DISS. ETH NO. 26129

Fibronectin as a key regulator of macromolecular crowding-enhanced extracellular matrix assembly

A thesis submitted to attain the degree of

DOCTOR OF SCIENCES of ETH ZURICH

(Dr. sc. ETH Zurich)

presented by

Jenna Leigh Graham

M. Sc. in Biomedical Engineering, Johns Hopkins University, USA

B. Eng in Biomedical Engineering, The Catholic University of America, USA

born on 20.05.1989

citizen of the United States of America

accepted on the recommendation of

Prof. Dr. Viola Vogel
Prof. Dr. Michael Raghunath
Prof. Dr. Denis Wirtz

2019

Abstract

Tissue engineers seek to replace damaged and diseased tissues in the body with *in vitro*-grown tissue substitutes. This involves seeding cells onto an engineered scaffold and providing the right chemical and physical cues to promote cell-mediated tissue assembly and tissue-specific remodeling. One of the key factors limiting the success of tissue engineering is the long culture time required for cells to assemble matrix in the highly dilute cell culture medium. However, the *in vivo* environment where matrix assembly naturally occurs is not dilute like cell culture medium, but rather highly crowded by macromolecules. Studies have shown that adding soluble macromolecules to cell culture medium to mimic the natural macromolecular crowding enables cells to more effectively build matrix by promoting molecular interactions.

Most mechanistic studies of how crowding enhances matrix assembly focus on the impact of crowding on collagen fiber assembly and largely ignore the highly abundant provisional matrix protein fibronectin. Fibronectin is the first matrix protein assembled by cells and it serves as a template to nucleate collagen fibers. Collagen cannot be assembled in the absence of fibronectin, and the tensional state of fibronectin impacts collagen binding. In this work we asked for the first time what role fibronectin plays in the underpinning mechanism of crowding-enhanced matrix assembly.

First, we took a close look at fibronectin and collagen I assembly over time and showed that the assembly of both is increased by the neutral crowding molecule Ficoll and the two are colocalized in the early stages of matrix assembly. We then asked how crowding enhances fibronectin assembly, since this process is cell tension-mediated and does not rely on enzymatic cleavage like collagen assembly does. We found that there were no changes in cell mechanical behavior, including contractility, that could explain the increased assembly. We then tuned to the fibronectin and found that Ficoll doubles the amount of surface adherent fibronectin, which can be readily harvested by fibroblasts and speed up fibrillogenesis, thus providing evidence of the first mechanism for crowding enhanced fibronectin assembly.

Next we asked what role fibronectin plays in the assembly of collagen in the presence of crowding. We used our well-validated Fn-FRET probe to reveal that Ficoll crowding upregulates the total amount of fibronectin fibers in a low-tension state through upregulating fibronectin assembly. Since unstretched fibronectin fibers have more collagen binding sites to nucleate the onset of collagen fibrillogenesis, our data suggests that the Ficoll-induced upregulation of low-tension fibronectin fibers contributes to enhanced collagen assembly in crowded conditions. We then manipulated the fibronectin assembly process by cross-linking fibronectin to the glass surface and found that fibroblasts could no longer harvest the coating to assemble early fibers. Remarkably, this suppressed the Ficoll-induced upregulation of collagen assembly, demonstrating that a fibronectin fiber template is still necessary, even when crowding is there to drive collagen processing and assembly.

Finally, we asked how our findings could be useful to tissue engineers. We showed that adding a preadsorbed fibronectin coating to a material doubles the early matrix assembly in the presence of

crowding. This is highly significant because the long culture time required to produce a tissue substitute *in vitro* is a key factor limiting the clinical success of tissue engineering.

In summary, we showed that the accelerated collagen I assembly as induced by crowding is regulated by cell access to fibronectin and we provided a preadsorbed fibronectin coating as a new tool for tissue engineers to better harness the power of macromolecular crowding to increase the speed of matrix assembly.

Zusammenfassung

Gewebe-Ingenieure streben an, beschädigtes und erkranktes Gewebe im Körper durch in vitro herangewachsene Gewebesubstitute zu ersetzen. Dies beinhaltet das Aussäen von Zellen auf ein konstruiertes Gerüst und die Bereitstellung der richtigen chemischen und physikalischen Signale, um die zellvermittelte Gewebe-Assemblierung und den gewebespezifischen Umbau zu fördern. Einer der Schlüsselfaktoren, die den Erfolg des Gewebe-Engineering einschränken, ist die lange Kulturzeit, die die Zellen benötigen, um die Matrix in dem stark verdünnten Zellkulturmedium zu assemblieren. Die In-vivo-Umgebung, in der die Matrix-Assemblierung auf natürliche Weise stattfindet, ist jedoch nicht wie Zellkulturmedium verdünnt, sondern von Makromolekülen stark überfüllt. Studien haben gezeigt, dass die Zugabe von löslichen Makromolekülen zum Zellkulturmedium zur Nachahmung des natürlichen makromolekularen Crowdings es den Zellen ermöglicht, durch Förderung molekularer Wechselwirkungen eine Matrix effektiver zu assemblieren.

Die meisten mechanistischen Studien konzentrieren sich jedoch auf die Auswirkungen des Crowdings auf die Assemblierung von Kollagenfasern und ignorieren weitgehend das reichlich vorkommende vorläufige Matrixprotein Fibronektin. Fibronektin ist das erste Matrixprotein, das von Zellen zu Fasern assembliert wird und als Vorlage für die Initiierung der Assemblierung von Kollagenfasern dient. Kollagen kann in Abwesenheit von Fibronektin nicht zu Fasern assembliert werden, und der Spannungszustand von Fibronektin beeinflusst die Kollagenbindung. In dieser Arbeit fragten wir zum ersten Mal, welche Rolle Fibronektin im Mechanismus der crowding-verstärkten Matrix-Assemblierung spielt.

Zuerst haben wir die Fibronektin- und Kollagen-I-Assemblierung im Zeitablauf genau angeschaut und gezeigt, dass die Assemblierung beider Moleküle durch das neutrale Molekül Ficoll verstärkt wird und beide Moleküle in den frühen Stadien der Matrix-Assemblierung kolokalisiert sind. Wir fragten dann, wie das Crowding die Fibronektin-Assemblierung verstärkt, da dieser Prozess durch die Zellspannung vermittelt wird und nicht wie die Kollagen-Assemblierung auf einer enzymatischen Spaltung beruht. Wir stellten fest, dass sich das zellmechanische Verhalten, einschließlich der Kontraktilität,was die verstärkte Assemblierung hätte erklären können, nicht verändert. Wir haben uns dann dem Fibronektin zugewendet und festgestellt, dass Ficoll die Menge des an der Oberfläche haftenden Fibronektins verdoppelt, das leicht von Fibroblasten geerntet werden kann und die Fibrillogenese beschleunigt. Dies liefert den Nachweis des ersten Mechanismus für die crowding-verstärkte Fibronektin-Assemblierung.

Als nächstes fragten wir, welche Rolle Fibronektin bei der Kollagen-Assemblierung in Gegenwart von Crowding spielt. Mithilfe unserer gut validierten Fn-FRET-Sonde konnten wir zeigen, dass Ficoll-Crowding die Gesamtmenge der Fibronektinfasern in einem spannungsarmen Zustand durch die Hochregulierung der Fibronektin-Assemblierung erhöht. Da ungestreckte Fibronektinfasern mehr Kollagenbindungsstellen aufweisen, um die Kollagenfibrillogenese zu initiieren, legen unsere Daten nahe, dass die Ficoll-induzierte Hochregulierung von Fibronektinfasern mit niedriger Spannung zu einer erhöhten Kollagen-Assemblierung unter Crowding-Bedingungen beiträgt. Anschließend manipulierten wir den Fibronektin-Assemblierungsprozess, indem wir Fibronektin mit der

Glasoberfläche vernetzten, und stellten fest, dass Fibroblasten die Beschichtung nicht mehr ernten konnten, um frühe Fasern zu assemblieren. Bemerkenswerterweise unterdrückte dies die Ficoll-induzierte Hochregulierung der Kollagen-Assemblierung, was zeigt, dass eine Fibronektin-Faser-Matrize immer noch notwendig ist, selbst wenn Crowding vorhanden ist, um die Kollagen-Verarbeitung und Assemblierung voranzutreiben.

Schließlich fragten wir, wie unsere Erkenntnisse im Bereich des Tissue Engineerings nützlich sein könnten. Wir haben gezeigt, dass das Hinzufügen einer voradsorbierten Fibronektinbeschichtung zu einem Material die frühe Matrix-Assemblierung in Gegenwart von Crowding verdoppelt. Dies ist von großer Bedeutung, da die lange Kulturzeit, die zur Herstellung eines Gewebeersatzes *in vitro* erforderlich ist, ein Schlüsselfaktor ist, der den klinischen Erfolg des Gewebe-Engineering einschränkt.

Zusammenfassend haben wir gezeigt, dass die crowding-induzierte beschleunigte Kollagen-I-Assemblierung durch den Zellzugriff auf Fibronektin reguliert wird, und wir haben Gewebe-Ingenieuren eine voradsorbierte Fibronektin-Beschichtung als neues Werkzeug bereitgestellt, um die Kraft des makromolekularen Crowdings besser zu nutzen und die Geschwindigkeit der Matrix-Assemblierung zu erhöhen.

Table of Contents

Abbreviation List

Alexa-647 Fn	fibronectin labeled with Alexa Fluor 647
BMP1	bone morphogenic protein 1
Col1	type I collagen
CR	carrageenan
DxS	dextran sulfate
ECM	extracellular matrix
F-actin	filamentous actin
Fn	fibronectin
FRET	Förster resonance energy transfer
FRET-Fn	fibronectin labeled for FRET
FVO	fractional volume occupancy
GdnHCl	guanidine hydrochloride
H3K9Ac	acetylation of histone 3 at lysine
H3K27me3	trimethylation of histone 3 at lysine 27
MMC	macromolecular crowding
MRTF-A	myocardin-related transcription factor-A
MSCs	mesenchymal stem cells
p-FAK	phosphorylated focal adhesion kinase
p-MLC2	phosphorylated myosin light chain 2
PSS	polysodium-4-styrene sulfonate
PVP	polyvinyl pyrolidone
TGF-β	transforming growth factor beta
YAP	yes-associated protein

1. Scope of the thesis

1.1. Motivation and Significance

Since the *in vitro* growth of engineered tissue substitutes is time consuming and thus expensive, a primary challenge taken on by tissue engineers is to define methods to speed up the assembly of native extracellular matrix (ECM) by cells *in vitro*. Important factors contributing to the success of a tissue engineered product besides the speed of assembly are its physical stability, how close the physical and biochemical properties are to native ECM, cell viability, cell proliferation, and cell phenotype. In recent years, macromolecular crowding has been applied to tissue engineering to improve the success of tissue assembly *in vitro*[1–3]. Molecular crowding results in much faster ECM assembly, as well as more native matrix architecture, enhanced matrix remodeling, and reduced cellular phenotypic drift (see Supplemental table 1 for a summary of literature concerning the use of crowding in tissue engineering).

The term macromolecular crowding describes the phenomenon where soluble macromolecules in a fluid take up space (excluded volume) and thereby affect the behavior of neighboring molecules whose available volume and thus conformational freedom are decreased[4,5], resulting in more compact protein conformations. Crowding also slows diffusion, enhances the interaction of molecules, their aggregation, and enhances adsorption of proteins onto surfaces[4,6–10]. Since the *in vivo* extracellular environment contains 9% - 45% volume fraction of macromolecules (FVO)[11], various artificial crowding agents have been added to cell culture to mimic *in vivo* crowding. One of the most commonly used crowding mimics is a mixture of two types of Ficoll (Supplemental table 1), a neutral, synthetic polysucrose[12–17] that has been FDA approved for clinical and *in vitro* applications[18,19]. The mixture of 37.5mg/mL 70kDa and 25mg/mL 400kDa Ficoll creates a crowded solution with an FVO of approx. 18% v/v which replicates the crowding level in blood plasma[2,12,20] and has proven effective in enhancing matrix assembly[11–17,21–23]. Even though negatively charged crowding molecules like carrageenan have a stronger enhancing effect on matrix assembly, they have an unequal impact on different matrix components (e.g. they have a much stronger enhancing effect on collagen I than fibronectin) and therefore result in a change in the composition of the ECM[22,24–26].

Crowding has been shown to enhance the assembly of a wide range of ECM molecules, including fibronectin, collagen types I-VII, laminin, fibrillin, vitronectin, heparin sulfate proteoglycan, hyaluronic acid, decorin, lysyl oxidase, tenascin C, and thrombospondin (see Chen et al.[2] for a more complete list). However, it is best described how crowding enhances assembly of collagen type I. Crowding enhances enzymatic cleavage of cell-secreted procollagen, both in a cell-free collagen gel assay and in cell culture[1,2,20,21,27–29], and crowding promotes collagen self-association in cell-free systems[2,30,31]. Additionally, crowding increases transglutaminase 2 and lysyl oxidase cross-linking of collagen, as shown in cell culture[1,2]. Finally, a fragment produced from the activation of procollagen C proteinase enhancer 1 has been found to act as a matrix metallopeptidase 2 inhibitor[21,32], thereby reducing the enzymatic digestion of the assembled collagen matrix.

In contrast to collagen, how crowding increases the assembly of fibronectin is not known. Fibronectin is the very first matrix molecule actively assembled into provisional ECM fibers by cells[33–37]. Though crowding drives supramolecular assembly, and should thus increase fibronectin-fibronectin binding, fibronectin fibrillogenesis is tightly regulated and requires fibronectin stretching to expose cryptic Fn-Fn binding sites[38–42]. Additionally, there is no enzymatic cleavage required to initiate fibronectin assembly, so crowding cannot be acting on fibronectin through this known mechanism. Given the important role of cell-fibronectin interactions in fiber assembly, crowding likely has another mechanism to increase fibronectin assembly that has not yet been identified.

It is also unknown what role fibronectin might play in the assembly of other ECM molecules in the presence of crowding. In early phases of ECM assembly, the initiation of collagen I polymerization into fibers needs to be nucleated. The nucleation of collagen I polymerization *in vivo* is initiated by fibronectin fibers which act as templates for collagen peptides to bind, similarly to the role of seeds that initiate biomineralization processes. In fact, even though collagen gels can be formed from a solution of collagen monomers *in vitro,* i.e. by lowering the pH and increasing the temperature, these initiation conditions are not typically exploited in cell culture and collagen matrix cannot be formed *in vivo* without the presence of fibronectin[43–46]. Importantly, though, early fibronectin-collagen binding is mechano-regulated as collagen peptides can tightly bind only to structurally relaxed but not to highly stretched fibronectin fibers[35,47]. Additionally, fibronectin binds to and enhances the procollagen cleavage activity of bone morphogenic protein 1[48,49] and plays a role in regulating the activity of the collagen cross-linker lysyl oxidase[50].

1.2. Objectives

Given the significant interactions between fibronectin and collagen assembly in cell culture, the main objective of this work is to understand the impact of macromolecular crowding on fibronectin assembly and the important role that this plays in assembly of other matrix components in the presence of crowding. We have divided this goal into 4 specific aims:

1. Study the time course of matrix assembly under crowding conditions with particular attention to how fibronectin and collagen I are interacting (Chapter 3)
2. Identify a mechanism for how macromolecular crowding enhances fibronectin assembly (Chapters 4&5)
3. Investigate the role of fibronectin as a template for collagen I fiber assembly in the presence of macromolecular crowding (Chapter 6&7)
4. Evaluate the impact of supplementing fibronectin on matrix assembly with macromolecular crowding (Chapter 8)

This thesis proceeds to address each of these specific aims. Chapter 2 will provide a general introduction to the extracellular matrix components fibronectin and type I collagen and how they are assembled, then introduce the phenomenon of macromolecular crowding, and finally provide an overview of all work that has been done in the tissue engineering field utilizing the matrix enhancing effect of macromolecular crowding. Chapter 3 will then provide a fluorescence microscopy-based investigation of the assembly of fibronectin and collagen by human skin fibroblasts in the presence

of the crowder Ficoll, with quantification at 16 hours, 2 days, and 6 days. Chapter 4 will then present an investigation into changes in cell mechanical behavior that could explain the increased fibronectin assembly in the presence of crowding, given that fibronectin assembly is a cell-mediated process. Chapter 5 will then turn to crowding effects on fibronectin that could contribute to increased assembly. Chapter 6 will show an investigation into the impact of crowding on the tensional state of fibronectin and its ability to nucleate collagen I fibers, utilizing our well-validated fibronectin-FRET probe[40,47,51–55]. Chapter 7 will then utilize crosslinking of a fibronectin coating to examine the importance of cells ability to harvest fibronectin for collagen I assembly in the presence of macromolecular crowding. Finally, chapter 8 will demonstrate how our findings can be useful to tissue engineers by investigating the impact of supplemental human plasma fibronectin on the speed of matrix assembly with crowding.

This thesis will also be supplemented by several appendices. Appendix A will provide protocols developed in this work. Appendix B will provide custom MATLAB code used to analyze microscopy images. Appendix C will show a comparison of two fibronectin matrix visualization methods: fluorescent conjugation and antibody staining. Appendix D will show how the threshold was optimized for Fn-FRET analysis. Finally, Appendix E will present findings regarding an as-of-yet unidentified toxicity effect of Ficoll purchased from Sigma Aldrich (as opposed to Ficoll from GE Healthcare, which was used consistently in this work).

This work has been published in the journal Biomaterials Science:

Fibrillar fibronectin plays a key role as nucleator of collagen I polymerization during macromolecular crowding-enhanced matrix assembly, by Jenna Graham, Michael Raghunath, and Viola Vogel, Biomaterials Science, 2019, 7, 4519-4535, DOI: 10.1039/C9BM00868C.

2. Introduction

2.1. Fibronectin

Fibronectin is a glycoprotein that is a critical component of the extracellular matrix. Fibronectin usually exists as a dimer of two nearly identical, approximately 250kDa subunits that are linked at their C-terminal end. In solution, the fibronectin dimer has a globular conformation. Although there is only one gene encoding for fibronectin, variable splicing results in many variant forms. There are two main classes of fibronectin found in the body, plasma and cellular. Plasma fibronectin is produced by hepatocytes in the liver and is found circulating in the blood plasma at a concentration of 300ug/mL[56]. Cellular fibronectin is secreted by matrix producing cells in various tissues of the body and has many more variants, enabling tissue specific control of cell- and ligand-binding[56]. Both cellular and plasma fibronectin are found incorporated into the same fibers in the extracellular matrix[57].

Fibronectin plays a key role in embryonic development, as evidenced by the fact that mice not expressing the FN gene experience embryonic lethality[58]. Fibronectin also plays a key role in wound healing as the first provisional matrix that is assembled by cells, along with fibrin. Fibronectin promotes infiltration and proliferation of cells to the wound cite, and also serves as a template for the assembly of other matrix components. Eventually, this provisional matrix is replaced by a more mature matrix with more collagens[59].

Fibronectin is a highly extensible protein that exists in several different tensional states in vitro[51]. When fibronectin is extended by tensional forces, cryptic binding sites are exposed, thus changing its binding activity for cells, biological molecules, and other matrix proteins[42]. In fact, binding sites for other fibronectin molecules are exposed when fibronectin is stretched and stretching of fibronectin is therefore necessary for fibronectin fiber assembly[38–42]. This is accomplished by cell traction forces. Figure 2.1 shows the structure of fibronectin and indicates cryptic binding sites.

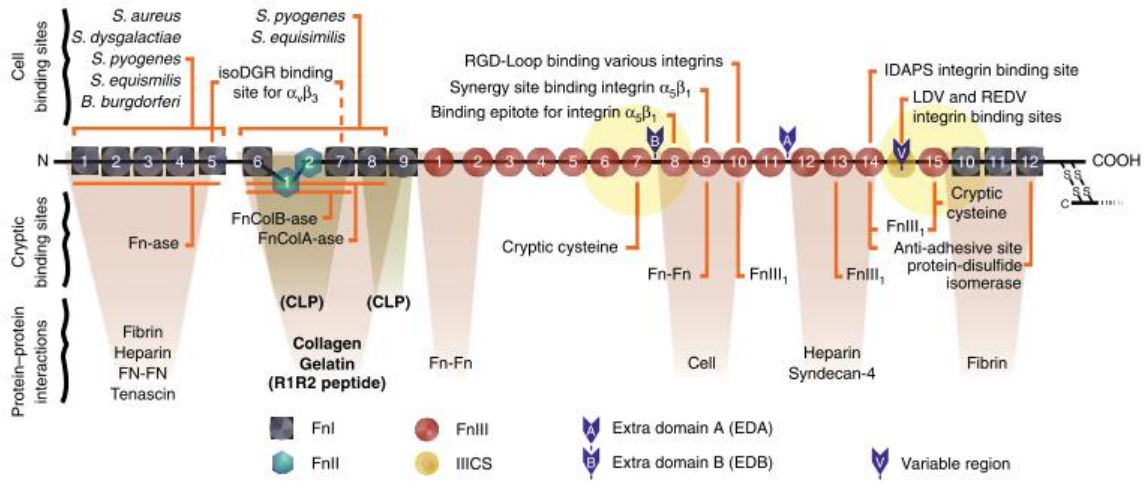

Figure 2.1 Domain structure of fibronectin with binding sites for cells and proteins indicated. Cryptic binding sites are also indicated. Reprinted from Nature Communications, vol. 6, article no. 8026, Kristopher E. Kubow, Radmila Vukmirovic, Lin Zhe, Enrico Klotzsch, Michael L. Smith, Delphine Gourdon, Sheila Luna, and Viola Vogel, Mechanical forces regulate the interactions of fibronectin and collagen I in extracellular matrix, Copyright (2015), with permission from Macmillan Publishers Limited[47].

Upon binding of cells to a surface coated with globular fibronectin, early-stage focal contacts form that are rich in both $\alpha_v\beta_3$ and $\alpha_5\beta_1$ integrins. With time, $\alpha_5\beta_1$ rich fibrillar adhesions coupled to myosin are pulled away from $\alpha_v\beta_3$ focal adhesions toward the cell nucleus by cell tension forces along actin stress fibers[60,61]. This movement of integrins toward the cell center results in extension of fibronectin molecules. Figure 2.2 depicts this process. Fibronectin readily deposits from the media onto surfaces and existing matricies or scaffolds in cell culture, so this process occurs even if there is no fibronectin coating added before cell seeding. Similarly *in vivo*, fibronectin is ever present in the blood and fluid surrounding cells and is therefore available for cell-mediated matrix assembly. Crosslinking of fibronectin to the substrate surface prevents this translocation of integrins and thereby interferes with fibronectin fiber assembly[60].

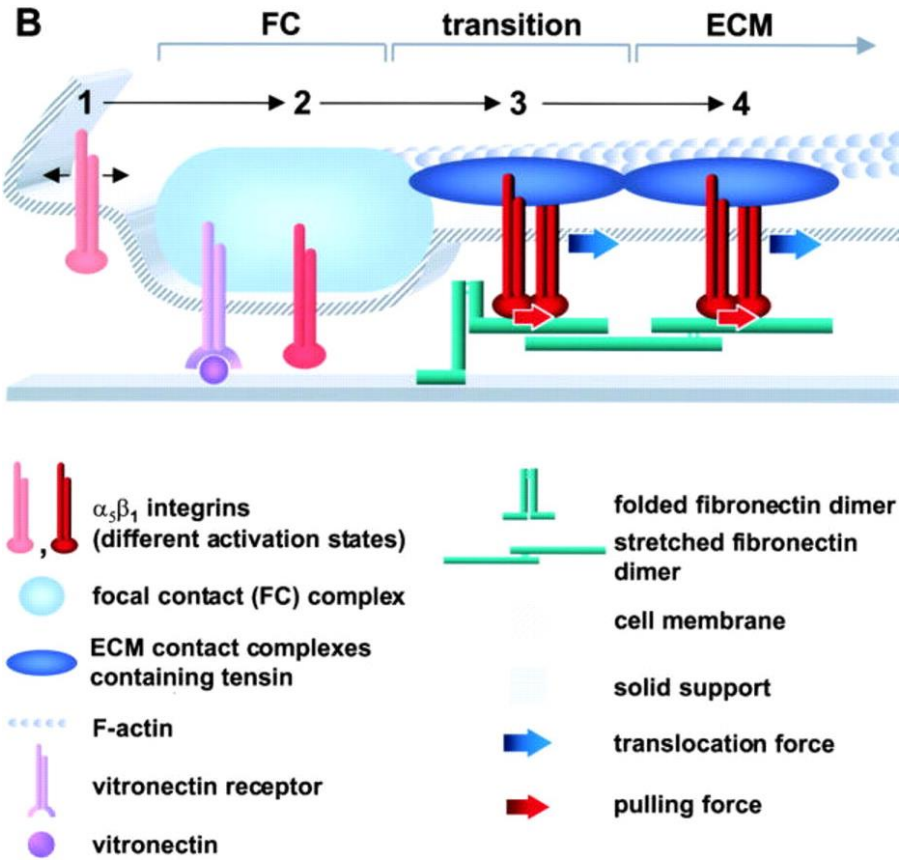

Figure 2.2 The fibronectin matrix assembly process requires cell-mediated traction forces that translocate $\alpha_5\beta_1$ integrins and thereby extend fibronectin dimers. Reprinted from The Journal of Cell Biology, vol. 148, no. 5, 1075-1090, Roumen Pankov, Edna Cukierman, Ben-Zion Katz, Kazue Matsumoto, Diane C. Lin, Shin Lin, Cornelia Hahn, and Kenneth M. Yamada, Integrin Dynamics and Matrix Assembly, Copyright (2000), with permission from The Rockefeller University Press[39].

The fact that fibronectin does not form fibers by self-assembly but rather requires cell involvement is quite important for its function *in vivo*. Fibronectin needs to remain in soluble form in the blood until it is needed to close a wound[62]. The fact that fibronectin-fibronectin binding sites are hidden in the globular state prevents self-assembly that would impede blood flow. Then, when fibronectin comes into contact with fibroblasts at a wound site, cell-mediated tensional forces change the conformation of fibronectin to expose cryptic Fn-Fn bindings sites, thereby regulating matrix assembly.

The conformation of fibronectin can be assessed *in vitro* with our well validated, custom built Förster resonance energy transfer (FRET) probe[40,47,51–55]. FRET is a technique that can detect the distance between two different fluorophores that are in close proximity to one another (0.5-10 nm). The donor fluorophore (in our case Alexa Fluor 488) is excited with a laser and, if the acceptor fluorophore is close enough, some of the excitation energy of the donor is transferred non-radiatively through

long-range dipole-dipole coupling to the acceptor fluorophore (in our case Alexa Fluor 546). The amount of energy that is transferred from the donor to the acceptor is inversely proportional to the sixth-power of the distance between them, and also affected by the degree of overlap of the donor emission spectrum and the acceptor absorption spectrum, the quantum yield of the donor, the absorption coefficient of the acceptor, and the relative orientation of the dipole moments. With this technique, we can get a readout in the form of the ratio of acceptor to donor light intensity that is very sensitive to the distance between the donor and acceptor. In order to use this technique to measure a large range of fibronectin conformations, we specifically label the cysteines in fibronectin type III modules $FNIII_7$ and $FNIII_{15}$ with acceptor dyes and then randomly label the amines with donor dyes[51,53,63]. We then add this FRET-Fn probe in low quantities (10% of total supplemented fibronectin) to cell culture and it gets incorporated into cell-assembled fibronectin fibers. Only a small portion of the total fibronectin is labeled to prevent transfer of light intensity between different fibronectin molecules (intermolecular FRET). This technique has been used in our group to show that fibronectin exists in different conformational states in cell culture[51], that fibronectin is unfolded by cell tensional forces[40,53], and that fibronectin becomes progressively more and more unfolded as the matrix ages (in the absence of ascorbic acid)[54].

In order to validate the FRET probe and also get an idea of what conformation of fibronectin corresponds to a given FRET ratio, increasing concentrations of the chemical denaturant guanidine hydrochloride (GdnHCl) have been used to slowly denature fibronectin and measure the corresponding FRET ratios[40,53]. Studies have shown that fibronectin in 1M GdnHCl is extended but has not lost its secondary structure, whereas fibronectin in 4M GdnHCl is fully denatured and has lost its secondary structure[53]. It is important to note, however, that the denaturation curve is measured in solution but the FRET that we measure in cell culture is from fibronectin in fibers. So we cannot know the exact conformation of fibronectin in fibers from this calibration, but it is still a valuable benchmark to get an estimate of the distance between donor and acceptor fluorophores, which is related to fibronectin conformation. The calibration procedure also allows comparison of results obtained with different batches of the FRET-Fn probe. Figure 2.3 depicts how the conformation of the FRET-Fn probe changes with denaturation, and also how it is thought to change with force.

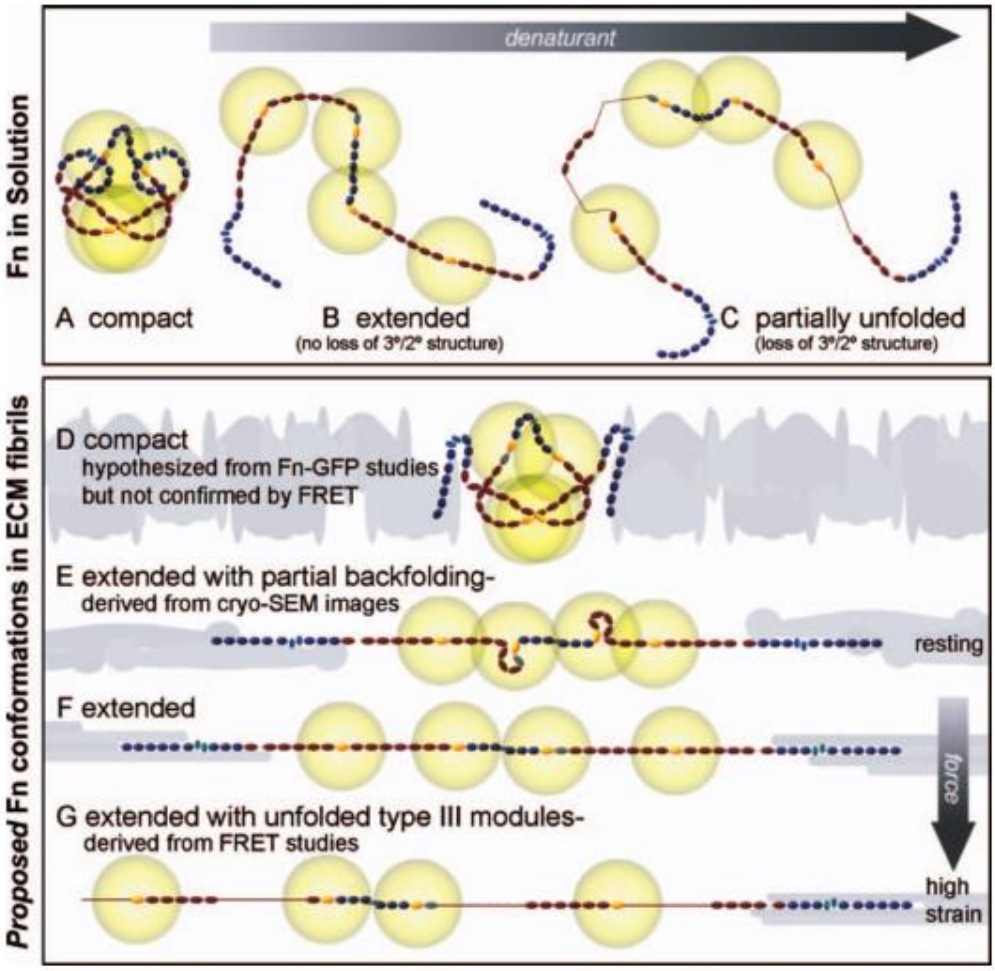

Figure 2.3 Diagram of the conformation of the FRET-Fn probe as it is denatured or extended by force. The gold modules represent the cysteines on $FNIII_7$ and $FNIII_{15}$ specifically labeled with acceptor fluorophores. The yellow circles represent the distance range within which FRET can occur. The donor fluorophores are not indicated, as they are randomly located on amines. A-C show conformational changes of fibronectin in response to a denaturant. Fibronectin is in a compact conformation in solution (A). A low concentration of denaturant (1M GdnHCl) destabilizes ionic interactions within the fibronectin dimer resulting in an extended conformation but no loss of secondary structure (B). A higher concentration of denaturant (4M GdnHCl) leads to unfolding and loss of secondary structure (C). D-G show predictions of how the conformation of fibronectin in a fibril changes with increasing force. Fn-GFP studies predict that fibronectin in an unstretched fibril is in a compact conformation (see original paper for Fn-GFP references) (D). However, cryo-SEM and FRET data suggest that fibronectin in an unstretched fibril is extended with partial backfolding, rather than compact (see original paper for cryo-SEM references) (E). Cell tension forces first result in extension of fibronectin dimers within a fibril (F). Higher forces result in unfolding of type III modules within a fibril (G). Reprinted from PLoS Biol, vol. 5, no. 10, e268, Smith ML, Gourdon D, Little WC, Kubow KE, Eguiluz RA, Luna-Morris S, and Viola Vogel, Force-Induced Unfolding of Fibronectin in the Extracellular Matrix of Living Cells, Copyright (2007), with permission from PLOS[53].

2.2. Type I Collagen

Type I collagen is the most abundant collagen in the human body and a very important structural component of the extracellular matrix. Collagen I is a triple helical protein made of up two α_1 chains and one α_2 chain. Cells produce and secrete heterotrimers of procollagen, which contain propeptides at each end that prevent collagen-collagen binding inside the cell. After secretion, the propeptides need to be cleaved off by enzymes called N- and C-proteinases, named after the end of the protein that they cleave. Once propeptides have been cleaved, collagen molecules can bind to one another and fiber assembly can begin (Figure 2.4).

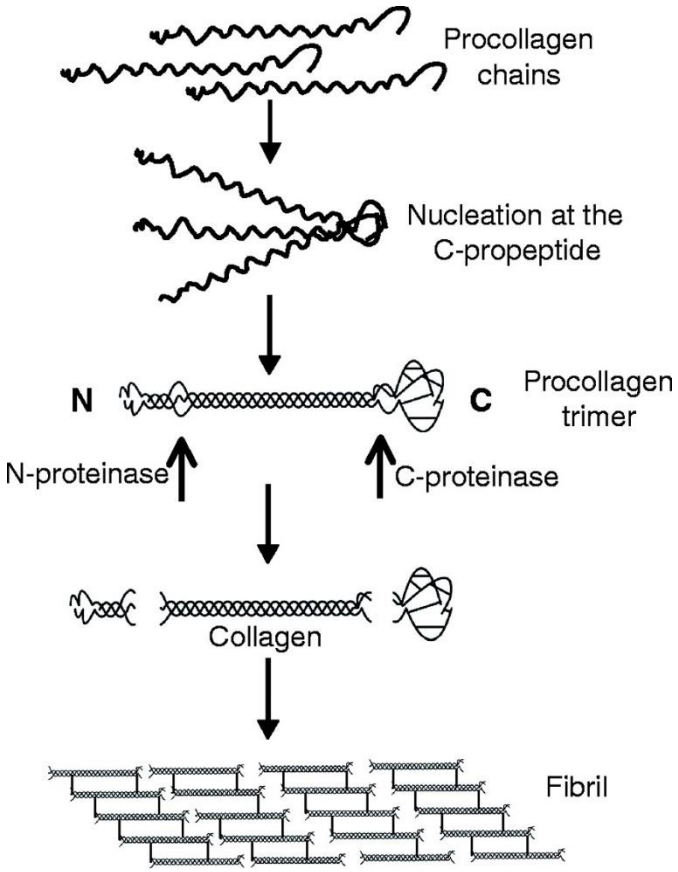

Figure 2.4 Diagram depicting the steps of collagen assembly. Procollagen chains synthesized in the endoplasmic reticulum associate at the C-terminal end to form a procollagen trimer inside the cell. The procollagen trimer is then secreted and N- and C-propeptides at each end are cleaved by N- and C- proteinases, respectively. Once cleaved, the collagen trimer can self-associate and assemble into fibrils with covalent cross-links between triple helical collagen molecules. Note: self-assembly only occurs ex vivo from a solution of collagen monomers. Not shown here is the nucleation step involving fibronectin that is required for collagen fiber formation in vitro and in vivo. Reprinted from Journal of Cell Science, vol. 118, no. 7, 1341-1353, Elizabeth G. Canty and Karl E. Kadler, Procollagen trafficking, processing and fibrillogenesis, Copyright (2005), with permission from The Company of Biologists Ltd[64].

In vitro, collagen assembly is often studied in a cell-free environment. Purified collagen with propeptides already removed is stable in a low temperature, acidic solution. Then upon neutralization and warming of the solution, collagen fiber formation is initiated. Fiber formation proceeds following a sigmoidal curve, with an initial lag phase followed by a period of steep growth that eventually levels off (Figure 2.5). Nucleation of new fibers occurs during the lag phase and then rapid elongation and thickening of fibers occurs during the growth phase. The final structure of the collagen network that is formed depends on the kinetics of nucleation and growth[30].

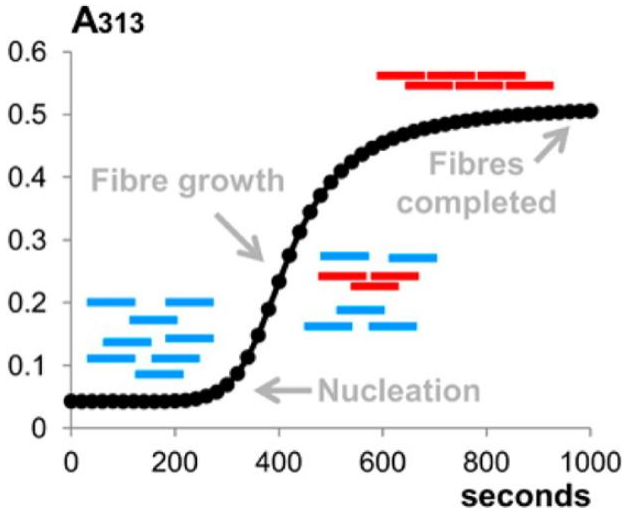

Figure 2.5 Collagen assembly in a cell-free assay follows a sigmoidal curve. Fiber assembly from an acidic solution of precleaved collagen monomers (0.8mg/mL) was initiated by neutralization and warming to 37°C. This diagram shows the increase in absorbance at 313nm (A_{313}, a measure of diffraction due to collagen fiber assembly, also called turbidity) over time as collagen self-assembles from a solution of monomers. Fibers must first be nucleated, which occurs during the initial period before turbidity increases. After nucleation, soluble collagen monomers readily bind to growing fibers during the growth phase, which is marked by rapidly increasing turbidity. Finally, as the free collagen monomers are depleted, growth slows and fiber formation is completed. Reprinted from The Journal of Physical Chemistry B, vol. 119, no. 12, 4350-4358, Jean-Yves Dewavrin, Muhammed Abdurrahiem, Anna Block, Mrinal Musib, Francesco Piazza, and Michael Raghunath, Synergistic Rate Boosting of Collagen Fibrillogenesis in Heterogeneous Mixtures of Crowding Agents, Copyright (2015), with permission from ACS Publications, Washington, DC[31].

Even though collagen is capable of self-assembly as described above, these conditions are not physiological and this is not how collagen is assembled *in vivo*. The assembly process *in vivo* and in cell culture is highly regulated and involves several interacting molecules. In fact, collagen binds to over 50 known molecules *in vivo* and these numerous interactions allow for highly regulated and highly diverse assemblies of collagen for different types of tissues in the body. Specifically, collagen I assembly requires the presence of fibronectin, integrins, and collagen V[46] to act as nucleators. For instance, McDonald et al. showed that inhibition of collagen binding to fibronectin by an interfering antibody inhibited collagen assembly by fibroblasts *in vitro*[43]. Additionally, Li et al. showed that inhibition of fibronectin assembly by $\alpha_2\beta_1$ and $\alpha_5\beta_1$ integrin blocking antibodies also inhibited collagen

assembly by vascular smooth muscle cells *in vitro*[65]. Wenstrup et al. showed in a study of Ehlers-Danlos syndrome that collagen I fibers do not form in the absence of collagen V *in vivo*[66].

Another very important cofactor for collagen assembly *in vitro* and *in vivo* is ascorbic acid. Without ascorbic acid present, cells are not able to efficiently release procollagen and most collagen assembly is prevented[64]. Therefore, ascorbic acid is often supplemented to cell culture media. It is important to consider the form of ascorbic acid because it is very unstable in solution and degrades quickly. L-ascorbic acid 2-phosphate magnesium salt is a form with increased stability that is often used in cell culture[67].

2.3. Interactions between fibronectin and collagen I

As previously mentioned, fibronectin is one of the key regulators of collagen I assembly. Several studies using fibronectin-null cells and fragments that prevent fibronectin assembly have shown that collagen I cannot be assembled in the absence of fibronectin[43–46,68]. Not only must fibronectin be present, but fibronectin fibers also act as a mechano-regulated template for collagen I assembly. The tensional state of fibronectin fibers has an impact on this process. Our group previously showed that collagen fibers nucleate at unstretched fibronectin, but not highly stretched fibronectin[47]. Collagen tended to colocalized mostly with fibronectin fibers with a higher FRET signal (Figure 2.6), and stretching of fibronectin fibers resulted in destruction of the multivalent binding site for gelatin and reduced binding of collagen. Fibronectin has also been shown to bind and enhance the activity of bone morphogenic protein 1 (a procollagen C-proteinase)[48] and lysyl oxidase (a collagen crosslinker)[50].

Interestingly, one alternative mechanism for collagen I assembly *in vivo* that may be fibronectin-independent has been postulated[69–71]. In an effort to explore the potential therapeutic benefit of targeting fibronectin to inhibit fibrosis, Moriya et al. found that collagen I assembly still occurred in response to liver injury in a fibronectin-deficient mouse model[69]. They identified TGF-β and type V collagen as necessary players in this pathway. At the same time, Kawelke et al. showed that fibronectin is actually protective against liver fibrosis because its expression limits TGF-β activity[70]. By inhibiting fibronectin expression, Moriya et al. eliminated this control against TGF-β activity and collagen I assembly. It is important to note, however, that though fibronectin gene expression was depleted in the liver in these studies, it is not clear that fibronectin was eliminated. Other organs still expressed fibronectin[72]. Additionally, mice were allowed to develop with normal fibronectin expression and it was only knockedout 4 weeks after birth, at which point there was certainly fibronectin present in assembled matrix. Therefore it is likely that fibronectin was still present to act as nucleator for collagen fiber assembly. These results then truly speak to the role of plasma fibronectin gene expression as a regulator of TGF-β activity.

Altock et al. further showed that, in contrast to inhibition of fibronectin expression, inhibition of fibronectin matrix assembly is an effective way to prevent fibrosis[71]. Together these results confirm the fact that fibronectin fibers are critical for collagen I assembly *in vivo*.

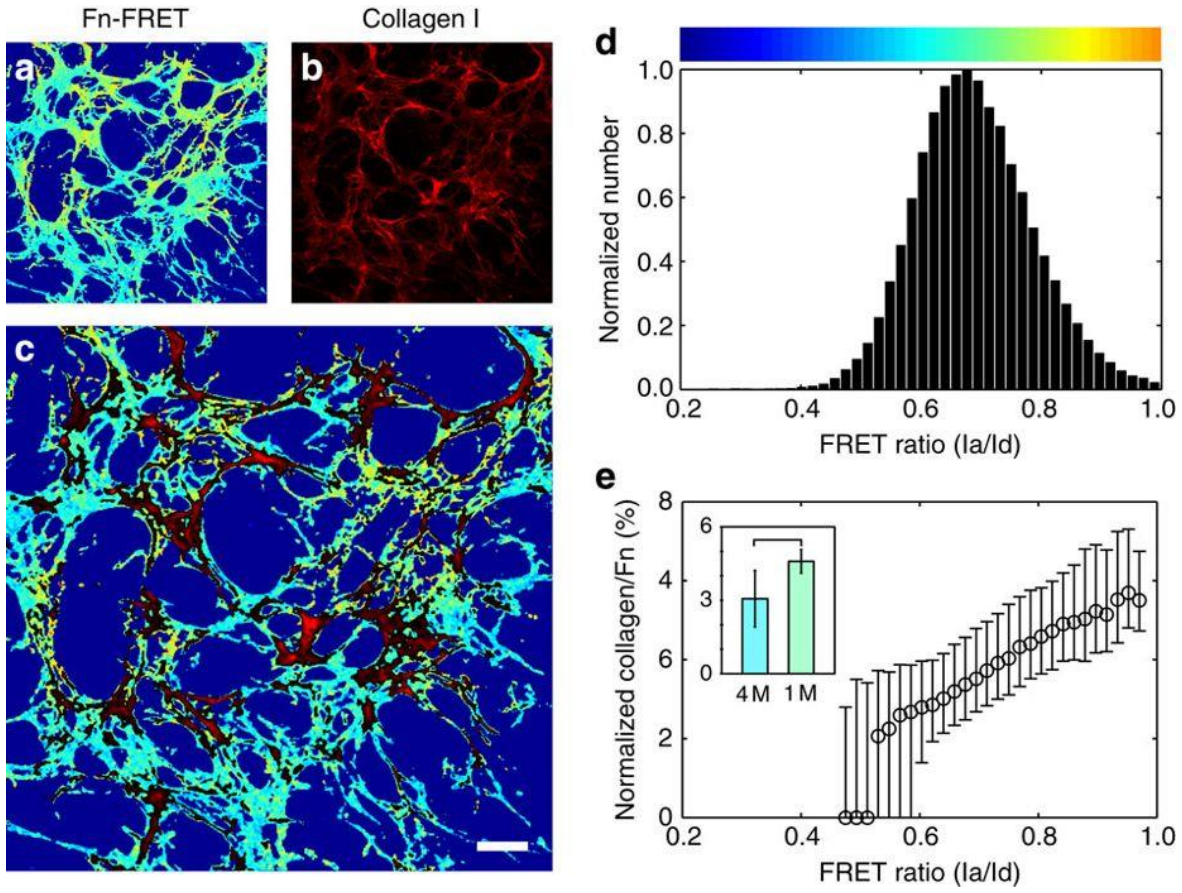

Figure 2.6 Data from Kubow et al. show that collagen fibers in early ECM co-localize with relaxed fibronectin fibers. (a) Fibronectin-FRET signal in a 3 day matrix assembled by fibroblasts in the presence of ascorbic acid. (b) Corresponding immunostained collagen I. (c) Overlay of Fn-FRET and collagen I to demonstrate co-localization. Only collagen I pixels above the median intensity are shown. (d) Histogram of FRET ratios. (e) Correlation of collagen intensity with Fn-FRET ratio shows that collagen tends to colocalize more with higher FRET fibronectin. Reprinted from Nature Communications, vol. 6, article no. 8026, Kristopher E. Kubow, Radmila Vukmirovic, Lin Zhe, Enrico Klotzsch, Michael L. Smith, Delphine Gourdon, Sheila Luna, and Viola Vogel, Mechanical forces regulate the interactions of fibronectin and collagen I in extracellular matrix, Copyright (2015), with permission from Macmillan Publishers Limited[47].

Collagen I also has an impact on fibronectin fiber tension. As a matrix matures, collagen fibers become more interconnected and are no longer restricted to the fibronectin template. They then take the primary mechanical load in the matrix and, as a result, fibronectin fibers become more relaxed[47]. Removing collagen by collagenase treatment and blocking of collagen-fibronectin binding both resulted in increased strain in fibronectin.

2.4. Macromolecular crowding

The fluid inside and outside of cells in our bodies is highly crowded by macromolecules. Though this fact is usually neglected in *in vitro* cell culture[2], macromolecular crowding has significant impacts on how other molecules behave. The extracellular fluid has 20-80 g/L of macromolecules, but the only source of macromolecules in cell culture media is from supplemented serum which is used at very low concentrations and results in a much lower level of crowding. Inside of cells, the crowding level is much higher and research has shown that this is a very important component regulating molecular interactions in the cytoplasm. Figure 2.7 shows an approximation of what crowding looks like inside and outside the cell, as well as a scale of different crowding levels found *in vitro* and *in vivo*.

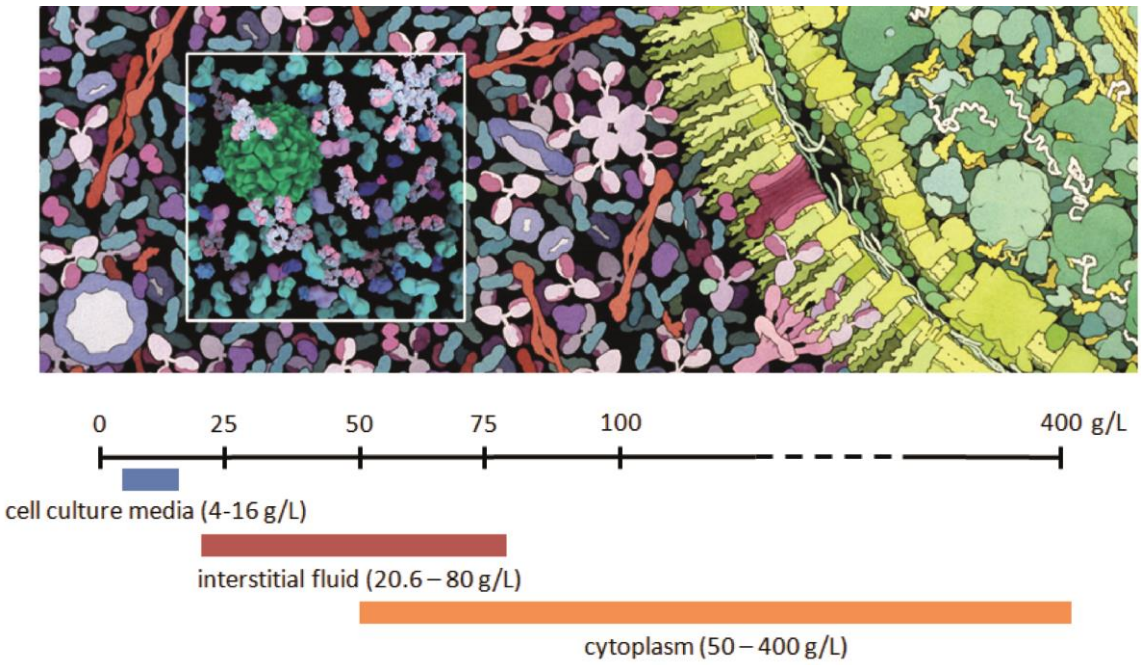

Figure 2.7 Diagram depicting the crowded environment inside and outside of the cell. (A) Artistic representation of E.coli (yellow/green) in blood serum (purple/blue). (B) Scale showing ranges of crowding in vitro and in vivo. Figure part A reprinted from Current Opinion in Structural Biology, vol. 20, no. 5, 640-648, Yutaka Ito and Philipp Selenko, Cellular structural biology, Copyright (2010), with permission from Elsevier[73].

The impact of crowding is described by the concept of excluded volume: macromolecules in a solution occupy space that other molecules then cannot occupy. As a result, the available volume that a molecule potentially could occupy is reduced (Figure 2.8). This results in thermodynamic changes (reduced entropy and increased free energy) that favor configurations that take up less space. Consequently crowding tends to cause protein compaction, aggregation, stabilization of complexes, and adsorption onto surfaces. All of these consequences relate directly to the excluded volume effect and can be understood by imagining that molecular arrangements that take up less space are thermodynamically preferred (i.e. compact proteins (Figure 2.9), two proteins as a complex

rather than separate, proteins on a surface rather than in the bulk media). Crowding also results in slowed diffusion since there are many other molecules blocking the path of a diffusing molecule.

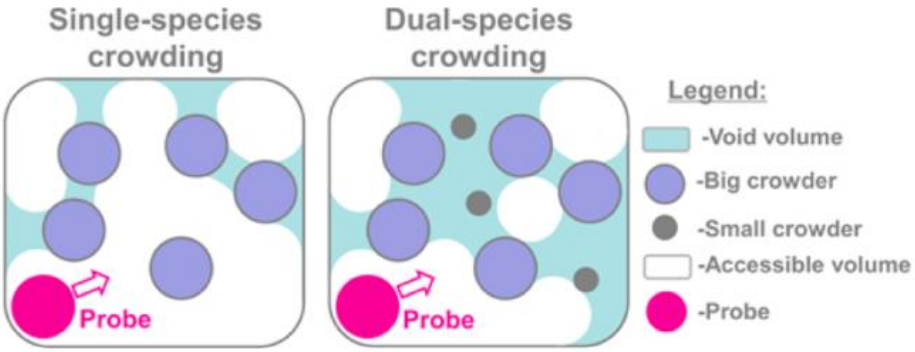

Figure 2.8 Diagram demonstrating how the presence of crowding molecules creates an excluded volume effect that limits the space that a probe molecule can occupy. The probe is not only excluded from the area where crowders are, but also from the narrow spaces in between the crowders that are too small for the probe to fit (indicated by the light blue area "void volume"). The addition of a few small crowders (dual-species crowding) creates a synergistic effect where the total volume excluded is more than the sum of the volume of the crowders. This is because the small crowders fill the large gaps in between the large crowders that could have accommodated the probe molecule, thereby further reducing the available space for the probe molecule. Many groups, including us, utilize this phenomenon by mixing two species of Ficoll (70kDa and 400kDa) to achieve an enhanced crowding effect. Reprinted from The Journal of Physical Chemistry B, vol. 119, no. 12, 4350-4358, Jean-Yves Dewavrin, Muhammed Abdurrahiem, Anna Block, Mrinal Musib, Francesco Piazza, and Michael Raghunath, Synergistic Rate Boosting of Collagen Fibrillogenesis in Heterogeneous Mixtures of Crowding Agents, Copyright (2015), with permission from ACS Publications, Washington, DC[31].

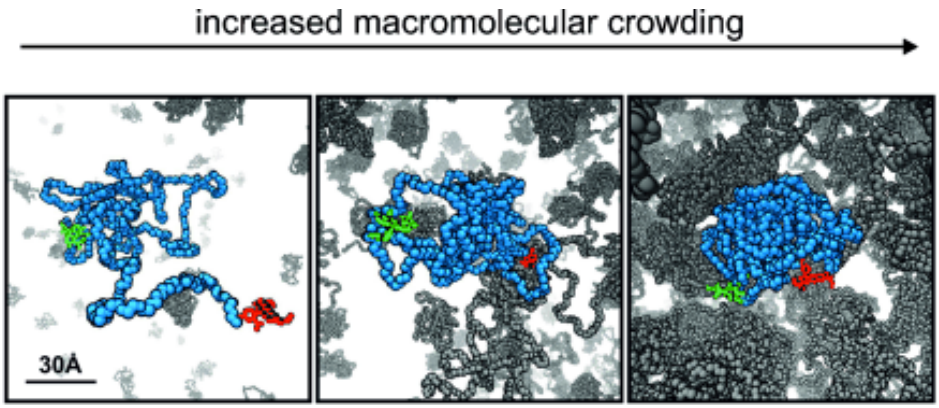

Figure 2.9 Diagram depicting how proteins favor a more compact conformation in a crowded environment because there is less available space and no two molecules can occupy the same space. In this simulation, both the probe molecule and the crowder molecule are polyethylene glycol (PEG). Reprinted from Angewandte Chemie International Edition, vol. 54, no. 8, David Gnutt, Mimi Gao, Oliver Brylski, Matthias Heyden, and Simon Ebbinghaus, Excluded-Volume Effects in Living Cells, Copyright (2014), with permission from Wiley Online Library[74].

Many studies have sought to explain the consequences of macromolecular crowding through both theoretical and experimental means, however, the high complexity of crowding in the cytoplasm and the possibility for more interactions between the crowders and probe molecules besides steric repulsion result in some interactions that cannot be predicted by simple excluded volume[75]. For example, Banks et al. showed that the intrinsically disordered protein FlgM does not simply adopt a more compact conformation with increasing level of crowding[76]. Instead, FlgM forms two distinct populations (compact and extended) at high levels of crowding. This complex behavior involves variable degrees of binding of the FlgM to the crowders, where the compact molecules exhibit few binding interactions and the extended molecules exhibit many binding interactions with the crowder. The biophysical community is still working hard to understand all the ways that crowding plays a role in the vast molecular interactions inside the cell and new studies are published continuously with different specific molecules in different types of crowded environments. However, the concentration of macromolecules in the extracellular fluid that is relevant in the consideration of matrix assembly is much lower than in the cytoplasm, and therefore some of the complexity is reduced. Additonally, when tissue engineers use simulated crowding to increase matrix assembly (as will be described in the next section), very simple solutions of inert crowders are used, so direct interactions between the crowders and matrix molecules is assumed to be low.

2.5. Applications of macromolecular crowding in tissue engineering

A recent wave of publications in the field of tissue engineering has demonstrated the power of macromolecular crowding to drive matrix assembly *in vitro*. In typical cell culture medium, which is very dilute and analogous to salt water, matrix assembly is a very inefficient process, a fact that has significantly limited the success of tissue engineering. However, studies have shown that macromolecular crowding can be mimicked in *in vitro* culture by the supplementation of artificial crowding molecules to the medium. The added crowding empowers cells to make their own matrix on a much shorter timeline, thereby making tissue engineering by self-assembly a much more realistic goal. Table 2.1 provides a summary of this literature.

Table 2.1 Summary of literature related to the use of crowding to enhance matrix assembly.

Cell/Tissue Type	Crowder	Key Findings	Reference
Human fibroblasts	500kDa Dextran Sulfate (DxS) 100 µg/mL	– Conversion of unprocessed procollagen in media to collagen in matrix – No impact of neutral Dextran at 100µg/mL	Lareu et al., Tissue Eng. (2007)[29]
Human lung fibroblasts	500kDa DxS 100µg/mL 200kDa polysodium-4-styrene sulfonate (PSS) 100µg/mL	– Accelerated activity of procollagen C-proteinase – Effective in 2D and 3D (2D>>3D) – No impact of 70kDa Ficoll, 400kDa Ficoll at 50mg/mL, or 10kDa DxS at 100ug/mL – Hydrodynamic radius and charge of crowder affect result	Lareu et al., FEBS Letters (2007)[28]
Human lung fibroblasts	500kDa DxS 100µg/mL Ficoll mixture (37.5mg/mL 70kDa + 25mg/ml 400kDa)	– Used crowding to create an *in vitro* fibrosis model to screen antifibrotic compounds – Faster, more granular matrix assembly with DxS than Ficoll	Chen et al., Br. J. Pharmacol. (2009)[20]
Several cell types	500kDa DxS 100µg/mL Ficoll mixture	– Assembly of many ECM components increased by DxS	Chen et al., Adv. Drug Deliv. Rev. (2011) [2]
Human lung fibroblasts	500kDa DxS 100µg/mL	– Matrix assembled by fibroblasts with crowding supported stable propagation of human embryonic stem cells better than Matrigel	Peng et al., J. Tissue Eng. Regen. M. (2012)[77]

Human mesenchymal stem cells	Ficoll mixture	– Increased matrix assembly, alignment – Feedback to cells: cytoskeletal alignment, increased adhesion, proliferation	Zeiger et al., PLoS One (2012)[12]
Porcine chondrocytes	Ficoll mixture	– Increased collagen and glycosaminoglycan production in 2D but not in 3D model (PGA unwoven fibers)	Chen et al., Tissue Eng. Part C (2013)[78]
Human corneal, lung, and dermal fibroblasts MSCs	Caregeenan type 1 (CR) 75µg/mL	– Increased collagen I and fibronectin deposition by all cell types. Degree of effect was cell type dependent.	Kumar et al., Adv. Sci. Tech. (2014)[79]
Human MSCs	Ficoll mixture	– Enhanced adipogenic differentiation (chemically induced): more lipid production, more ECM – Adipo-ECM generated under crowding also promoted enhanced differentiation	Ang et al., Tissue Eng. Part A (2014)[14]
Human fibroblasts MSCs	Polyvinyl pyrolidone (PVP)	– PVP has a similar ECM enhancing effect as Ficoll but can achieve higher FVO without increased viscosity.	Rashid et al., Tissue Eng. Part C (2014)[11]
Human lung fibroblasts, tenocytes, osteoblasts	500kDa DxS 100µg/mL CR 75µg/mL	– Low serum (0.5%) resulted in higher collagen I production with crowding – Generated cell-sheet that could be released from pNIPAAm substrate – Many matrix components enhanced by CR	Satyam et al., Adv. Mater. (2014)[22]
Cell-free collagen gel formation	400kDa Ficoll 0-25mg/mL	– Rate of collagen nucleation and fiber growth can be tuned by crowding level resulting in altered fiber diameter and organization	Dewavrin et al., Acta. Biomater. (2014)[30]
Bovine vascular endothelial cells	Ficoll mixture	– Greater amount of collagen IV produced, more aligned	Liu et al., Meter. Res. Soc. Symp. Proc. (2014)[13]

Rat vocal fold fibroblasts	Ficoll mixture	– Increased collagen I assembly with crowding and TGFβ-1, toward the goal of *in vitro* fibrosis drug screening	Graupp et al., Laryngoscope (2014)[23]
Human corneal fibroblasts	Ficoll mixture	– Production of a cell-sheet that could be released from temperature responsive polymer in 6 days – No change in ECM gene expression or αSMA expression – Effective in medium containing both bovine and human serum	Kumar et al., Sci. Rep. (2015)[15]
Cell-free collagen gel formation	40kDa and 360kDa PVP 70kDa and 200kDa Dextran 70kDa and 400kDa Ficoll	– Mixtures of different size crowders have a synergistic effect that results in higher volume exclusion than the simple sum of hydrodynamic radii	Dewavrin et al., J. Phys. Chem. B (2015)[31]
Human corneal fibroblasts	500kDa DxS 100µg/mL CR 75ug/mL	– Similar matrix enhancing effect of DxS and CR – DxS caused some changes in gene expression toward myofibroblast, whereas CR didn't	Kumar et al., Tissue Eng. Part C (2015)[80]
Human MSCs	Ficoll mixture + 10kDa DxS 100µg/mL	– Produced ECM that retained glycosaminoglycans and growth factors and supported hematopoietic stem and progenitor cell expansion	Prewitz et al., Biomaterials (2015)[17]
Organotypic skin culture (human keratinocytes and fibroblasts)	Ficoll mixture	– Improved organotypic coculture with crowding, improved ECM assembly and promoted formation of a collagen VII-rich dermal-epidermal junction	Benny et al., Tissue Eng. Part A (2015)[16]
Human bone-marrow MSCs (bmMSCs)	Ficoll mixture	– Enhanced brown-adipocyte differentiation as well as "browning" of bmMSC-derived white adipocytes, attributed to MMC induced 3D ECM that encapsulated cells	Lee et al., Sci. Rep. (2016)[81]
Human dermal fibroblasts	CR 75µg/mL	– Optimized oxygen tension and serum concentration in culture with CR: 2% oxygen tension and 0.5% serum lead to the most matrix with CR	Satyam et al., Acta. Biomater. (2016)[82]

Human bmMSCs	CR 75µg/mL	– CR enhanced matrix assembly at both 2% and 20% oxygen tension – Matrix gene expression, surface markers, and transcription factors not affected – Differentiation potential was sensitive to oxygen tension and crowding	Cigognini et al., Sci. Rep. (2016)[24]
Human corneal fibroblasts	CR 75µg/mL	– Optimized oxygen tension and serum concentration in culture with CR: 2% oxygen tension and 0.5% serum lead to the most matrix with CR	Kumar et al., J. Tissue Eng. Regen. M. (2017)[25]
Adipose stem cells	Ficoll mixture	– Osteogenesis and adipogenesis enhanced by MMC, chondrogenesis inhibited in medium with human or bovine serum – MMC was not beneficial in xeno-free/serum-free medium	Patrikoski et al., Stem Cells Int. (2017)[83]
Reconstituted porcine kidney matrix	400kDa Ficoll	– Crowding level modulated the fibrillation kinetics and matrix architecture, as well as distribution of ECM components	Magno et al., Acta Biomater. (2017)[84]
Drop-on-demand bioprinting	PVP	– Controlled the architecture of bioprinted collagen hydrogel with PVP, could vary architecture within gel	Ng et al., Biomater. Sci. (2018)[85]
Human chondrocytes	CR 100µg/mL	– Some benefit of MMC in chondrocyte culture, but not as much as other cell types	Graceffa et al., J. Tissue Eng. Regen. M. (2019)[86]
Human dermal fibroblasts	CR Ficoll DxS	– Tested several different cocktails of crowders with different components and molecular weight, found polydispersity and negative charge to be important factors driving matrix assembly	Gaspar et al., Acta Biomater. (2019)[26]

This literature shows that many different cell types enhance ECM production in crowded conditions, and the assembly of many different ECM components is enhanced (Figure 2.10). A number of different crowders have been successfully used to enhance matrix assembly, including the neutral crowders Ficoll, Dextran, and polyvinyl pyrolidone (PVP), and the negatively charged crowders dextran sulfate (DxS), carrageenan (CR), and polysodium-4-styrene sulfonate (PSS). Several different properties of the crowder affect how much matrix is assembled, including the hydrodynamic radius, the charge, and the size distribution (polydispersity). Larger crowders tend to have a stronger effect,

owing to the fact that matrix proteins are also quite large (100s of kDa) and crowders of similar size to the probe molecule tend to have the largest excluded volume effect. Negatively charged crowders enhance matrix assembly much more than neutral crowders, but they also promote the assembly of a granular matrix that does not match the architecture of native matrix as well as that produced in the presence of neutral crowders. Negatively charged crowders also have a stronger effect on collagen assembly than fibronectin assembly, so they tend to change the composition of the matrix compared to that produced with neutral crowders. However, in order for neutral crowders to be effective, they need to have sufficient polydispersity. Dewavrin et al. showed that there is a synergistic effect when crowders of different sizes are mixed together that results in higher volume exclusion than expected from the combined volume of the crowders[31] (see Figure 2.8 above). This has been proven true in the case of Ficoll, which is very effective as a mixture of 70kDa and 400kDa components, but each alone are much less effective[28].

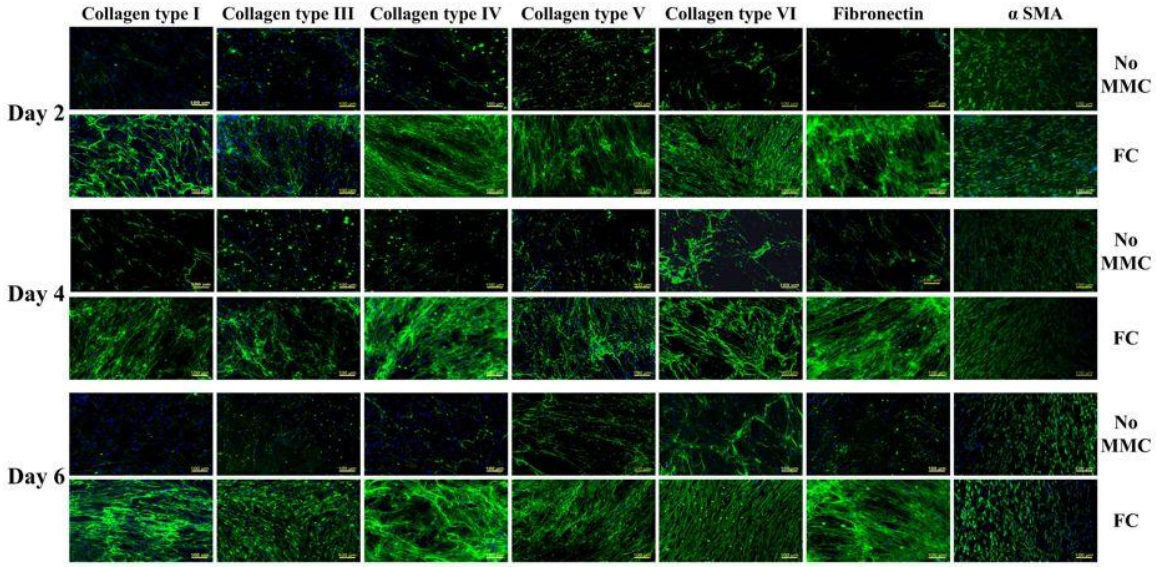

Figure 2.10 Immunocytochemistry images of various matrix components assembled by human corneal fibroblasts in 2 days, 4 days, and 6 days in the absence and presence of a mixture of two molecular weights of Ficoll (37.5mg/mL 70kDa + 25mg/mL 400kDa). 100µL ascorbic acid phosphate was added. The αSMA stain in the last column indicates that no unintended phenotypic change (myofibroblast differentiation) occurred in the presence of crowders. Reprinted from Scientific Reports, vol. 5, no. 1, 8729, Pramod Kumar, Abhigyan Satyam, Xingliang Fan, Estelle Collin, Yury Rochev, Brian J. Rodriguez, Alexander Gorelov, Simon Dillon, Lokesh Joshi, Michael Raghunath, Abhay Pandit, and Dimitrios I. Zeugolis, Macromolecularly crowded in vitro microenvironments accelerate the production of extracellular matrix-rich supramolecular assemblies, Copyright (2015), with permission from Nature Publishing Group[15].

Several different applications for crowding related to its matrix enhancing abilities have been demonstrated. Benny et al. were able to significantly improve the outcome of an organotypic skin co-culture model and were the first to successfully create a collagen VII-rich dermal-epidermal junction *in vitro*, a very important structural component of natural skin[16] (Figure 2.11). Satyam et al.

and Kumar et al. both showed that a matrix reinforced cell-sheet could be generated in the presence of crowding and then released from a temperature responsive polymer substrate, demonstrating the power of crowding to quickly produce tissue substitutes in vitro with enough mechanical integrity to be handled in the clinic[15,22]. Another approach in tissue engineering is the production of scaffolds in a cell-free system that are later seeded with cells. Several studies have demonstrated that crowding can be used to modulate the architecture of a scaffold by altering the rate of fiber nucleation and growth. Dewavrin et al. showed this in collagen cell formation[30] and Magno et al. showed this for reconstitution of procine kidney matrix[84]. Ng et al. demonstrated how this could be harnessed to spatially control the architecture of a matrix produced by drop-on-demand bioprinting to produce a structurally complex scaffold[85]. Recent efforts to optimize matrix assembly in the presence of crowding have shown that serum level and oxygen tension are important factors impacting the amount of matrix produced. A serum level of 0.5% and an oxygen tension of 2% have been found to be optimal for matrix assembly by human corneal and dermal fibroblasts[25,82].

A different but related application for the matrix enhancing power of crowding is the development of an *in vitro* fibrosis model to screen antifibrotic compounds[20]. Similarly, Ranamukhaarachchi et al. recently showed how crowding could be used in an *in vitro* cancer model to alter collagen gel architecture and study the impact of confinement on tumor cell invasive behavior[87].

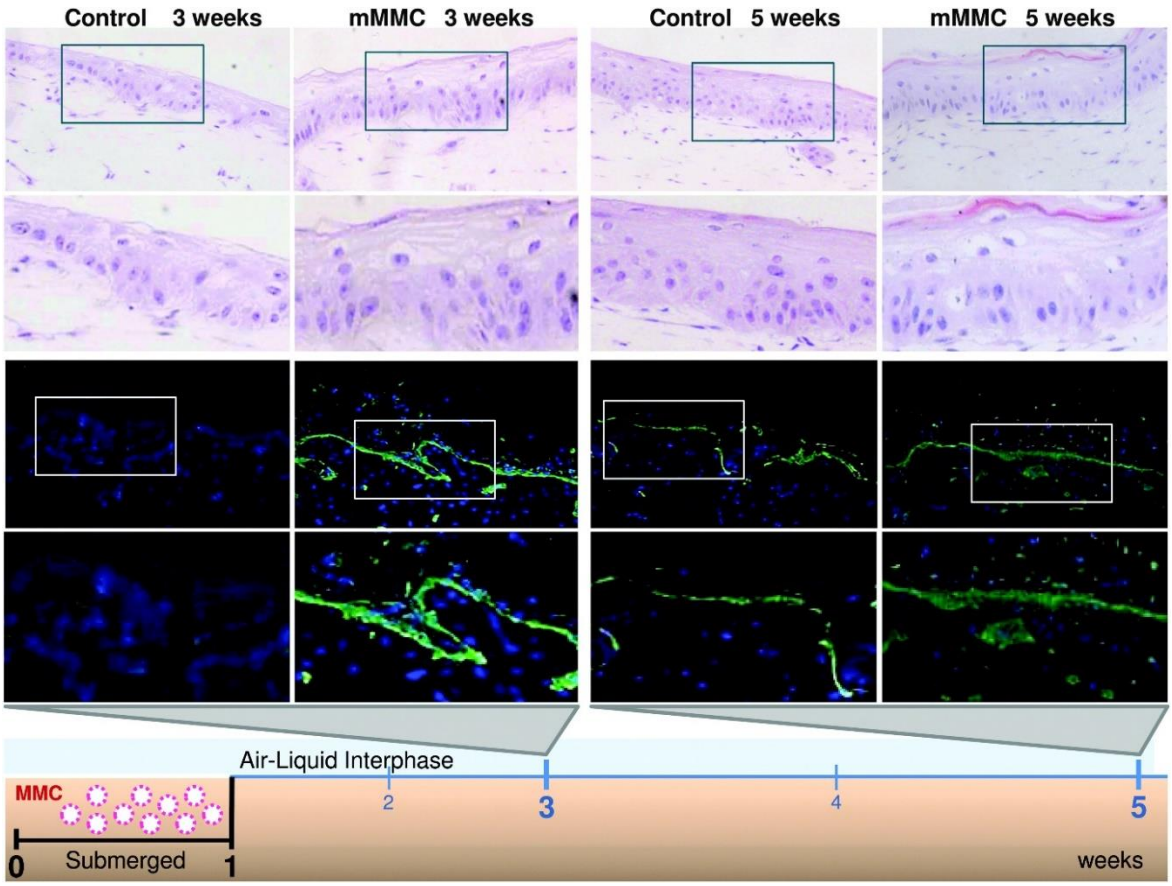

Figure 2.11 Ficoll mixture enhanced the formation of a collagen VII-rich dermal-epidermal junction (DEJ) in an organotypic skin co-culture. Keratinocytes were seeded on top of a collagen gel containing skin fibroblasts. The co-culture was submerged for 1 week and then cultured further at the air-liquid interface for a total of 3 weeks and 5 weeks. The presence of the crowder Ficoll lead to appearance of a collagen VII-rich DEJ already by 3 weeks, when none was present in control. After 5 weeks there was a collagen VII-rich DEJ in control, but it was more developed in the presence of Ficoll. The first set of images is hematoxylin and eosin staining. The second set of images is immunofluorescence with collagen VII in green and nuclei in blue. Reprinted from Tissue Engineering Part A, vol. 21, no. 1-2, 183-192, Paula Benny, Cedric Badowski, E. Birgitte Lane, and Michael Raghunath, Making More Matrix: Enhancing the Deposition of Dermal–Epidermal Junction Components In Vitro and Accelerating Organotypic Skin Culture Development, Using Macromolecular Crowding, Copyright (2015), with permission from Mary Ann Liebert, Inc.[16]

Also important to tissue engineering is the propagation and differentiation of stem cells, and crowding has also proven very useful in this area. Several studies have shown that crowding enhances chemically induced differentiation of mesenchymal stem cells (MSCs) towards osteogenic and adipogenic lineages[14,83]. Interestingly, it does not improve chondrogenic differentiation. Lee et al. showed that crowding induced spontaneous conversion of bone marrow MSC-derived white adipocytes to brown adipocytes, and this was attributed to the production of a 3D encapsulating ECM that promoted enhanced cell-matrix engagement[81]. Additionally, Peng et al. showed that matrix

produced in the presence of crowding supported better propagation of human embryonic stem cells and more stable cell phenotype compared to matrigel[77]. Similarly, Prewitz et al. showed that matrix produced with crowding supported expansion of hematopoietic stem and progenitor cells[17].

Though most of the research has focused on the impact of crowding on the ECM, there have been some reports of cellular effects. Generally, crowding is understood to be tolerated very well by cells, as evidenced by stable or increased proliferation and no metabolic effects[15,79,82]. Some studies have mentioned feedback from changes in ECM that result in changes in cell phenotype as well. For instance, increased adhesion strength and cytoskeleton alignment with the crowding induced ECM[12]. Importantly, several studies have shown that crowding results in more stable phenotype of cells over long-term cell culture. For example corneal fibroblasts, which are known to differentiate into myofibroblasts *in vitro*, were able to produce a tissue substitute that could be released from temperature-responsive polymer in 6 days without any increase in α-smooth muscle actin expression[15]. Interestingly, studies have shown that even though there is much more matrix assembled in the presence of crowding, there is no increase in ECM gene expression[15,24,80]. Often there is even a decrease due to negative feedback from the enhanced matrix assembly. This further drives home the idea that crowding impacts matrix assembly through thermodynamic changes in the medium rather than changes in cell phenotype.

Even though crowding has been successful at enhancing matrix in many different situations, there are some cases where crowding has been unsuccessful. Chen et al. tried to use crowding to enhance cartilage formation by porcine chondrocytes and found that even though matrix assembly in 2D was enhanced, when applied to a 3D model of chondrocytes in a matrix of polylactic acid-coated polyglycolic acid fibers, crowding was actually detrimental to tissue formation[78]. This finding and the fact that chondrogenic differentiation of MSCs is not improved by crowding show that cartilage is an area where the benefits of crowding have not been easy to realize. Patrikoski et al. recently found that crowding does not work well to enhance ECM assembly in xeno-free/serum-free medium[83]. This is a very important topic for clinical translation and something that will need to be addressed in the future. Importantly, though, crowding is successful in medium with human serum.

2.6. Mechanistic explanations how crowding enhances matrix assembly

Collagen I has been the primary focus of much of the crowding literature related to tissue engineering, and, consequently, the mechanistic understandings regarding how crowding enhances ECM assembly all involve collagen I assembly. Bateman et al. already showed in 1986 that crowding increases the rate of procollagen cleavage through the enhanced interaction of procollagen and procollagen proteinases[1], and this finding has been confirmed by studies both in cell culture and in a cell-free assay[1,2,20,21,27–29]. More recent studies have shown that crowding also increases association of collagen molecules with one another, leading to enhanced supramolecular assembly[2,30,31]. In an uncrowded medium, there is a lot of soluble procollagen but the rate of cleavage and fiber formation are both very slow so there is very little matrix in the cell layer. In a crowded medium, on the other hand, the increase in procollagen processing and supramolecular assembly result in conversion of unprocessed procollagen in the media to matrix fibers in the cell layer[1,11,12,21,28,29,88] (Figure 2.12). In a cell-free solution of collagen monomers, this increased assembly occurs through an increased rate of both fiber nucleation and growth[30], but whether crowding also increases collagen fiber nucleation in cell-culture where fibronectin and collagen V are involved has not been studied. Results have also shown that crowding increases crosslinking of collagen by transglutaminase 2 and lysyl oxidase[1,2]. Lastly, matrix metalloproteinase 2 activity was shown to be reduced by a fragment produced by the activation of procollagen C proteinase enhancer 1, which is enhanced in crowded conditions[21,32].

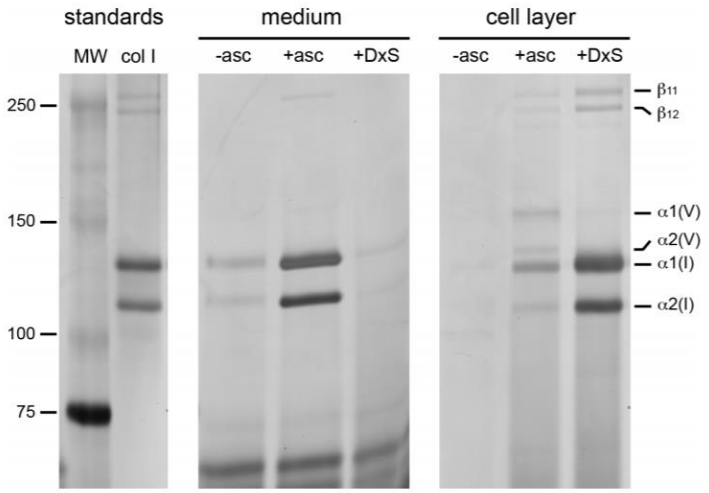

Figure 2.12 SDS-PAGE gel of collagen in the medium and cell layer showing that crowding results in conversion of soluble collagen into insoluble collagen in the cell layer. –asc refers to control without ascorbic acid in which there is very little collagen. With the addition of ascorbic acid (+asc) there is a lot of collagen released to the media, but very little has been converted into matrix. This represents the low efficiency matrix assembly in the uncrowded environment. Then, upon addition of 100µg/mL 500kDa DxS (+DxS), the collagen is no longer in the media but rather in the cell layer. Nearly all collagen was converted from soluble form to matrix in response to DxS. Reprinted from Tissue Engineering, vol. 13, no. 2, Ricky R. Lareu, Irma Arsianti, Harve Karthik Subramhanya, Peng Yanxian, and Michael Raghunath, In vitro enhancement of collagen matrix formation and crosslinking for applications in tissue engineering: a preliminary study, Copyright (2007), with permission from Mary Ann Liebert, Inc., New Rochelle, NY[29].

3. Matrix assembly in response to treatment with different crowding agents

In this chapter we present our investigation of the time course of matrix assembly by human dermal fibroblasts in response to treatment with the neutral crowding agent Ficoll, with particular attention given to the spatial correlation of fibronectin and collagen I. Then we present a comparison of the matrix assembly in response to several different crowding agents.

These experiments were planned by Jenna Graham (JG) and Prof. Dr. Viola Vogel (VV). JG conducted the experiments and analyzed the data. Dr. Jens Möller helped with time lapse microscopy of fibronectin harvesting. JG, VV, and Prof. Dr. Michael Raghunath (MR) discussed the data and wrote the text (exerpt from manuscript).

3.1. Ficoll increases assembly of fibronectin and collagen I fibers in the first 16 hours and they are colocalized

To take a close look at the impact of crowding on the early phases of ECM assembly, and particularly the interaction between fibronectin and collagen I, we cultured primary human dermal fibroblasts in the absence or presence of the standard Ficoll mixture (37.5mg/mL 70kDa + 25mg/mL 400kDa, GE Healthcare). Before adding fibroblasts, we adsorbed human plasma fibronectin to the glass substrate (50µg/mL, 1 hour). It was previously shown that fibroblasts harvest fibronectin from the substrate surface and incorporate it into fibers, along with soluble plasma fibronectin from serum and their own cell produced cellular fibronectin[89,90], as also observed here (Figure 3.1). Note that we observed the cells to stop scraping off fibronectin from the surface while rounding up and going through a cell division, as can be seen in the last frame of Figure 3.1. We then sparsely seeded fibroblasts at 5,000 cells/cm^2 and allowed them to adhere for 1 hour. We chose to start with a very low cell seeding density to allow for better visualization of the interaction of fibroblasts with the fibronectin coating and early matrix assembly. Next, the media were exchanged and fibroblasts were exposed to Ficoll (+Ficoll) or cultured in standard medium without crowders (-Ficoll). In both cases, 50µg/mL of human plasma fibronectin and 100µM L-ascorbic acid 2-phosphate were supplemented to the cell culture media to promote matrix assembly. A small portion (10%) of the fibronectin supplemented to the media and in the coating was fluorescently labeled (Alexa-647) to enable its visualization. Significant matrix assembly took place during the first 16 hours, both in the absence and presence of Ficoll (Figure 3.2A-B). Early fibronectin and collagen I fibers were colocalized in both conditions, as shown by the intensity linescans in Figure 3.2A-B. Ficoll did not have an impact on cell density after 16 hours (Figure 3.2C). Quantification of fibronectin and collagen I by summing the respective fluorescent pixel intensities showed that there was already more of both matrix proteins with Ficoll treatment after only 16 hours (Figure 3.2D-E). Notably, the effect of Ficoll on fibronectin deposition was stronger than on collagen I (1.9x vs 1.7x, respectively). Additionally, the fibronectin matrix assembled with Ficoll covered approximately twice the area of that assembled without Ficoll (2.1x, Figure 3.2F). Respective greyscale images of each channel can be found in Figure 3.3.

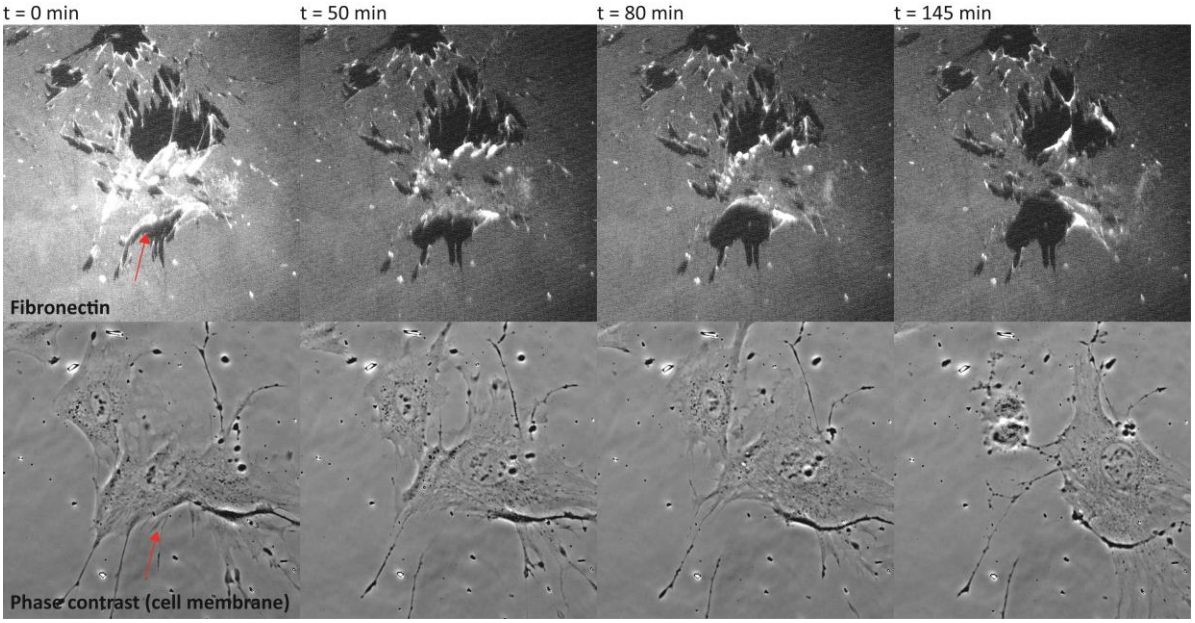

Figure 3.1 Series of images from a time-lapse widefield microscopy movie showing how fibroblasts scrape off an adsorbed fibronectin coating. The top row is Alexa-647 fibronectin and the bottom row is the corresponding phase contrast image showing cell membranes. The red arrow in the first image indicates an area where fibronectin will be scraped off by the cell. Note that cells stop scraping off fibronectin from the surface while rounding up and going through a cell division, as can be seen in the last frame.

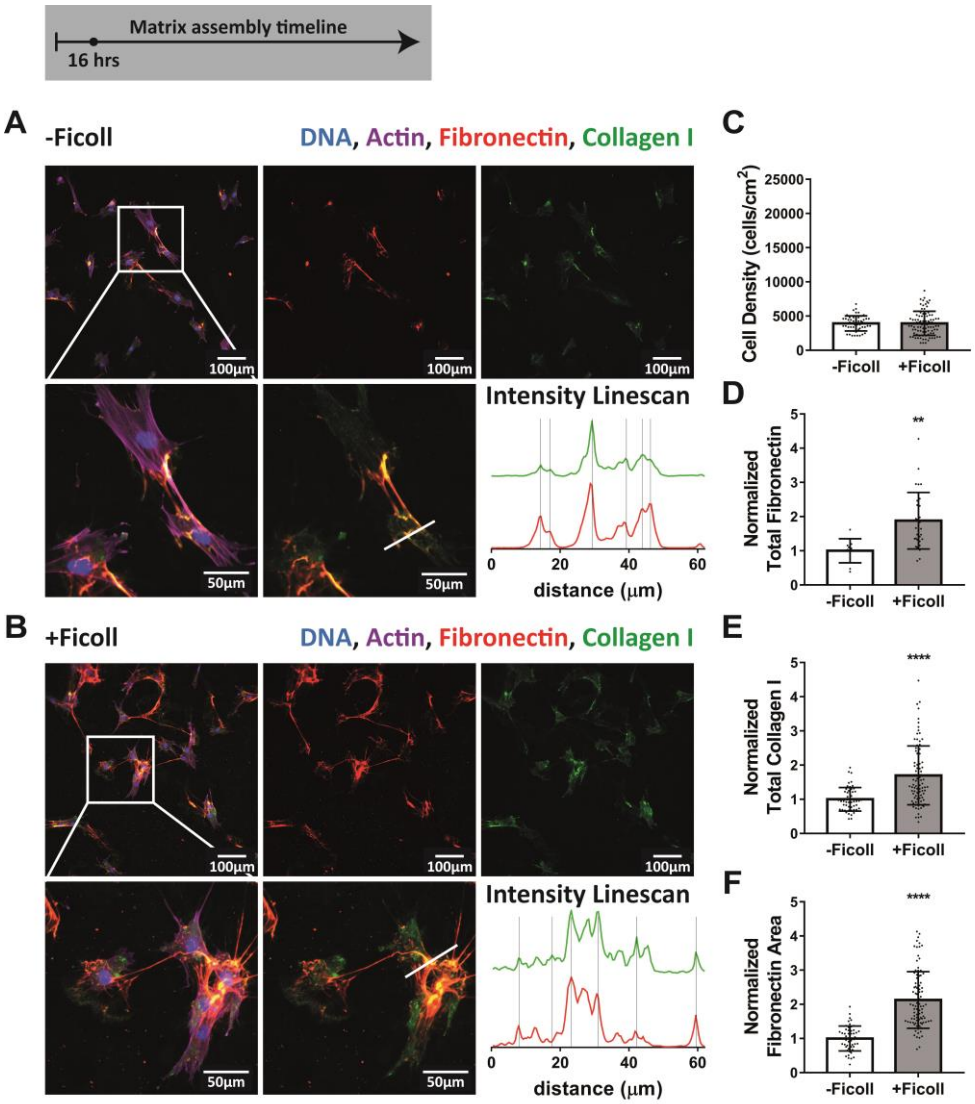

*Figure 3.2 Ficoll supplementation accelerates ECM assembly within the first 16 hours and fibronectin and collagen I are colocalized. (A) ECM assembled without Ficoll. The first row shows a widefield fluorescence image of fibroblasts and matrix followed by images of Alexa-647-labeled fibronectin and antibody-stained collagen I alone. The second row shows a magnified area of the image above, followed by an image of matrix only and intensity linescans of fibronectin and collagen I along the white line indicated in the matrix only image. (B) ECM assembled with Ficoll mixture (37.5mg/mL 70kDa Ficoll + 25mg/mL 400kDa). (C) Cell density. (D) Summed intensity of Alexa-647-labeled fibronectin. (E) Summed intensity of antibody-stained collagen I. (F) Area of substrate covered by fibronectin fibers as quantified using a threshold set to distinguish fibers from background and coating. 30-100 images were analyzed for each condition (10 for Total Fibronectin in -Ficoll condition). D-F show values normalized to the mean without Ficoll. Glass substrates preadsorbed with 50μg/mL plasma fibronectin (10% Alexa-647-labeled). Cells cultured in MEM Alpha supplemented with 10% fetal bovine serum, 1% penicillin-streptomycin, 100μM L-ascorbic acid 2-phosphate, and 50μg/mL plasma fibronectin (10% Alexa-647-labeled). ** indicates p<0.01, **** indicates p<0.0001.*

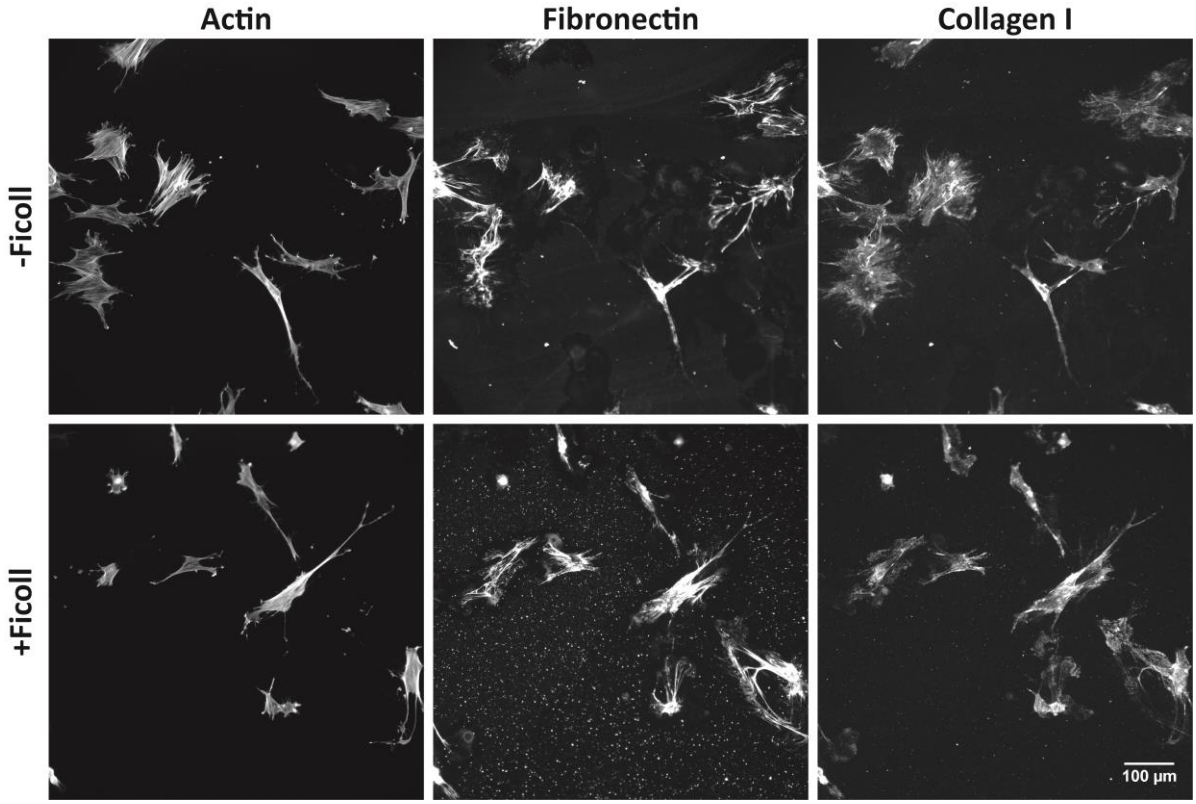

Figure 3.3 Widefield greyscale images captured with a 20x objective of cells and matrix assembled in 16 hours +/-Ficoll (37.5mg/mL 70kDa + 25mg/mL 400kDa). Glass substrates preadsorbed with 50µg/mL plasma fibronectin (10% Alexa-647-labeled). Cells cultured in MEM Alpha supplemented with 10% fetal bovine serum, 1% penicillin-streptomycin, 100µM L-ascorbic acid 2-phosphate, and 50µg/mL plasma fibronectin (10% Alexa-647-labeled). Images are from the same data set as shown in Figure 3.2.

3.2. Collagen I fibers mostly continue to colocalize with fibronectin fibers after 2 days of Ficoll exposure

Assembly of fibronectin and collagen I fibers remained enhanced under Ficoll treatment as fibroblasts were cultured for 2 days with respect to the control (Figure 3.4). Importantly, as matrix assembly progressed, collagen I was still colocalized with fibronectin during the first few days, as shown by the intensity line scans in Figure 3.4A-B. Cell density had more than doubled since 16 hours and was still not impacted by Ficoll (Figure 3.4C). Quantification of matrix proteins showed that Ficoll increased fibronectin fiber assembly more than collagen I also at this time point (2.6x vs 1.8x, Figure 3.4D-E). Ficoll induced fibronectin matrix covered about twice the area compared to control without Ficoll (Figure 3.4F). Respective greyscale images of each channel can be found in Figure 3.5.

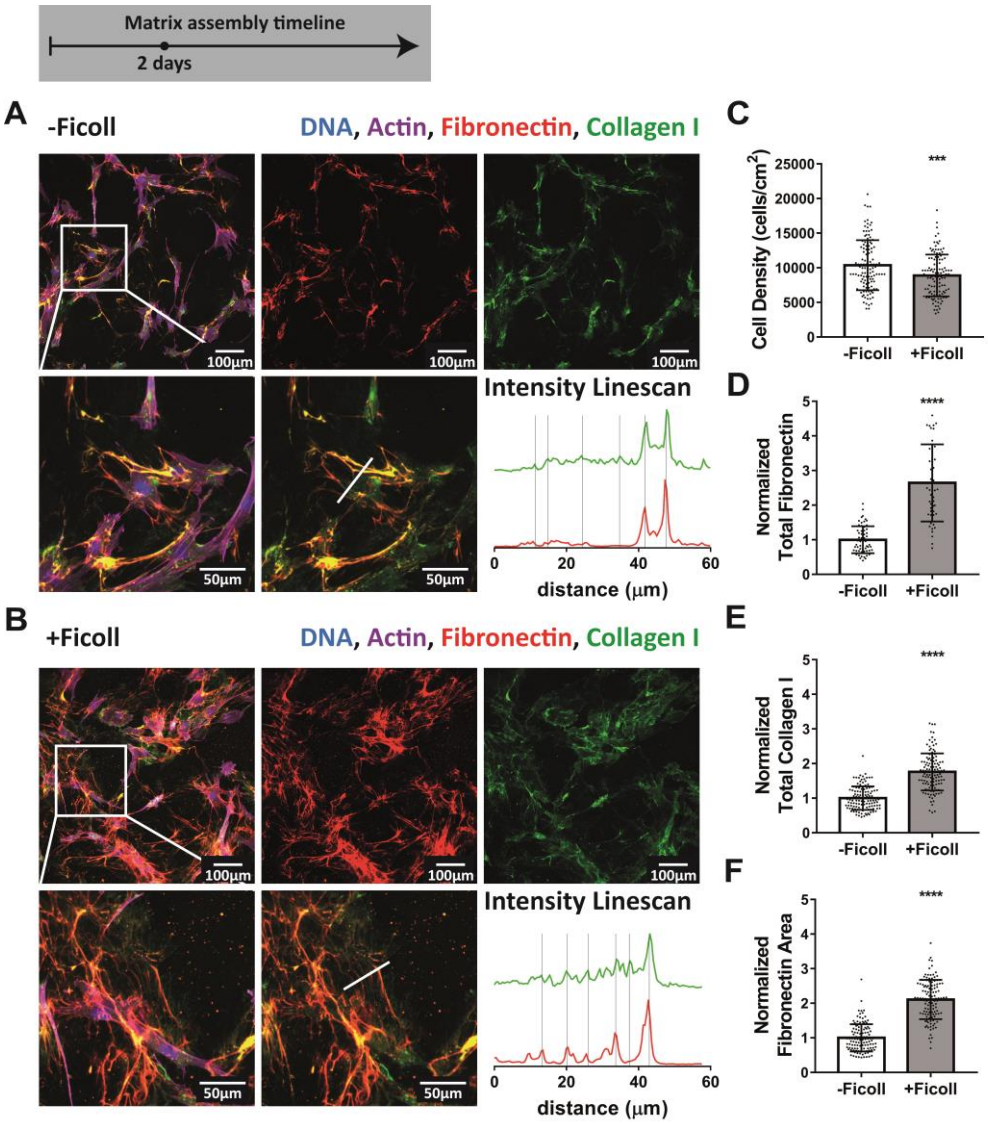

*Figure 3.4 Ficoll treatment continues to accelerate assembly of fibronectin and collagen I throughout 2 days and they are still mostly colocalized. (A) ECM assembled without Ficoll. The first row shows a widefield fluorescence image of fibroblasts and matrix followed by images of Alexa-647-labeled fibronectin and antibody-stained collagen I alone. The second row shows a magnified area of the image above, followed by an image of matrix only and intensity linescans of fibronectin and collagen I along the white line indicated in the matrix only image. (B) ECM assembled with Ficoll. (C) Cell density. (D) Summed intensity of Alexa-647-labeled fibronectin. (E) Summed intensity of antibody-stained collagen I. (F) Area of substrate covered by fibronectin fibers as quantified using a threshold set to distinguish fibers from background and coating. 50-120 images were analyzed for each condition. D-F show values normalized to the mean without Ficoll. Glass substrates preadsorbed with 50μg/mL plasma fibronectin (10% Alexa-647-labeled). Cells cultured in MEM Alpha supplemented with 10% fetal bovine serum, 1% penicillin-streptomycin, 100μM L-ascorbic acid 2-phosphate, and 50μg/mL plasma fibronectin (10% Alexa-647-labeled). *** indicates p<0.001, **** indicates p<0.0001.*

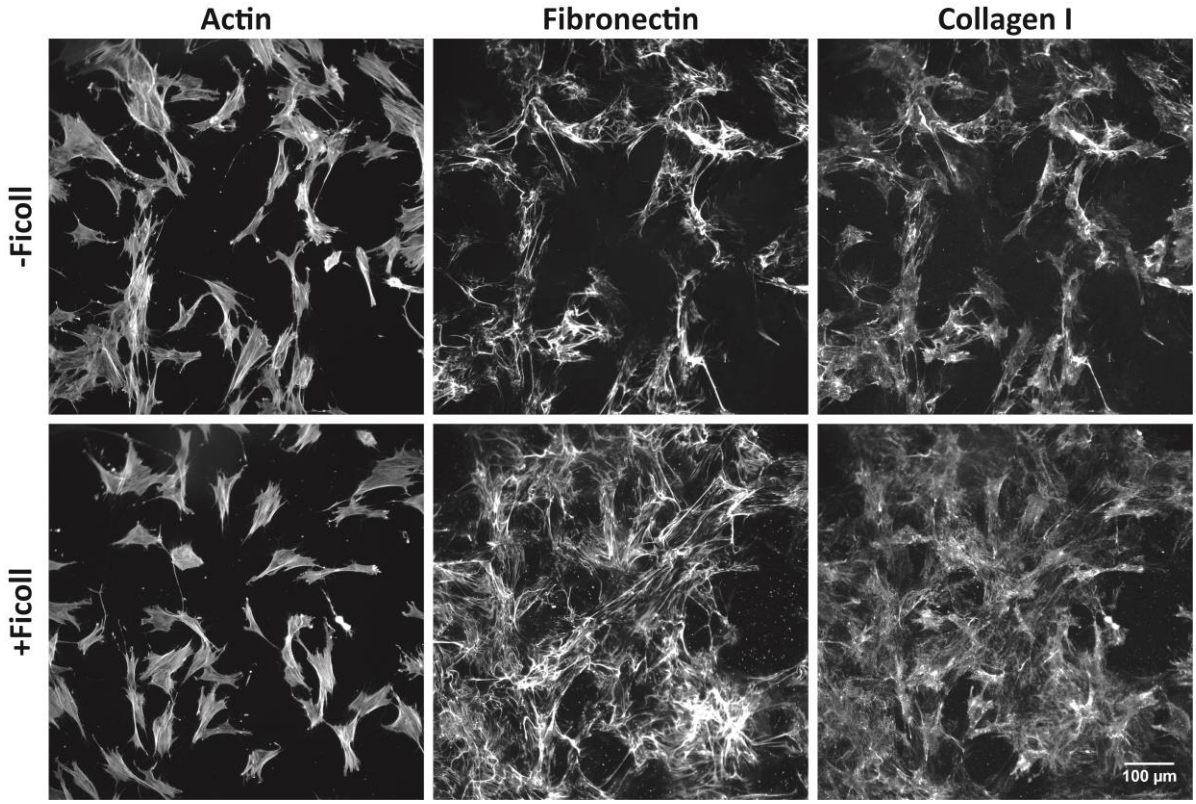

Figure 3.5 Widefield greyscale images captured with a 20x objective of cells and matrix assembled in 2 days +/-Ficoll (37.5mg/mL 70kDa + 25mg/mL 400kDa). Glass substrates preadsorbed with 50µg/mL plasma fibronectin (10% Alexa-647-labeled). Cells cultured in MEM Alpha supplemented with 10% fetal bovine serum, 1% penicillin-streptomycin, 100µM L-ascorbic acid 2-phosphate, and 50µg/mL plasma fibronectin (10% Alexa-647-labeled). Images are from the same data set as shown in Figure 3.4.

3.3. A dense matrix was assembled in 6 days both with and without Ficoll

To ask how effective Ficoll treatment is during the early versus late phases of cell culture, we continued the experiment further to six days, at which point the fibroblasts had reached confluence and developed a very dense matrix (Figure 3.6A-B). The collagen I fibers showing the brightest immunolabel signal were still generally in close proximity to the fibronectin fibers, both with and without Ficoll, as can be appreciated in the z-stack shown in Figure 3.7. However, the depth and density of the matrix made it difficult to determine if collagen I was still strictly co-localized with fibronectin. Previous studies suggest that, by this time point, collagen I fibers have become increasingly interconnected and are no longer restricted to the fibronectin template[47]. After 6 days, fibroblasts had reached a confluent state and the cell density was the same with and without Ficoll (Figure 3.6C). Quantification of fibronectin and collagen I showed that matrix assembly in non-Ficoll treated samples caught up significantly and the differences with Ficoll were quite small compared to earlier time points (Figure 3.6D-E). Respective greyscale images of each channel can be found in Figure 3.8.

Taken together, this time series from 16 hours to 6 days highlights the fact that Ficoll substantially accelerated the early matrix assembly process, while its effect evened out by 6 days when non-Ficoll-treated cultures caught up in terms of matrix assembly. Figure 3.9 shows that the results were the same when fibronectin was quantified not by Alexa-647-labeling of plasma fibronectin, but by antibody staining, as is standard in the field.

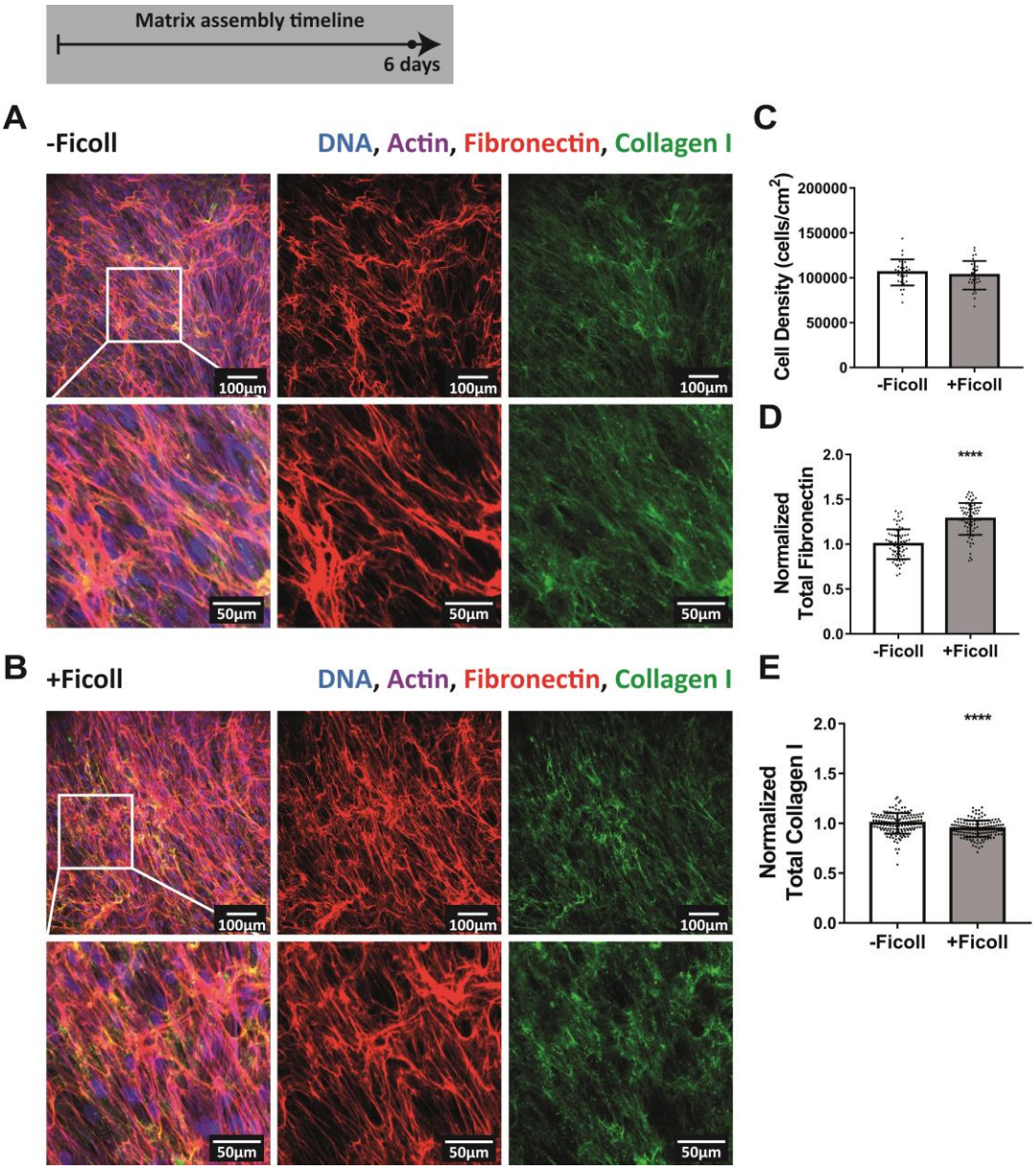

*Figure 3.6 Extracellular matrix assembly after 6 days with and without Ficoll. (A) ECM assembled without Ficoll. The first row shows a widefield fluorescence image of fibroblasts and matrix followed by images of Alexa-647-labeled fibronectin and antibody-stained collagen I alone. The second row shows a magnified area of the image above: first cells and matrix, followed by images of fibronectin and collagen I alone. (B) ECM assembled with Ficoll. (C) Cell density. (D) Summed intensity of Alexa-647-labeled fibronectin. (E) Summed intensity of antibody-stained collagen I. 70-150 images were analyzed for each condition (30 images analyzed for cell density). D-E show values normalized to the mean without Ficoll. Glass substrates preadsorbed with 50µg/mL plasma fibronectin (10% Alexa-647-labeled). Cells cultured in MEM Alpha supplemented with 10% fetal bovine serum, 1% penicillin-streptomycin, 100µM L-ascorbic acid 2-phosphate, and 50µg/mL plasma fibronectin (10% Alexa-647-labeled). **** indicates p<0.0001.*

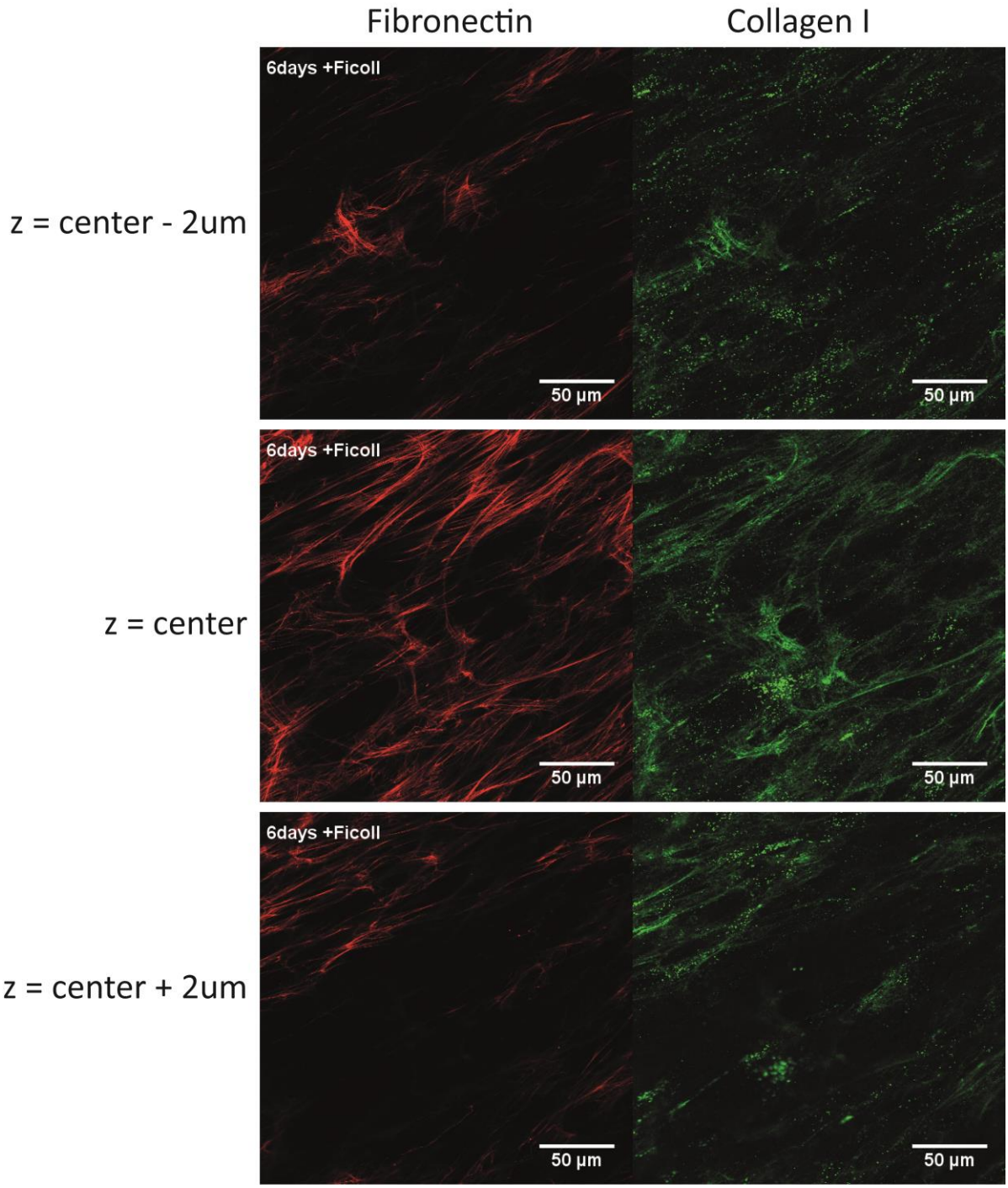

Figure 3.7 Confocal z-stack of 6-day matrix assembled in the presence of Ficoll.

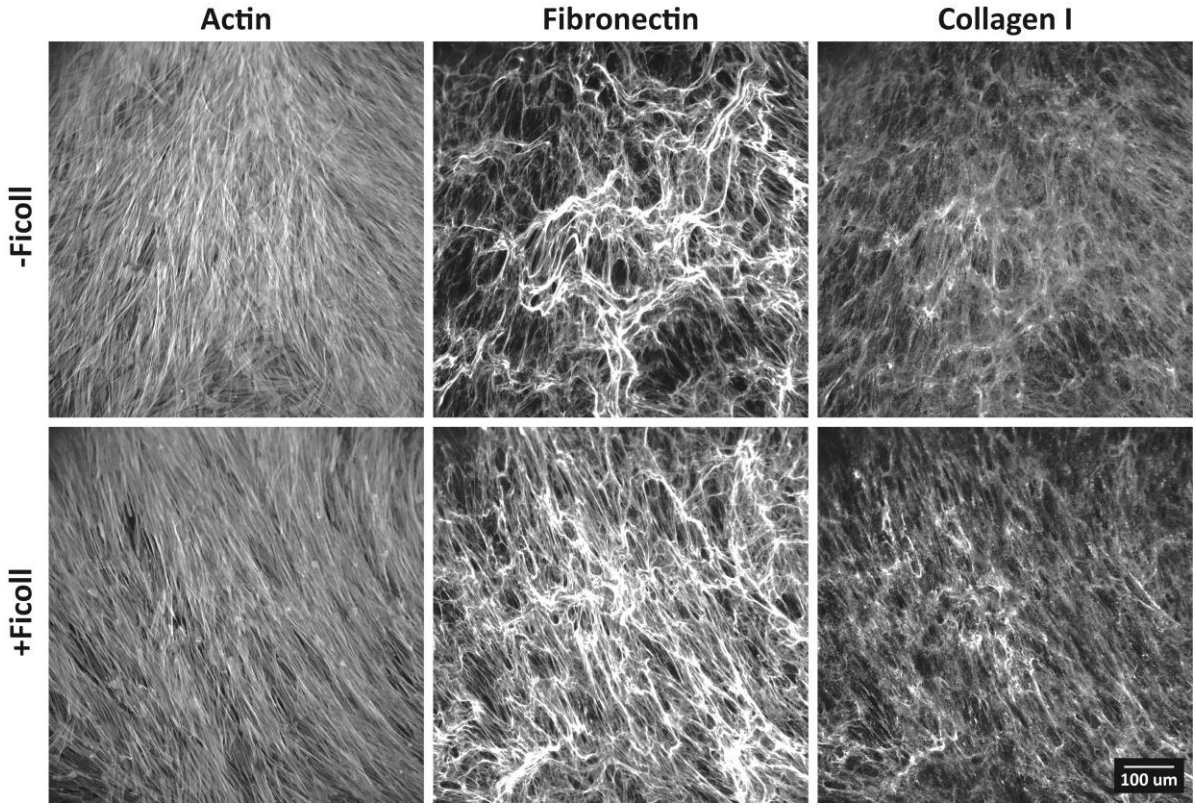

Figure 3.8 Widefield greyscale images captured with a 20x objective of cells and matrix assembled in 6 days +/-Ficoll (37.5mg/mL 70kDa + 25mg/mL 400kDa). Glass substrates preadsorbed with 50µg/mL plasma fibronectin (10% Alexa-647-labeled). Cells cultured in MEM Alpha supplemented with 10% fetal bovine serum, 1% penicillin-streptomycin, 100µM L-ascorbic acid 2-phosphate, and 50µg/mL plasma fibronectin (10% Alexa-647-labeled). Images are from the same data set as shown in Figure 3.6.

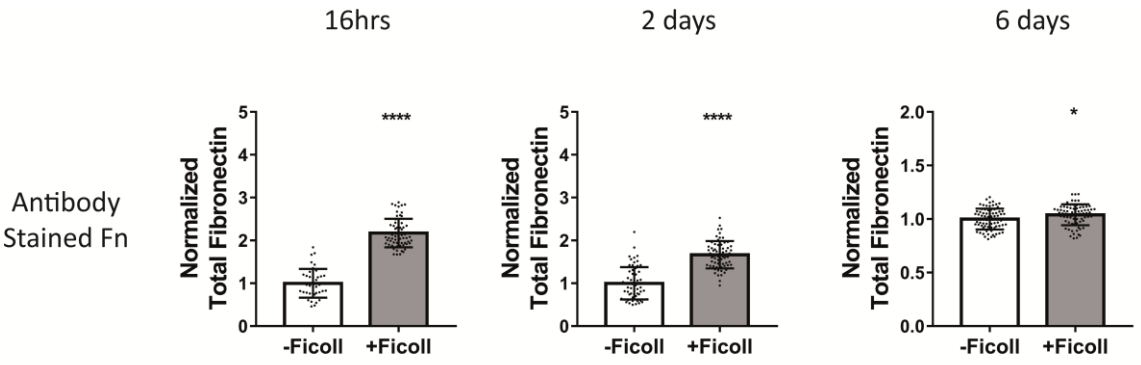

*Figure 3.9 Fibronectin matrix assembly quantified by antibody staining. Reported values are the summed intensity of fibronectin fluorescence signal, normalized to the average in -Ficoll control. * indicates p<0.05, **** indicates p<0.0001*

3.4. Comparison of different crowding agents

In order to get a better idea of how crowding impacts matrix assembly, we also compared different crowding agents. We looked at several crowders that are commonly used in the tissue engineering field: the neutral crowders Dextran and PVP, and negatively charged carageenan (CR). Figure 3.10 shows images of matrix assembled in 48 hours. In this case the cells were allowed to adhere to glass preadsorbed with fibronectin for 24 hours before media was changed and crowders were added, so the matrix is one day older than what was shown previously (Figure 3.4 and 3.5), but the amount of time exposed to crowders is the same. Interestingly, we notice that these early matricies were quite different depending on the crowder used. The carrageenan matrix had much more collagen than the others, as expected based on literature[26]. This collagen was quite granular, also as expected. In the samples treated with Dextran, it appears as though there was more coating that had not been disturbed compared to Ficoll treated samples. We also noticed that all samples treated with PVP showed a colocalization of matrix with cells and a lack of matrix in the space between cells. This is quite different from what we have seen with Ficoll, where the matrix was well distributed around the glass surface. Both of these results suggest altered harvesting of the coating with different crowders compared to Ficoll: less harvesting with Dextran and more with PVP. The PVP result could also mean that the cell adhesion to fibronectin is stronger so they carry it with them instead of leaving it on the surface. We cannot say for sure from this data. Quantification of cell density showed that all crowders caused a mild increase in proliferation, except for 40kDa PVP which showed no change. Quantification of collagen I showed that the standard Ficoll mixture had the strongest enhancing effect of neutral crowders on collagen I assembly. This experiment was only completed once and would need to be repeated to draw concrete conclusions, but it suggests that not all crowders affect matrix assembly the same and points to Ficoll as the best choice among neutral crowders to increase collagen I assembly. We continued with Ficoll for the remainder of this work.

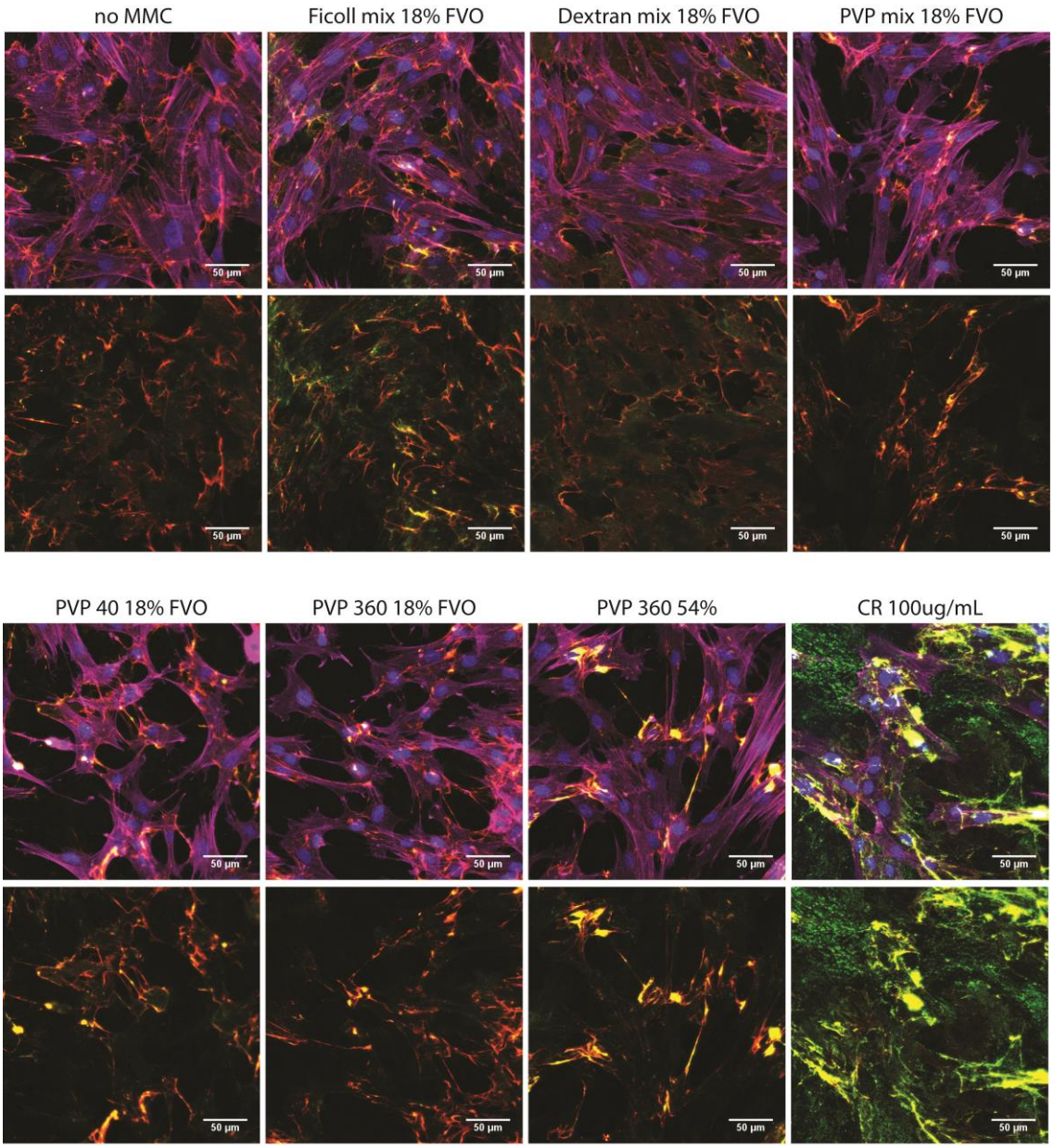
no MMC
Ficoll mix 18% FVO
Dextran mix 18% FVO
PVP mix 18% FVO
PVP 40 18% FVO
PVP 360 18% FVO
PVP 360 54%
CR 100ug/mL
50 µm

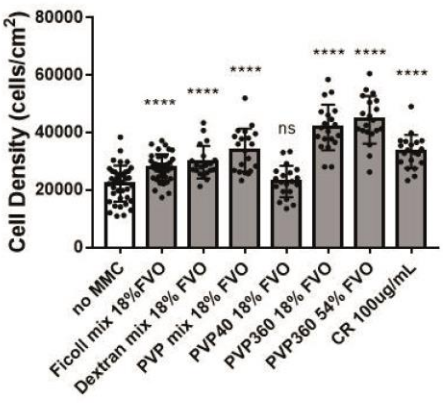
Cell Density (cells/cm2)
80000
60000
40000
20000
0
****
ns
no MMC
Ficoll mix 18%FVO
Dextran mix 18% FVO
PVP mix 18% FVO
PVP40 18% FVO
PVP360 18% FVO
PVP360 54% FVO
CR 100ug/mL

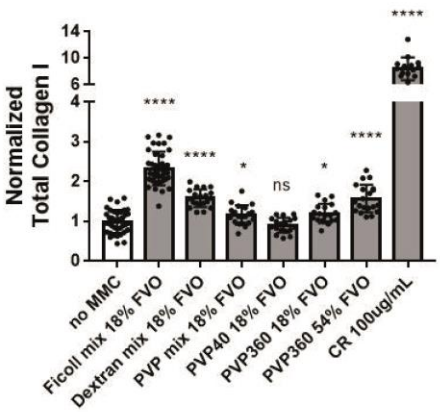
Normalized Total Collagen I
14
10
6
4
3
2
1
0
****
*
ns
no MMC
Ficoll mix 18% FVO
Dextran mix 18% FVO
PVP mix 18% FVO
PVP40 18% FVO
PVP360 18% FVO
PVP360 54% FVO
CR 100ug/mL

*Figure 3.10 Matrix assembled in 48 hours on glass preadsorbed with fibronectin (after 24 hour adhesion period) in the presence of different crowding agents. Ficoll mix 18% FVO refers to the standard mixture of Ficoll (37.5mg/mL 70kDa + 25mg/mL 400kDa). Dextran mix 18% FVO: 9.13mg/mL 70kDa + 4.44mg/mL 500kDa neutral Dextran. PVP mix 18% FVO: 10.75mg/mL 40kDa + 1.89 mg/mL 360kDa PVP. PVP40 18% FVO: 21.5mg/mL 40kDa PVP. PVP360 18% FVO: 3.78mg/mL 360kDa PVP. PVP360 54% FVO: 11.34mg/mL 360kDa PVP. CR 100µg/mL. Cell density and collagen assembly were quantified. Cell seeding density was 5,000 cells/cm^2. * indicates p<0.1, **** indicated p<0.0001.*

4. Increased fibronectin assembly is not attributable to changes in the mechanical functions of fibroblasts

In this chapter we present a screening of different mechanosensitive cell and nuclear markers looking for a change in mechanical cell behavior that might explain the increase in fibronectin assembly in the presence of Ficoll.

These experiments were planned by JG and VV, Dr. Nikhil Jain (NJ), and Dr. Lina Aires (LA). JG conducted the experiments and analyzed the data. NJ and LA helped with staining protocols for nuclear markers. JG, VV, and MR discussed the data and wrote the text (excerpt from manuscript).

Given that fibronectin fibrillogenesis depends on traction forces, we next asked whether Ficoll upregulates cell contractility or any other cell functions related to matrix assembly. We cultured cells as before, except without fibronectin supplementation since this is not standard in the field, and analyzed them after 24 hours exposure to Ficoll. We measured cell spreading area and found no change with Ficoll (Figure 4.1A). We then measured phosphorylation of focal adhesion kinase (pFAK), which is downstream of integrin ligation[91], and found that this was also not changed by Ficoll treatment (Figure 4.1B). We then assessed cell contractility by measuring the phosphorylation of myosin light chain 2 (p-MLC2), which was unchanged (Figure 4.1C), as well as the amount of filamentous actin (F-actin) per cell, which increases with cell traction forces, and also remained unchanged (Figure 4.1D). Fibroblasts could also have increased migration and/or membrane activity that results in increased harvesting of the fibronectin coating. We estimated the area of coating harvested per cell by dividing the total area per image where the fibronectin coating had been removed by the number of cells in that image. This was also unchanged with Ficoll (Figure 4.1E). We then measured several nuclear markers that are known to be sensitive to mechanical interactions of cells with their environment. We found no changes in the ratio of lamin A to lamin B, the nuclear-to-cytoplasmic ratio of transcription factors yes-associated protein (YAP) and myocardin-related transcription factor-A (MRTF-A), or the histone markers acetylation of histone 3 at lysine 9 (H3K9Ac) and trimethylation of histone 3 at lysine 27 (H3K27me3) (Figure 4.1F-J). Taken together, these results show that there were no apparent changes in cell behavior that could explain the increased fibronectin fiber assembly with Ficoll.

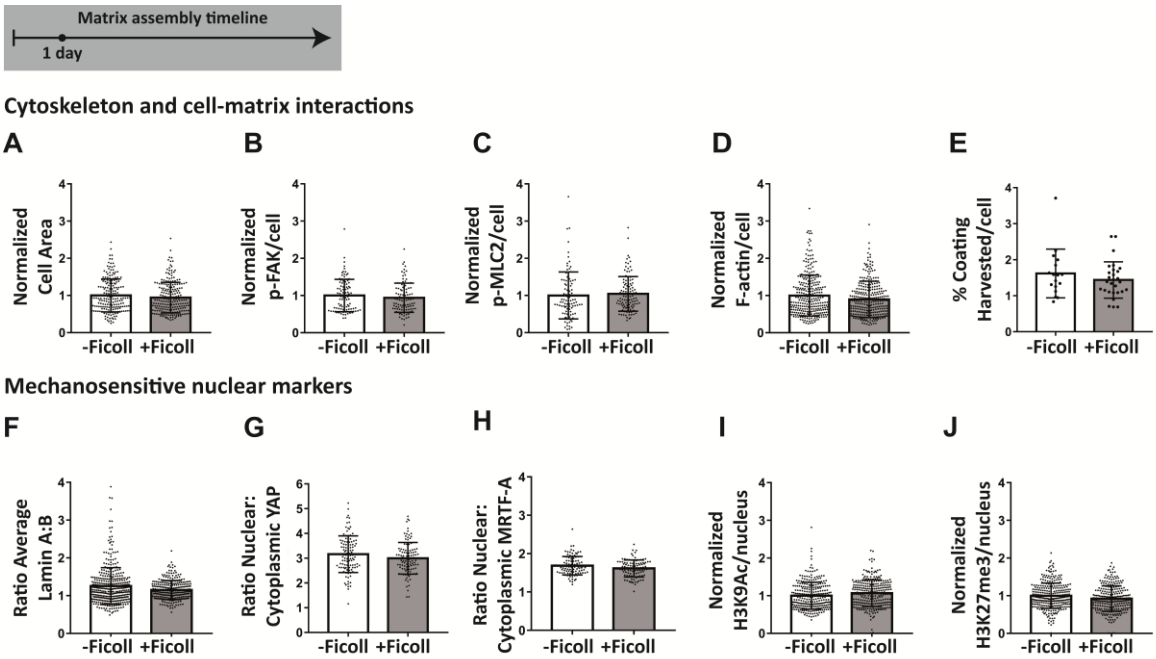

Figure 4.1 Ficoll has no major effect on vital cell mechanical functions. Protein levels were assessed at the single cell level by immunofluorescence microscopy after 24 hours of Ficoll treatment compared to control. (A) Cell area. (B) Summed intensity of phosphorylated focal adhesion kinase per cell. (C) Summed intensity of phosphorylated myosin light chain 2 per cell. (D) Summed intensity of filamentous actin per cell. (E) Percent of image field of view with fibronectin coating removed, divided by the number of cells in the image. Approximately 20 images analyzed per condition. (F) Ratio of average intensity of lamin A to lamin B. (G) Ratio of average intensity of yes-associated protein in the nucleus to the cytoplasm. (H) Ratio of average intensity of myocardin-related transcription factor-A in the nucleus to the cytoplasm. (I) Summed intensity of acetylation of histone 3 at lysine 9 in the nucleus. (J) Summed intensity of trimethylation of histone 3 at lysine 27 in the nucleus. For A-D and F-J, each data point represents one cell. At least 100 individual cells were analyzed per condition. All values except ratios were normalized to the average without Ficoll. Glass substrates preadsorbed with 50µg/mL unlabeled plasma fibronectin. Cells cultured in MEM Alpha supplemented with 10% fetal bovine serum, 1% penicillin-streptomycin, and 100µM L-ascorbic acid 2-phosphate, but no additional plasma fibronectin (aside from that in serum).

5. Ficoll increases the amount of fibronectin at the glass surface where it is easily accessible for cell mediated fiber assembly

In this chapter we continue our search for a mechanism explaining how crowding enhanced fibronectin assembly, focusing now on the fibronectin.

These experiments were planned by JG and VV. JG conducted the experiments and analyzed the data. JG, VV, and MR discussed the data and wrote the text (excerpt from manuscript).

Next we asked whether Ficoll regulates cell access to fibronectin since crowding has been shown to increase the adsorption of molecules from the bulk fluid onto surfaces[92,93]. In order to assemble fibers, cell surface integrins need to bind to fibronectin, much of which is soluble in the medium, either coming from serum supplement or secreted by the cells themselves. Ficoll could cause increased adsorption of soluble fibronectin from the medium to the glass surface during extended cell culture. To investigate this, we cultured cells for 2 days with and without Ficoll and, after sample fixation, analyzed antibody-stained fibronectin on the glass surface in areas where the coating was left undisturbed (no apparent harvesting, no cells, no fibers). We switched to antibody staining for fibronectin quantification to ensure that we labeled both cellular and plasma fibronectin, and because this is standard in the field. We also did not add supplemental plasma fibronectin to the medium to correlate with previous studies where this had not been done (data with supplemental fibronectin shown in Figure 5.2). As evident from the images in Figure 5.1A, the amount of fibronectin at the surface was increased significantly in the presence of Ficoll. Quantification of the intensity of fibronectin stain showed 2.3x more fibronectin per area on the glass surface in the Ficoll treated condition (Figure 5.1B). This means that, though the glass substrates were initially preadsorbed with fibronectin, Ficoll treatment caused additional soluble fibronectin from the media to deposit to the glass surface over 2 days of culture.

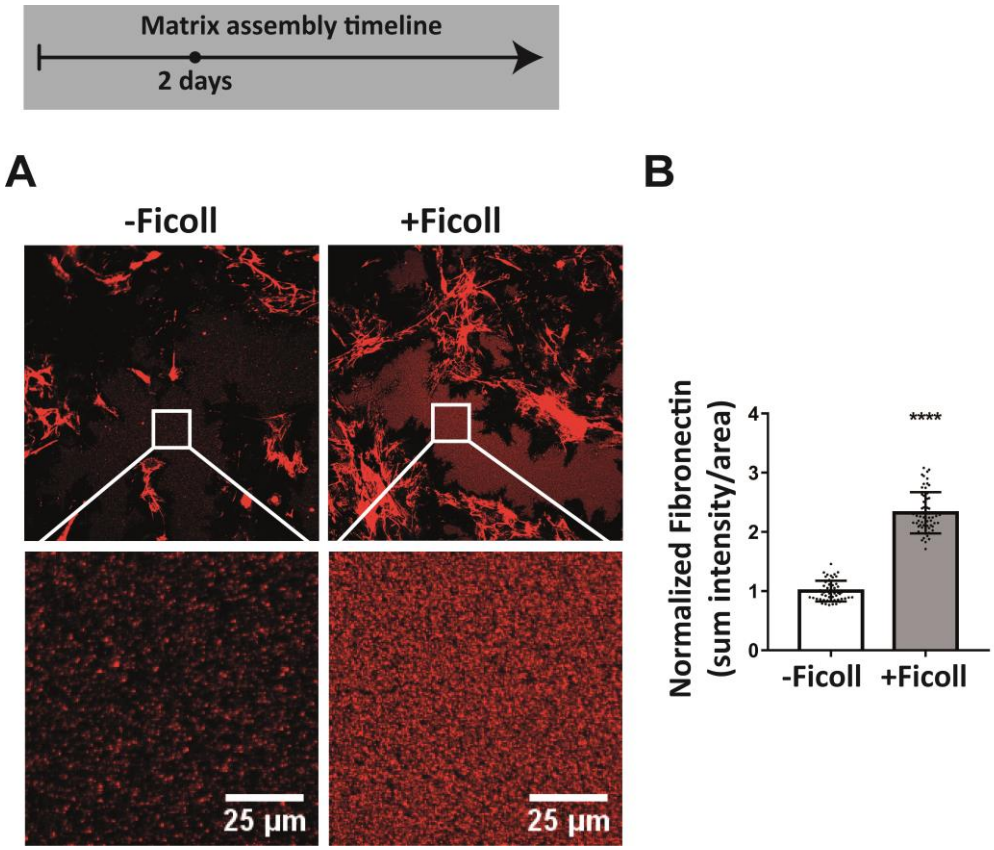

*Figure 5.1 Ficoll increases fibronectin adsorption to the glass surface during cell culture. (A) Widefield immunofluorescence images of antibody-stained fibronectin after 2 days culture with and without Ficoll, with insets below showing undisturbed areas of fibronectin coating (no fibroblasts or matrix fibers) that were analyzed. (B) Summed fibronectin intensity divided by area. Glass substrates preadsorbed with 50µg/mL unlabeled plasma fibronectin. Cells cultured in MEM Alpha supplemented with 10% fetal bovine serum, 1% penicillin-streptomycin, and 100µM L-ascorbic acid 2-phosphate, but no additional plasma fibronectin (aside from that in serum). **** indicates p<0.0001.*

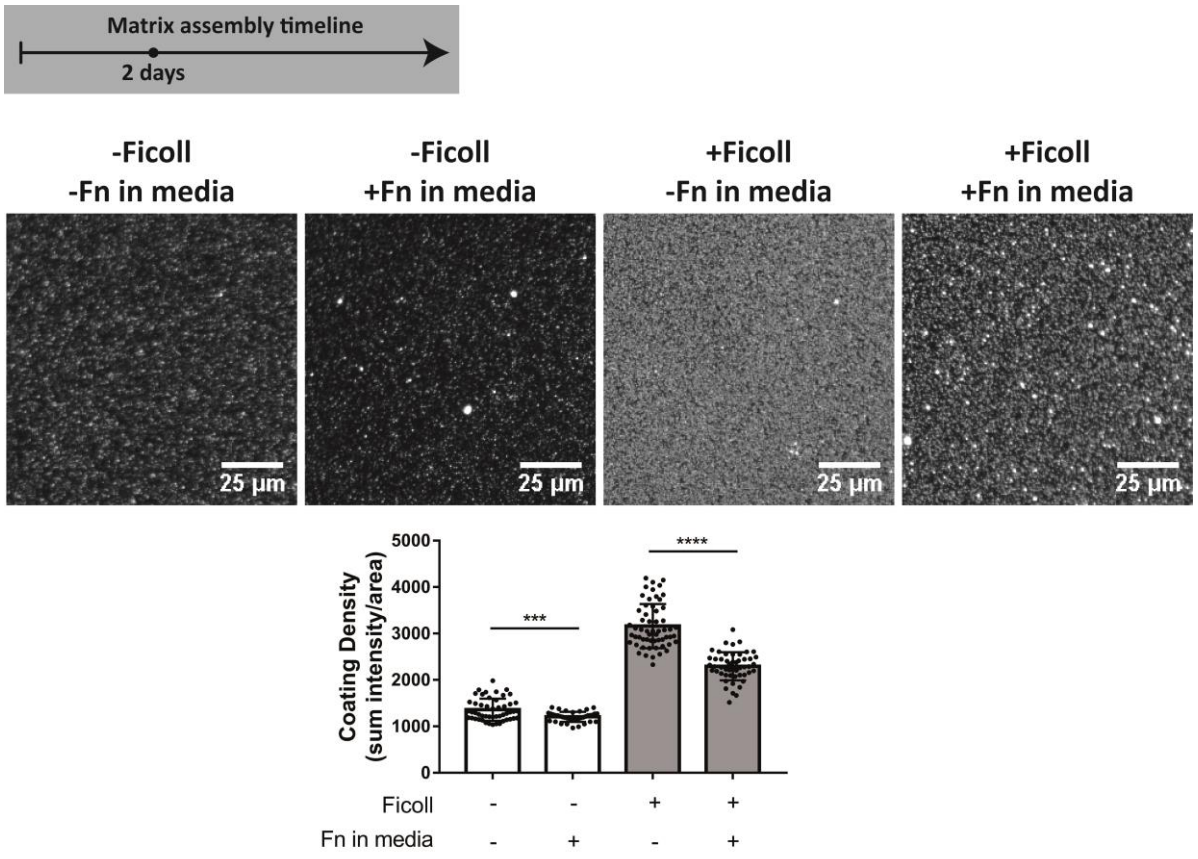

*Figure 5.2 Fibronectin on the glass surface after 2 days culture +/-Ficoll, both with and without 50µg/mL human plasma fibronectin supplemented to the medium. Reported values are the summed intensity of fibronectin antibody-stain divided by the area. *** indicates p<0.001, **** indicates p<0.0001.*

6. With the Ficoll-induced increase in fibronectin matrix there is more un-stretched fibronectin to act as a template for collagen I assembly

In this chapter we focus on the role of fibronectin in collagen assembly in the presence of crowding. It is well understood that fibronectin acts as a template for fibronectin[43–46], but whether or not this is still essential in the presence of Ficoll that drives procollagen processing and assembly is not known. Here we present an investigation into the tensional state of fibronectin, which impacts its ability to nucleate collagen fibers.

These experiments were planned by JG and VV. JG conducted the experiments and analyzed the data. Mario Benn (MB) helped with FRET experiments and provided FRET-labeled fibronectin. Dr. Simon Arnoldini (SA) provided MATLAB code that was adapted by JG for FRET analysis. JG, VV, and MR discussed the data and wrote the text (excerpt from manuscript).

Since collagen I assembly is nucleated by binding to low tension rather than highly stretched fibronectin fibers, as fiber stretching destroys the multivalent binding motif by which collagen peptides bind to several fibronectin type I and II modules in a row[47], similarly to how fiber stretching destroys the binding sites of bacterial adhesins[94,95], we next asked if Ficoll results in a greater total amount of un-stretched fibronectin fibers that could initiate polymerization of collagen I during the early stages of matrix assembly with our well validated FRET-fibronectin probe[40,47,51–55,63,96–101]. Ten percent of the supplemented plasma fibronectin was FRET-labeled and was incorporated into the matrix assembled by cells, as observed before[40,53]. The glass was preadsorbed with unlabeled fibronectin to distinguish freshly assembled ECM fibers from that adsorbed to the glass substrate. Cell seeding density was doubled (10,000 cells/cm^2) to ensure that we had enough fibronectin-FRET signal in an early stage of matrix assembly. Figure 6.1A shows representative images of FRET ratios after 2 days, with and without Ficoll. A histogram of all FRET ratios compiled from 21 images for each condition appears in Figure 6.1B. The overall peak tensional state of the matrix did not change, which is consistent with our finding that cell contractility did not increase (Figure 4.1). However, the total number of high-FRET pixels was higher upon Ficoll treatment (Figure 6.1B). To further assess fibronectin's conformational states, we used different concentrations of the chemical denaturant guanidine hydrochloride (GdnHCl) to gradually denature fibronectin in solution, measured the resulting fibronectin-FRET ratios, and created a calibration curve for our FRET-labeled fibronectin probe, as done before[40,53] (Figure 6.2). Fibronectin in 1M GdnHCl is extended compared to the globular state in PBS, but has not yet lost its secondary structure, whereas fibronectin in 4M GdnHCl has lost its secondary structure and is completely denatured[52]. Fibronectin fibrillogenesis is initiated by stretch-induced opening of cryptic fibronectin-fibronectin binding sites[35] and, as cells start bundling fibronectin profilaments into thicker fibers[102], they can get further stretched up to 3-4 times their equilibrium length in cell culture[63]. To quantify the amount of low tension fibronectin, we then quantified the total number of pixels in each image with a FRET ratio above that of fibronectin in 1M GdnHCl (i.e. FRET ratio = 0.34). There was a 30% increase in the amount of low-tension fibronectin with Ficoll at 2 days compared to -Ficoll control (Figure 6.1C). Taken together, the overall tensional

state of the fibronectin fibers was not changed with Ficoll, but the total number of FRET pixels representing un-stretched fibronectin, and thus potential nucleation sites for collagen I, was significantly higher upon Ficoll treatment.

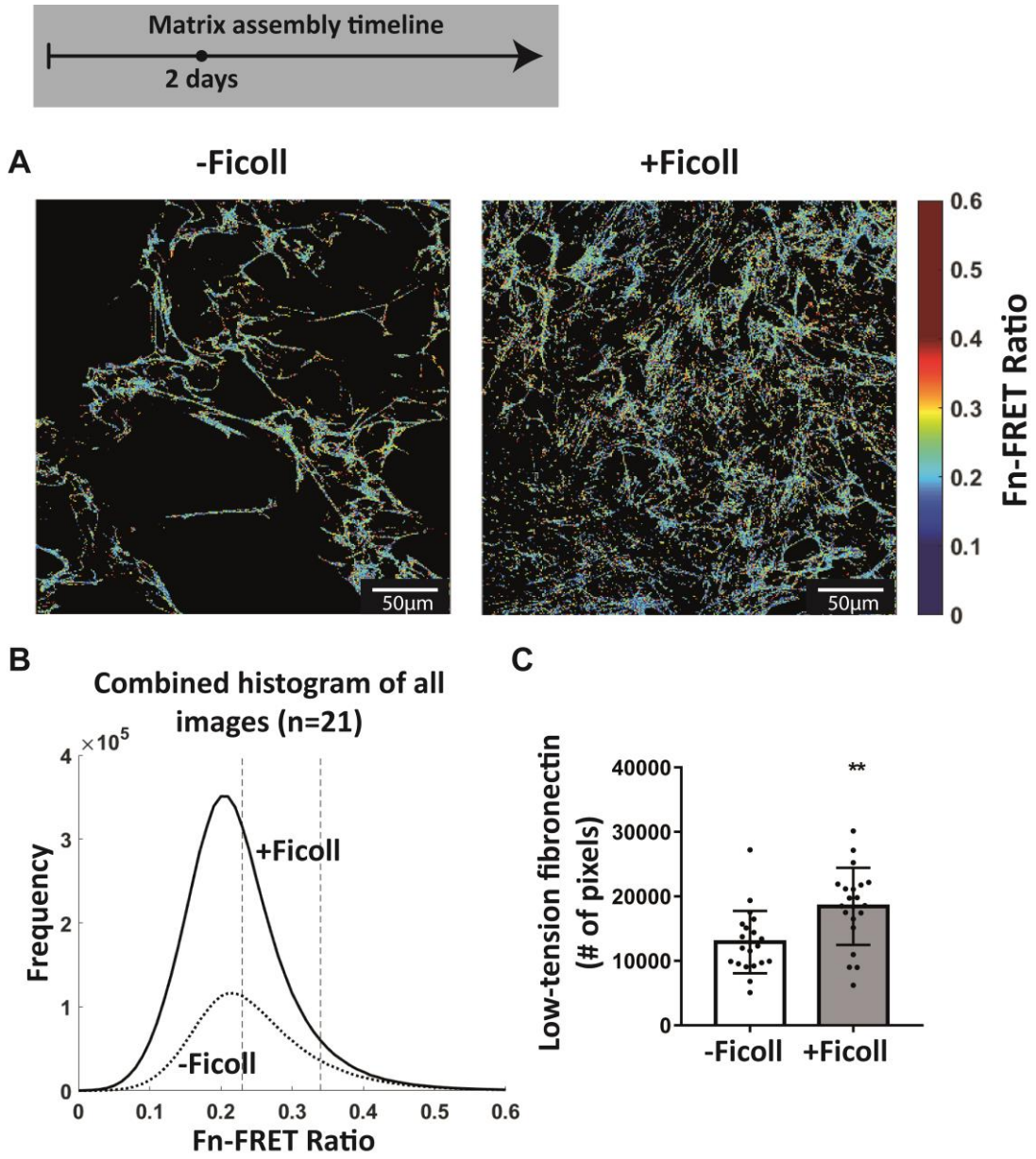

*Figure 6.1 Ficoll increases the number of nucleation sites that can induce collagen I polymerization as assessed by fibronectin-FRET, even though the distribution of fibronectin strains is not significantly altered. (A) Confocal images of the fibronectin-FRET ratios at the glass surface (where early matrix fibers are assembled) after 2 days in culture without and with Ficoll. (B) Representative FRET ratio histograms compiled from 21 images for each condition: 7 images each from 3 different samples. The dotted vertical lines represent the average FRET ratios in 4M GdnHCl (left) and in 1M GdnHCl (right) – see Supplemental Figure 6.2 for calibration curve. (C) Number of pixels with FRET ratio above that of fibronectin in 1M GdnHCl. Each point represents a single measurement from one image. Glass substrates preadsorbed with 50µg/mL unlabeled plasma fibronectin. Cells cultured in MEM Alpha supplemented with 10% fetal bovine serum, 1% penicillin-streptomycin, 100µM L-ascorbic acid 2-phosphate, and 50µg/mL plasma fibronectin (10% FRET-labeled). ** indicates p<0.01.*

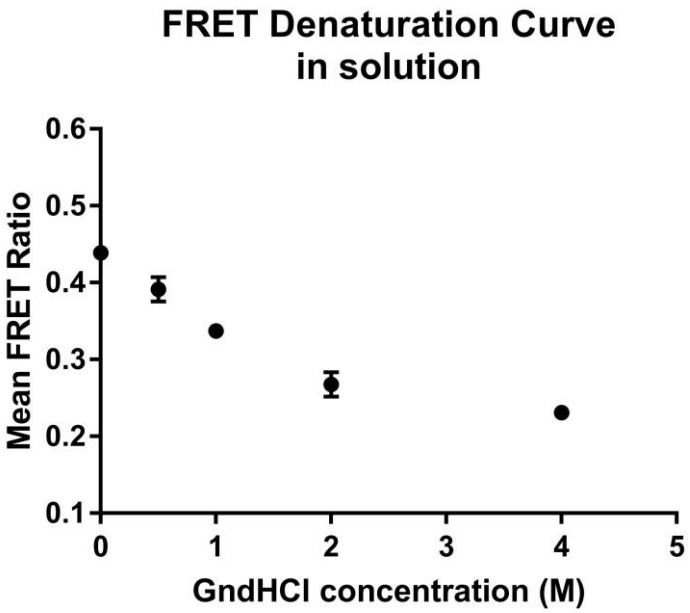

Figure 6.2 Fibronectin-FRET denaturation curve. The Fn-FRET probe was gradually denatured in increasing concentrations of the chemical denaturant guanidine hydrochloride and the FRET ratio was measured in solution. Reported values are the average FRET ratio for 5 individual measurements at each concentration of GdnHCl.

7. Cross-linking adsorbed fibronectin to the substrate inhibits the Ficoll-accelerated matrix assembly

In this chapter we continue our investigation of the role of fibronectin as a template for collagen in the presence of crowding. We interfere with the fibroblasts ability to harvest fibronectin on the surface by cross-linking the coating and look at the impact on crowding's ability to enhance collagen assembly.

These experiments were planned by JG, JM, and VV. JG conducted the experiments and analyzed the data. JM helped with cross-linking of fibronectin to the glass substrate. JG, VV, and MR discussed the data and wrote the text (excerpt from manuscript).

To ask how important surface adsorbed fibronectin might be in the accelerated matrix assembly process as induced by Ficoll, we covalently cross-linked fibronectin to the glass substrate before cell seeding to prevent fibroblasts from scraping off the coating and found that this significantly delayed early assembly of fibronectin fibers. Figure 7.1A shows antibody-stained fibronectin and collagen I assembled on a cross-linked fibronectin coating after 2 days. The dark, cell-shaped areas in the fibronectin channel in Figure 7.1A are shadows where the fibronectin antibody was not able to access the coating, which we confirmed by removing the cells with trypsin (Figure 7.2). Even though it is known that Ficoll drives the cleavage and assembly of collagen I, we found that Ficoll did not increase collagen I fiber assembly when the fibroblasts could not pull the fibronectin coating off the substrate to accelerate early fibronectin fibrillogenesis (Figure 7.1B). In contrast, collagen I fiber assembly was more than doubled by Ficoll on adsorbed fibronectin that the fibroblasts could harvest during the early phase fibrillogenesis (Figure 7.1C-D). This is an important novel finding that, even though Ficoll was there to promote the enzymatic cleavage and supramolecular assembly of collagen, the fibronectin fiber template was still essential for collagen I fiber assembly.

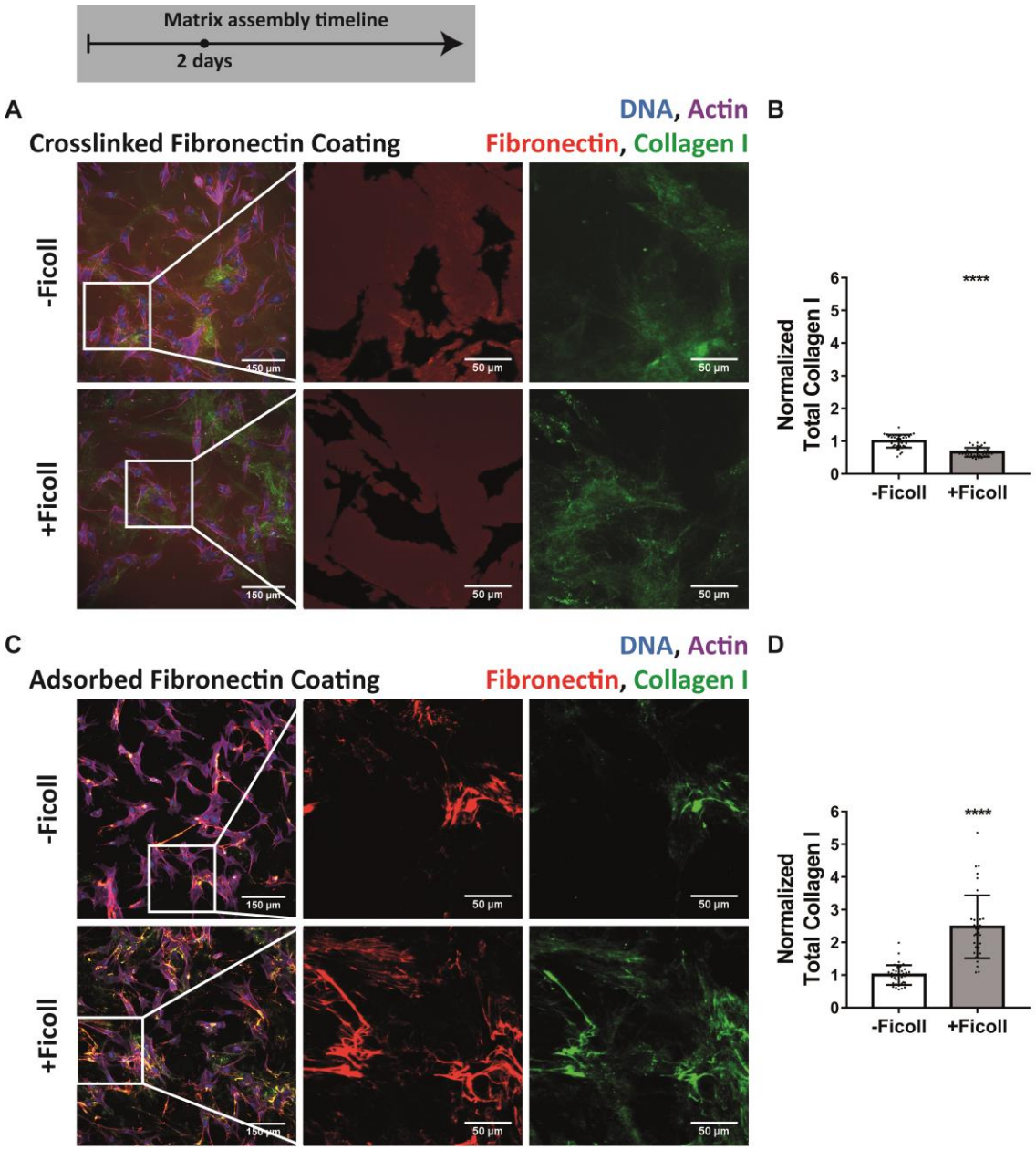

*Figure 7.1 Ficoll does not increase collagen I fiber assembly when the preadsorbed fibronectin coating is cross-linked to the substrate prior to cell seeding. (A) Widefield immunofluorescence images of matrix assembled on cross-linked fibronectin coating (50µg/mL, unlabeled) after 2 days of culture. The first image is of fibroblasts and matrix, followed by magnified images of fibronectin and collagen I alone. Dark areas in fibronectin channel are cell shadows, not harvested coating – see Figure 7.2 for confirmation. (B) Summed intensity of collagen I, normalized to the mean without Ficoll. (C-D) Same for adsorbed fibronectin coating (50µg/mL, unlabeled). Cells cultured in MEM Alpha supplemented with 10% fetal bovine serum, 1% penicillin-streptomycin, and 100µM L-ascorbic acid 2 phosphate, but no additional plasma fibronectin (aside from that in serum). **** indicates p<0.0001.*

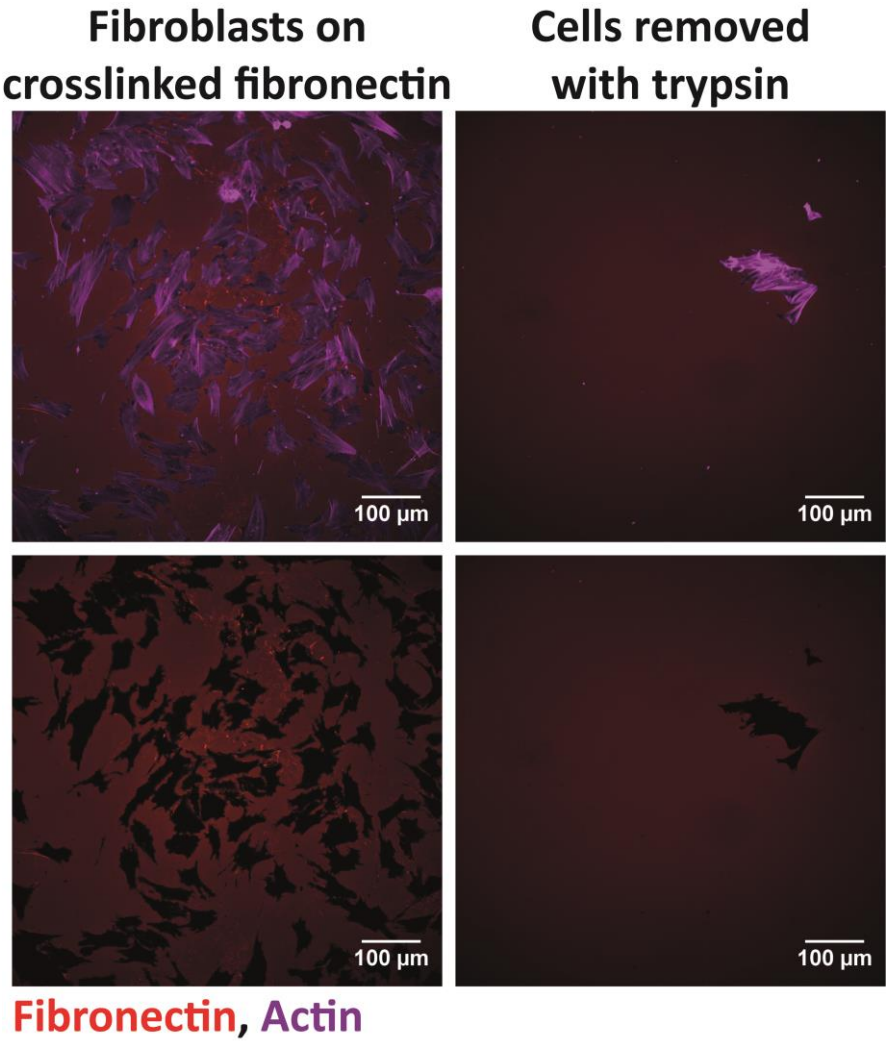

Figure 7.2 In order to confirm that the dark areas in the fibronectin channel on cross-linked fibronectin coating are shadows from the cells rather than digested or harvested coating (see Figure 7.1), one sample was treated with trypsin before fixing and staining. The sample was otherwise treated the same as all others. On the left is a standard sample with cells, and on the right is a sample where cells have been removed by trypsin (except for one that remained adherent). The top images show both cells and fibronectin, whereas the bottom images show only the fibronectin channel. The fact that all dark areas in the fibronectin channel disappeared with trypsin treatment (except the one where a cell remained) confirms that the cross-linked coating is still intact and the dark areas are places where the fibronectin antibody could not access the coating.

Cross-linking the fibronectin coating delays fibronectin fiber assembly since cells cannot harvest the coating, but eventually cells will assemble fibers on top of the coating from soluble fibronectin. We cultured cells for 72 hours on cross-linked fibronectin coating (without Ficoll treatment) and noticed that there were more fibronectin fibers assembled at this timepoint than after 48 hours. In this case there was also more collagen I, and the collagen I colocalized with fibronectin fibers, rather than cross-linked coating (Figure 7.3). This further confirms our finding that collagen I assembly requires a template of fibronectin fibers, but a coating of globular fibronectin is not sufficient.

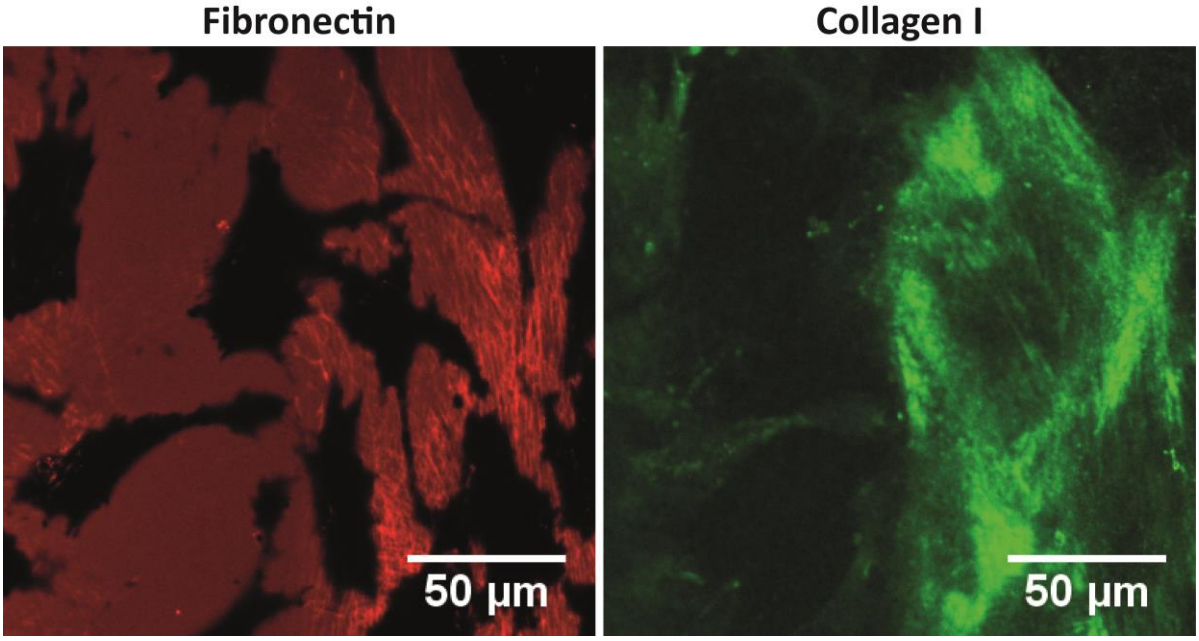

Figure 7.3 Representative image showing that collagen fibers are only assembled where there are fibronectin fibers on a cross-linked fibronectin coating. Procedure was the same as that used in Figure 7.1, except cells were cultured for a total of 72 hours to allow more time for fibronectin fibers to eventually be assembled from soluble fibronectin on the cross-linked coating that the fibroblasts could not harvest. This image is from a sample without Ficoll. The same behavior was seen in the presence of Ficoll. Fibronectin and collagen both visualized by antibody-staining.

8. Preadsorbing fibronectin to the glass substrate further accelerates matrix assembly under crowding conditions

In this chapter we present a way for tissue engineers to utilize our findings to improve crowding-induced matrix assembly.

These experiments were planned by JG and VV. JG conducted the experiments and analyzed the data. JG, VV, and MR discussed the data and wrote the text (excerpt from manuscript).

To ask how bioengineers can take advantage of our findings, we assessed the impact of preadsorbing fibronectin to the glass substrate on matrix assembly in crowded conditions. We cultured fibroblasts with Ficoll for 2 days on uncoated glass (standard protocol in the community) or glass coated with 50µg/mL adsorbed human plasma fibronectin. We found that the cell density was significantly higher when the glass was preadsorbed with fibronectin (Figure 8.1A), likely due to both increased cell adhesion and proliferation, and that there was much more fibronectin and collagen I fiber assembly than without precoating (Figure 8.1B-C). We then added 50µg/mL supplemental soluble plasma fibronectin to the medium, in addition to the preadsorbed fibronectin coating, to see if it further improved matrix assembly beyond the coating alone. Note that 10% serum contains only 2-3µg/mL of fibronectin [103]. Figure 8.1D-F shows that addition of supplemental soluble fibronectin minorly increased cell density but did not impact fibronectin or collagen I assembly. These results show that including fibronectin as a coating before cell seeding markedly improved the matrix assembly with macromolecular crowding in 2 days, but there was no further benefit of also supplementing soluble fibronectin to the medium.

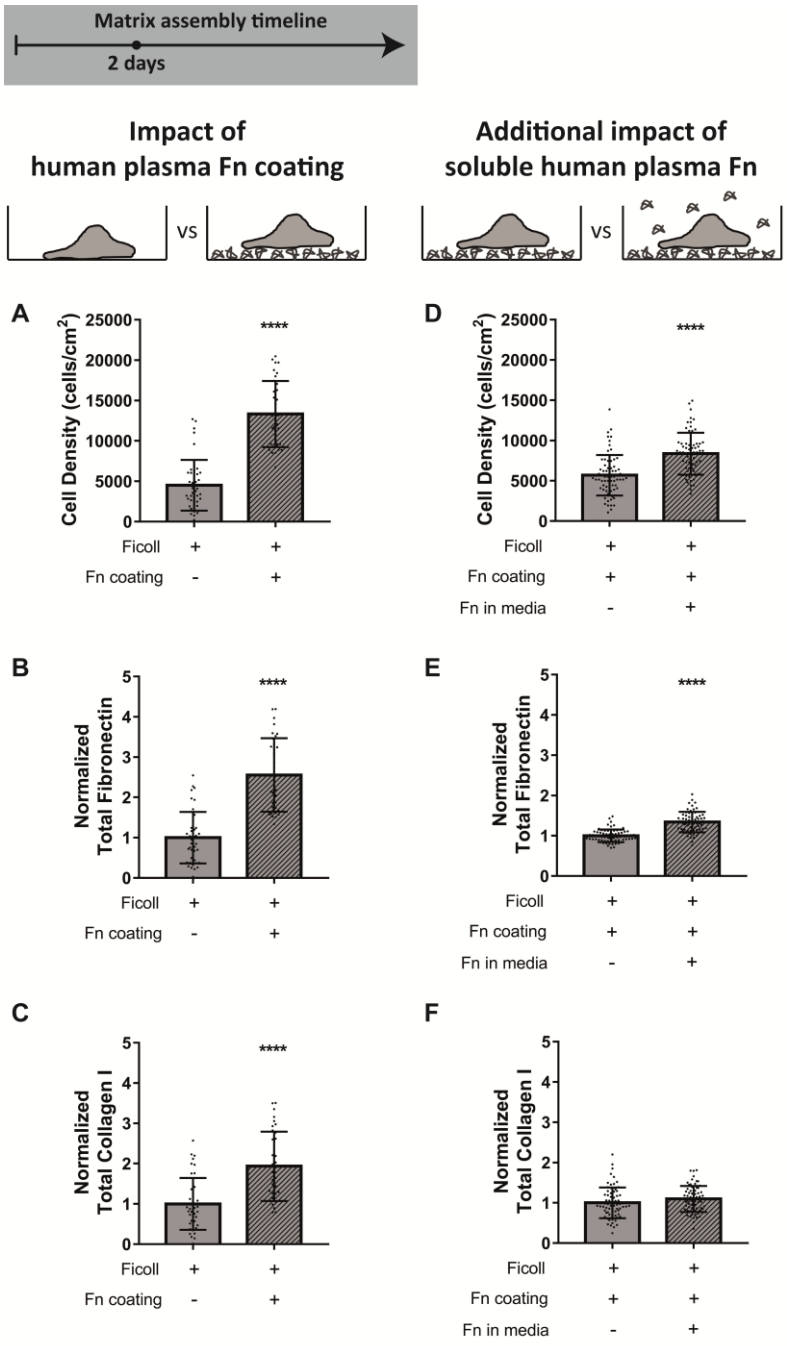

*Figure 8.1 Supplementation of fibronectin as an adsorbed coating improves matrix assembly in the presence of Ficoll after 2 days. (A-C) Tissue production in the presence of Ficoll on uncoated glass compared to glass coated with 50µg/mL adsorbed human plasma fibronectin (unlabeled). (A) Cell density. (B) Summed intensity of antibody-stained fibronectin. (C) Summed intensity of antibody-stained collagen I. B and C are normalized to the mean value on uncoated glass. (D-F) Additional impact of adding 50µg/mL soluble human plasma fibronectin (unlabeled) when there is already an adsorbed fibronectin coating. Cells cultured in MEM Alpha supplemented with 10% fetal bovine serum, 1% penicillin-streptomycin, and 100µM L-ascorbic acid 2 phosphate. **** indicates p<0.0001.*

9. Conclusion and Outlook

Since methods to accelerate matrix production are urgently needed in the fields of tissue engineering and regenerative medicine, our goal here was to shed light on the underpinning mechanisms by which Ficoll exposure upregulates ECM assembly, as previously reported [11–17,21–23,82,83]. Rather than just accelerating pro-collagen cleavage and supramolecular assembly, previously thought to be the main drivers[2,3], we show here that Ficoll also significantly enhances fibronectin assembly (Chapter 3) and that the rate of fibronectin fibrillogenesis regulates the collagen I assembly process. Towards the mechanistic side, we found that fibronectin and collagen I are colocalized during early ECM assembly both with and without crowders (Chapter 3), and that even though the cell mechanical functions are not significantly impacted (Chapter 4), Ficoll causes a significant increase in soluble fibronectin adsorbing from the medium to the substrate surface (Chapter 5). We observed a high density of bright fibronectin spots at the glass surface, but only in the presence of Ficoll (Chapters 3 and 5), suggesting that crowding causes aggregation of fibronectin, which likely contributes to further increasing the amount of fibronectin that the cells can harvest. The 2-fold increase in fibronectin at the glass surface seen with Ficoll correlates well with the 2-fold increase in early fibronectin fiber assembly (Chapter 3). Even though the cell spreading area and the area of coating harvested per cell are not significantly affected by Ficoll (Chapter 4), there is a significantly higher amount of fibronectin on the surface which the fibroblasts can scrape off. Fibronectin harvesting from the substrate is much more effective than from the medium because surface adsorbed fibronectin is in a more open conformation with greater accessibility of cell-binding sites than fibronectin in solution[52,104]. Additionally, fibroblasts can more readily exert tensional forces on surface-bound than on freely floating fibronectin, which is important since cells have to stretch fibronectin to induce its fibrillogenesis[35,39,102].

By exploiting our well-established fibronectin-FRET probe[40,47,51–55,63,96–101], we could show that Ficoll significantly increases the total amount of low-tension fibronectin fibers (Chapter 6). This observation is highly significant since we showed previously that fibronectin stretching destroys the multivalent binding motif for the collagen peptide[35,47], and consequently, only the low-tension fibronectin fibers can nucleate the initial collagen I polymerization process in cell culture. A very recent study showed that fibronectin also binds both procollagen and the C-proteinase BMP-1, thereby acting as a template to increase their interaction[49]. This suggests that the increase in fibronectin matrix with crowding could directly contribute to enhanced cleavage of procollagen, implicating yet another role for fibronectin in matrix assembly with crowding.

Since the rate by which fibronectin can be scraped off plays a key role in Ficoll-enhanced ECM assembly, we next asked whether chemical cross-linking to the substrate might slow the matrix assembly rate. Indeed we found that crosslinking of the pre-adsorbed fibronectin layer to the substrate abolished the previously described ability of Ficoll to upregulate matrix assembly (Chapter 7). This is a remarkable finding since it was shown previously that Ficoll upregulates procollagen cleavage and supramolecular assembly[1,2,20,21,27–31], and still, if the cells cannot efficiently harvest surface bound fibronectin to build fibers, Ficoll does not upregulate ECM assembly. We thus

illuminate for the first time the essential role of fibronectin in the underpinning mechanism by which Ficoll upregulates ECM assembly.

But what can tissue engineers learn from having deeper insights into the driving mechanism? Our finding that cross-linking of fibronectin to the glass surface also prevents collagen assembly, even in the presence of a neutral crowder (Chapter 7), demonstrates that paying attention solely to the crowder is not enough to catalyze collagen assembly *in vitro*. While it is common among tissue engineers to expose their materials to the medium before cell seeding, we show here that preadsorbing human plasma fibronectin greatly accelerates ECM production compared to the uncoated sample (Chapter 8) and that crosslinking of the preadsorbed fibronectin layer to the substrates destroys the accelerating effect of Ficoll supplementation (Chapter 7). We found that after 6 days there is no longer a large difference in the matrix assembled with and without Ficoll (Chapter 3). Results in the literature are mixed about whether the increased matrix with crowding persists over long culture times or if the matrix assembly without crowding eventually catches up[11,15,17,24,26] (summarized in Table 9.1). However, there seems to be a consensus that crowding increases the speed of early matrix assembly, as we too have shown (Chapter 3). This increase in speed in the early phases is highly valuable in tissue engineering, where the weeks to months traditionally needed to produce a substitute tissue *in vitro* result in high costs, a long wait-time for the patient, and changes in cell phenotype, limiting clinical success.

As tissue engineers move away from the use of standard fetal bovine serum towards animal-free media[83], it will become even more important to consider whether to supplement the media with fibronectin and at what concentrations. As we have shown here, it is highly beneficial to supplement purified human plasma fibronectin in the form of an adsorbed coating (Chapter 8). This may be even more impactful in cases where the cells do not efficiently produce fibronectin on their own. Our mechanistic insights give tissue engineers important new parameters to consider which can be tuned to effectively increase the ECM assembly process.

Table 9.1 Summary of findings regarding the effect of Ficoll on the amount of collagen I matrix at late timepoints. Only studies with standard Ficoll mixture (37.5mg/mL 70kDa + 25mg/mL 400kDa) as the crowder and supplemental ascorbic acid in culture media were included. Entries without references specified are from the same study as the row above.

Protein	Cell type	Crowder	Time point	Fold change in collagen	Method	Reference
Collagen I	Dermal fibroblasts	Ficoll	7 days	No change	SDS-PAGE of pepsin digested cell layers	Gaspar et al., Acta Biomater. (2019)[26]
			14 days	1.3x		
Collagen I	Dermal fibroblasts	Ficoll	6 days	Increased (fold-change not clear)	Immunofluorescence, thresholded area of matrix normalized to cell count	Rashid et al. Tissue Eng. Part C (2014)[11]
	Mesenchymal stem cells			>5x		
Total collagen	Mesenchymal stem cells	Ficoll + dextran sulfate	10 days	0.5x	Sircol assay of pepsin digested decellularized ECM layers	Prewitz et al., Biomaterials (2015)[17]
Collagen I	Mesenchymal stem cells	Ficoll	7 days	No change	SDS-PAGE of pepsin digested cell layers	Cigognini et al., Sci. Rep. (2016)[24]
			14 days	No change		
Collagen I	Corneal fibroblasts	Ficoll	6 days	>3x	SDS-PAGE of pepsin digested media and cell layers	Kumar et al. Sci. Rep. (2015)[15]

10. Materials and Methods

10.1. Isolation of human plasma fibronectin

Fibronectin was isolated from human plasma as described previously[53], with minor modifications. First, plasma (Blood Bank Zurich, Switzerland) was spun at 3220xg for 40 minutes at 8°C. 10mM EDTA was added to the supernatant and then the supernatant was passed through a PD-10 desalting column (GE Healthcare #17-0851-01). Next the supernatant was passed through a poly-prep chromatography column (Bio-Rad #7311550) pre-packed the day before with gelatin-sepharose 4B (VWR #17-0956-01) to bind fibronectin. The column was then washed with column buffer (PBS + 10mM EDTA), followed by 1M NaCl in column buffer, and 0.2M Arginine (Carl Roth #1655) in column buffer until the 280nm absorbance of the flow-through was <0.1. Finally, the fibronectin was eluted with 1M Arginine in column buffer and stored at -80°C until usage. The quality of fibronectin purification was confirmed by western blot and Coomassie staining. Before usage in cell culture, fibronectin was slowly thawed at 4°C overnight and the solvent was changed to PBS through dialysis with a Slide-A-Lyzer Dialysis Cassette (ThermoFischer Scientific #66003).

10.2. Substrate cleaning and fibronectin preadsorption

Glass coverslips were cleaned by soaking in 2% HellmaneX solution (Hellma #9-307-010-507) with sonication for 30 minutes, followed by another 30 minutes without sonication, and subsequently washed with deionized water and blown dry. Coverslips were then coated by adsorbing human plasma fibronectin from solution (50µg/mL in PBS, 1 hour, room temperature) and subsequently washed with PBS. Coverslips were sterilized before cell culture by 15 minutes of UV exposure in a biosafety cabinet.

10.3. Cell culture with crowded media

Normal human dermal fibroblasts (PromoCell, Vitaris AG, Switzerland) were cultured in standard medium consisting of MEM Alpha (Biowest #L0475), 10% fetal bovine serum (Biowest #S181H), and 1% penicillin-streptomycin (Gibco #15140122). Fibroblasts were regularly passaged with 0.25% Trypsin-EDTA (Invitrogen #25200-056) before reaching confluence and used at passage #6-9. Medium with crowders was prepared by dissolving 37.5mg/mL of 70kDa Ficoll (GE Healthcare #GE17-0310) and 25mg/mL of 400kDa Ficoll (GE Healthcare #GE17-0300) in standard medium in a 37°C water bath. Once dissolved, Ficoll containing medium was filtered through a 0.22µm syringe filter. Standard medium with no crowder was also filtered for control samples. This crowding formulation remained consistent throughout the study.

The following other crowders were also used in the same way as Ficoll from GE Healthcare: 70kDa Dextran (Sigma #31390), 500kDa Dextran (Pharmacia Biotech #17-0320-01), 40kDa PVP (Sigma #9003-39-8 PVP40), 360kDa PVP (Sigma #9003-39-8 PVP360), Carrageenan (Sigma #C1013), 70kDa Sigma Ficoll (#F2878), 400kDa Sigma Ficoll (#F2637).

10.4. Extracellular matrix assembly

For ECM assembly experiments, fibroblasts were cultured on coverslips coated with adsorbed fibronectin placed inside standard 12-well polystyrene tissue culture plates. After coating, coverslips were washed with PBS and fibroblasts were plated in standard medium at 5,000 cells/cm^2 and allowed to adhere for 1 hour in a humidified incubator with 5% CO_2. Afterwards, media were changed to +/- Ficoll as appropriate and supplemented with 100µM L-ascorbic acid 2-phosphate (Sigma #A8960) and 50µg/mL human plasma fibronectin purified in house (see methods section "Isolation of human plasma fibronectin"). Fibroblasts were cultured for 16 hours, 2 days, or 6 days. Media were changed after 3 days for the 6-day samples. Ascorbic acid and fibronectin were freshly added upon media change.

10.5. Immunofluorescence and microscopy

ECM assembly was visualized by immunofluorescence microscopy. Unless labeled-fibronectin was used, fibronectin was stained with BD primary antibody #610077 (1:200) and donkey anti-mouse-488 secondary antibody (Invitrogen #A-21202, 1:200). Collagen was visualized with Abcam primary antibody #34710 (1:200) and donkey anti-rabbit-546 secondary antibody (Invitrogen #A10040, 1:200). Actin was visualized with Phalloidin 647 or 488 (Invitrogen, 1:500) and DNA with Hoechst 33342 (Thermo Scientific #62249, 1:200). Samples were first blocked in 5% w/v BSA (AppliChem GmbH #A1391) in water for 1 hour, then incubated with primary antibody in 5% BSA for 1 hour at room temperature, followed by washing with 1% BSA and incubation with secondary antibody in 5% BSA for 1 hour at room temperature. Samples were then permeabilized with 0.3% Triton X-100 (AppliChem #A4975) for 15 minutes, washed, and stained with actin and DNA dyes. Samples were finally mounted with fluorescent mounting medium (Dako #S3023) and allowed to dry overnight at room temperature before imaging.

Phosphorylated FAK was immunolabeled with Abcam primary antibody #81298 (1:400) and phosphorylated myosin light chain 2 was immunolabeled with Cell Signaling Technologies primary antibody #3671 (1:50). Both were visualized with donkey anti-rabbit-546 secondary antibody (Invitrogen #A10040, 1:200). MRTF-A was immunolabeled with Abcam primary antibody #49311 (1:100), H3K9Ac with Abcam primary antibody #4441 (1:150), and H3K27me3 with Cell Signaling Technologies primary antibody #9733 (1:1600). Each of these were then visualized in individual samples with goat anti-rabbit 488 secondary antibody #A-11034 (1:200). Lamin A and lamin B were co-stained with primary antibodies ab8980 (Abcam, 1:200) and ab16048 (Abcam, 1:500) and secondary antibodies donkey anti-mouse 488 (Invitrogen #A-21202, 1:200) and donkey anti-rabbit 546 (Invitrogen #A10040), respectively. Staining proceeded as above, except permeabilization occurred just after fixing and before primary and secondary antibody incubations.

Images for quantification of ECM assembly and cell/nuclear markers were taken on a Leica DMI6000B epifluorescence microscope with 20x 0.7NA HC PlanApo objective. A mosaic of 20 images (5x4 grid) was captured to avoid bias in selecting areas to image. An ROI was selected to avoid corners where fluorescent lamp intensity was weaker. Some images were also taken with a Leica SP5 confocal microscope to better visualize small details and appreciate the dimensionality of the matrix.

10.6. Labeling of fibronectin

Unless specified otherwise, fibronectin matrix assembly was visualized by substituting 10% of the coating and supplemented soluble fibronectin with fluorescently-labeled fibronectin (5µg/mL labeled + 45µg/mL unlabeled). Fibronectin was randomly labeled with fluorescent probes on surface accessible lysine residues by amide bond formation, as described before[102] with minor modifications. After purification of fibronectin, the solvent was changed from 1M Arginine to labelling buffer (0.1M $NaHCO_3$ in PBS, pH 8.5) through dialysis with a Slide-A-Lyzer Dialysis Cassette (ThermoFischer Scientific #66003). Fibronectin in the dialysis cassette was then incubated with a molar excess of Alexa Fluor 647 succinimidyl ester (Invitrogen #A20006). The molar excess depended on the freshness of the dye and varied from 5-50 (lower values for more fresh dye). Fibronectin was then dialyzed again to change the solvent to PBS.

For FRET measurements, fibronectin was randomly labeled with Alexa 488 donor fluorophores on its amines via succinimidyl ester conjugation and specifically labeled with Alexa 546 acceptor fluorophores on the cysteines in fibronectin type III modules $FNIII_7$ and $FNIII_{15}$ via maleimide conjugation, based on previous protocols[51,53,63] and as described by Ortiz Franyuti et al[101]. To validate successful labeling, the sensitivity of the FRET-probe to progressive denaturation in increasing concentrations of guanidine hydrochloride (GdnHCl, Sigma #G4505) was verified with a procedure slightly modified from what was described previously[53]. A coverslip was coated with 2% BSA for 30 minutes, then washed with distilled water and blown dry. FRET-labeled fibronectin was dissolved in solutions of GdnHCl ranging from 4M to 0M (dH2O control). A 2.5uL drop of each solution was placed on the coverslip and was imaged in 5 ROIs above the glass-droplet interface with the same microscope settings as used for the matrices (see methods section “Imaging of FRET in cell-assembled matrices”). Average FRET ratios were calculated for each concentration and plotted as a denaturation curve.

10.7. Quantification of extracellular matrix and cell density

ECM assembly was quantified by summing fibronectin and collagen intensity per image after background subtraction with a custom MATLAB script. Cell density was quantified by automated segmentation of nuclei with a custom MATLAB script for 16 hour and 2 day samples. 6 day samples were counted manually because the density was too high for automatic segmentation.

10.8. Quantification of fibronectin adsorbed to the glass surface

Fibroblasts were cultured on fibronectin coated glass as described above, except without soluble fibronectin added to the media. After 2 days, samples were fixed, stained, and imaged as described above. The amount of fibronectin on the surface was quantified by measuring the fluorescence intensity in an area where the fibronectin layer looked uniform and there were no cells or matrix fibers. The summed intensity was divided by the area of the ROI and reported as fibronectin density. One ROI per image was analyzed. Some images showed abnormally high fluorescence intensity at

the glass surface. This could be due to autofluorescence from HellmaneX solution that was not fully washed. These images with abnormal coating were identified by viewing all images simultaneously and they were excluded from the analysis

10.9. Quantification of cell/nuclear markers and percentage of coating harvested

Cell areas were estimated by manual tracing. Intensity of F-actin, p-FAK, and p-MLC2 per cell were summed in the manually traced cell outline after background subtraction. Only spread cells with few cell-cell contacts were analyzed. The percentage of the coating harvested per cell was measured by setting a threshold to distinguish the intact coating and fibronectin fibers from areas of the glass where the coating had been removed (darker areas). The area below the threshold was measured and divided by the total area to get the percentage of the coating that was harvested. This value was then divided by the number of cells identified by automatic segmentation of the nuclei. YAP and MRTF-A nuclear-to-cytoplasmic ratios were measured manually in ImageJ software. Lamin A, Lamin B, H3K9Ac, and H3K27me3 were quantified by automatic nuclear segmentation in MATLAB.

10.10. Matrix assembly with FRET-labeled fibronectin

Fibroblasts were cultured in glass bottom Lab-tek chambers (Thermo Fisher Scientific #155411) that had been previously coated with unlabeled fibronectin (as described above). Cells were plated at 10,000 cells/cm^2 to achieve greater matrix assembly and ensure that there was enough signal to analyze FRET. After 1 hour cell adhesion, media were changed to +/-Ficoll and supplemented with 100µM L-ascorbic acid 2-phosphate, 45µg/mL unlabeled fibronectin, and 5µg/mL FRET-labeled fibronectin. Cells were cultured for 2 days, then washed with PBS and fixed with 4% PFA for 20 minutes.

10.11. Imaging of FRET in cell-assembled matrices

Samples were imaged in PBS immediately after fixation with an Olympus FV1000 confocal microscope with a 40x water immersion objective. Samples were excited with a 488nm laser and both the donor and acceptor emission were collected simultaneously. Two day old matrices were imaged in one focal plane where a majority of the matrix, particularly the smallest fibers, were in focus. A Kalman line filter was applied as a software setting at the time of image acquisition.

10.12. Analysis of FRET in cell-assembled matrices

Images of FRET labeled fibronectin were analyzed with custom MATLAB code as described previously [53]. Briefly, dark current background from the detector was subtracted from both the donor and acceptor images. Next, images were smoothed with a 2x2 pixel averaging filter. A threshold was applied to exclude low intensity signal from the fibronectin coating and background (selecting only for fibronectin fibers), as well as any saturated pixels. Then bleedthrough from the donor channel into the acceptor channel was corrected for by subtracting 20% of the donor image from the acceptor image, pixel-by-pixel. Finally, FRET ratios were calculated by dividing the pixel intensities of the acceptor image by the donor image.

10.13. Cross-linking fibronectin to the coverslip

For cross-linked fibronectin coating, coverslips were first plasma treated (Harrick Plasma PDC-32G) for 30 seconds at maximum power. Coverslips were then incubated for 15 minutes with 2% (3-Aminopropyl)triethoxysilane (Sigma-Aldrich #A3648) solution in DI water (made fresh). After rinsing with DI water, coverslips were treated with 0.125% glutaraldehyde (Sigma-Aldrich #G4004) in water for 30 minutes. Coverslips were washed again and coated with 50µg/mL fibronectin in PBS for 1 hour. After washing with PBS, coverslips were sterilized with UV for 15 minutes before cell plating. Cell culture proceeded as described above. Ascorbic acid was supplemented to the media, but not plasma fibronectin.

10.14. Statistical analysis

Unpaired, parametric t-tests were performed with GraphPad Prism software to test for statistical significance. P-values relative to control are indicated by stars in figures and defined in figure captions.

References

1. Bateman, J. F., Cole, W. G., Pillow, J. J. & Ramshaw, J. A. Induction of procollagen processing in fibroblast cultures by neutral polymers. *J. Biol. Chem.* **261,** 4198–203 (1986).

2. Chen, C., Loe, F., Blocki, A., Peng, Y. & Raghunath, M. Applying macromolecular crowding to enhance extracellular matrix deposition and its remodeling in vitro for tissue engineering and cell-based therapies. *Adv. Drug Deliv. Rev.* **63,** 277–290 (2011).

3. Benny, P. & Raghunath, M. Making microenvironments: A look into incorporating macromolecular crowding into in vitro experiments, to generate biomimetic microenvironments which are capable of directing cell function for tissue engineering applications. *J. Tissue Eng.* **8,** 2041731417730467 (2017).

4. Ellis, R. J. Macromolecular crowding: obvious but underappreciated. *Trends Biochem. Sci.* **26,** 597–604 (2001).

5. Mourao, M. A., Hakim, J. B. & Schnell, S. Connecting the Dots: The Effects of Macromolecular Crowding on Cell. *Biophys. J.* **107,** 2761–2766 (2014).

6. Zimmerman, S. B. & Minton, A. P. Macromolecular Crowding: Biochemical, Biophysical, and Physiological Consequences. *Annu. Rev. Biophys. Biomol. Struct.* **22,** 27–65 (1993).

7. Chebotareva, N. A., Kurganov, B. I. & Livanova, N. B. Biochemical effects of molecular crowding. *Biochemistry. (Mosc).* **69,** 1239–51 (2004).

8. Weiss, M. Crowding, diffusion, and biochemical reactions. *Int. Rev. Cell Mol. Biol.* **307,** 383–417 (2014).

9. Kuznetsova, I. M., Turoverov, K. K. & Uversky, V. N. What macromolecular crowding can do to a protein. *Int. J. Mol. Sci.* **15,** 23090–140 (2014).

10. Rivas, G. & Minton, A. P. Macromolecular Crowding In Vitro , In Vivo , and In Between. *Trends Biochem. Sci.* **41,** 970–981 (2016).

11. Rashid, R. *et al.* Novel Use for Polyvinylpyrrolidone as a Macromolecular Crowder for Enhanced Extracellular Matrix Deposition and Cell Proliferation. *Tissue Eng. Part C Methods* **20,** 994–1002 (2014).

12. Zeiger, A. S., Loe, F. C., Li, R., Raghunath, M. & Van Vliet, K. J. Macromolecular crowding directs extracellular matrix organization and mesenchymal stem cell behavior. *PLoS One* **7,** e37904 (2012).

13. Liu, F. D., Zeiger, A. S. & Van Vliet, K. J. Time-Dependent Extracellular Matrix Organization and Secretion from Vascular Endothelial Cells due to Macromolecular Crowding. *MRS Proc.* **1623,** mrsf13-1623-f02-10 (2014).

14. Ang, X. M. *et al.* Macromolecular crowding amplifies adipogenesis of human bone marrow-derived mesenchymal stem cells by enhancing the pro-adipogenic microenvironment. *Tissue Eng. Part A* **20,** 966–81 (2014).

15. Kumar, P. *et al.* Macromolecularly crowded in vitro microenvironments accelerate the production of extracellular matrix-rich supramolecular assemblies. *Sci. Rep.* **5,** 8729 (2015).

16. Benny, P., Badowski, C., Lane, E. B. & Raghunath, M. Making More Matrix: Enhancing the Deposition of Dermal–Epidermal Junction Components In Vitro and Accelerating Organotypic Skin Culture Development, Using Macromolecular Crowding. *Tissue Eng. Part A* **21,** 183–192 (2015).

17. Prewitz, M. C. *et al.* Extracellular matrix deposition of bone marrow stroma enhanced by macromolecular crowding. *Biomaterials* **73,** 60–9 (2015).

18. Harada, M. *et al.* Allogeneic bone marrow transplantation from a major ABO-incompatible donor. Infusion of hemopoietic stem cells isolated by Ficoll-Hypaque method. *Transplantation* **35,** 191–2 (1983).

19. Laessker, A. N., Hardarsson, T., Forsberg, A.-S., Mukaida, T. & Holmes, P. V. in *Cryopreservation of Mammalian Gametes and Embryos. Methods in Molecular Biology* (eds. Nagy, Z., Varghese, A. & Agarwal, A.) 355–365 (Humana Press, 2017). doi:10.1007/978-1-4939-6828-2_27

20. Chen, C. Z. *et al.* The Scar-in-a-Jar: studying potential antifibrotic compounds from the epigenetic to extracellular level in a single well. *Br.J.Pharmacol.* **158,** 1196–1209 (2009).

21. Peng, Y. & Raghunath, M. in *Tissue Engineering* (ed. Eberli, D.) (IntechOpen, 2010). doi:10.5772/8573

22. Satyam, A. *et al.* Macromolecular crowding meets tissue engineering by self-assembly: a paradigm shift in regenerative medicine. *Adv. Mater.* **26,** 3024–34 (2014).

23. Graupp, M. *et al.* Establishing principles of macromolecular crowding for in vitro fibrosis research of the vocal fold lamina propria. *Laryngoscope* **125,** E203–E209 (2015).

24. Cigognini, D. *et al.* Macromolecular crowding meets oxygen tension in human mesenchymal stem cell culture - A step closer to physiologically relevant in vitro organogenesis. *Sci. Rep.* **6,** 30746 (2016).

25. Kumar, P., Satyam, A., Cigognini, D., Pandit, A. & Zeugolis, D. I. Low oxygen tension and macromolecular crowding accelerate extracellular matrix deposition in human corneal fibroblast culture. *J. Tissue Eng. Regen. Med.* 6–18 (2017). doi:10.1002/term.2283

26. Gaspar, D., Fuller, K. P. & Zeugolis, D. I. Polydispersity and negative charge are key modulators of extracellular matrix deposition under macromolecular crowding conditions. *Acta Biomater.* **88,** 197–210 (2019).

27. Hojima, Y., Behta, B., Romanic, A. M. & Prockop, D. J. Cleavage of Type I Procollagen by C- and N-Proteinases Is More Rapid If the Substrate Is Aggregated with Dextran Sulfate or Polyethylene Glycol. *Anal. Biochem.* **223,** 173–180 (1994).

28. Lareu, R. R. *et al.* Collagen matrix deposition is dramatically enhanced in vitro when crowded with charged macromolecules: The biological relevance of the excluded volume effect. *FEBS Lett.* **581,** 2709–2714 (2007).

29. Lareu, R. R., Arsianti, I., Subramhanya, H. K., Yanxian, P. & Raghunath, M. In vitro enhancement of collagen matrix formation and crosslinking for applications in tissue engineering: a preliminary study. *Tissue Eng.* **13,** 385–391 (2007).

30. Dewavrin, J.-Y., Hamzavi, N., Shim, V. P. W. & Raghunath, M. Tuning the architecture of three-dimensional collagen hydrogels by physiological macromolecular crowding. *Acta Biomater.* **10,** 4351–9 (2014).

31. Dewavrin, J.-Y. *et al.* Synergistic rate boosting of collagen fibrillogenesis in heterogeneous mixtures of crowding agents. *J. Phys. Chem. B* **119,** 4350–8 (2015).

32. Mott, J. D. *et al.* Post-translational proteolytic processing of procollagen C-terminal proteinase enhancer releases a metalloproteinase inhibitor. *J. Biol. Chem.* **275,** 1384–90 (2000).

33. Grinnell, F. Fibronectin and wound healing. *J. Cell. Biochem.* **26,** 107–116 (1984).

34. Mosher, D. F. Assembly of fibronectin into extracellular matrix. *Curr. Opin. Struct. Biol.* **3,** 214–222 (1993).

35. Vogel, V. Mechanotransduction involving multimodular proteins: converting force into biochemical signals. *Annu. Rev. Biophys. Biomol. Struct.* **35,** 459–88 (2006).

36. Fernandez-Sauze, S., Grall, D., Cseh, B. & Van Obberghen-Schilling, E. Regulation of fibronectin matrix assembly and capillary morphogenesis in endothelial cells by Rho family GTPases. *Exp. Cell Res.* **315,** 2092–2104 (2009).

37. Singh, P., Carraher, C. & Schwarzbauer, J. E. Assembly of Fibronectin Extracellular Matrix. *Annu. Rev. Cell Dev. Biol.* **26,** 397–419 (2010).

38. Baneyx, G. & Vogel, V. Self-assembly of fibronectin into fibrillar networks underneath dipalmitoyl phosphatidylcholine monolayers: role of lipid matrix and tensile forces. *Proc. Natl. Acad. Sci. U. S. A.* **96,** 12518–12523 (1999).

39. Pankov, R. *et al.* Integrin dynamics and matrix assembly: tensin-dependent translocation of alpha(5)beta(1) integrins promotes early fibronectin fibrillogenesis. *J. Cell Biol.* **148,** 1075–90 (2000).

40. Baneyx, G., Baugh, L. & Vogel, V. Fibronectin extension and unfolding within cell matrix fibrils controlled by cytoskeletal tension. *Proc. Natl. Acad. Sci.* **99,** 5139–5143 (2002).

41. Hynes, R. O. The Extracellular Matrix: Not Just Pretty Fibrils. *Science (80-.).* **326,** 1216–1219 (2009).

42. Vogel, V. Unraveling the Mechanobiology of Extracellular Matrix. *Annu. Rev. Physiol.* **80,** 353–387 (2018).

43. McDonald, J. A., Kelley, D. G. & Broekelmann, T. J. Role of fibronectin in collagen deposition: Fab' to the gelatin-binding domain of fibronectin inhibits both fibronectin and collagen organization in fibroblast extracellular matrix. *J. Cell Biol.* **92,** 485–92 (1982).

44. Sottile, J. & Hocking, D. C. Fibronectin Polymerization Regulates the Composition and Stability of Extracellular Matrix Fibrils and Cell-Matrix Adhesions. *Mol. Biol. Cell* **13,** 3546–3559 (2002).

45. Sottile, J. *et al.* Fibronectin-dependent collagen I deposition modulates the cell response to fibronectin. *Am. J. Physiol. Physiol.* **293,** C1934–C1946 (2007).

46. Kadler, K. E., Hill, A. & Canty-Laird, E. G. Collagen fibrillogenesis: fibronectin, integrins, and minor collagens as organizers and nucleators. *Curr. Opin. Cell Biol.* **20,** 495–501 (2008).

47. Kubow, K. E. *et al.* Mechanical forces regulate the interactions of fibronectin and collagen I in extracellular matrix. *Nat. Commun.* **6,** 8026 (2015).

48. Huang, G. *et al.* Fibronectin Binds and Enhances the Activity of Bone Morphogenetic Protein 1. *J. Biol. Chem.* **284,** 25879–25888 (2009).

49. Saunders, J. T. & Schwarzbauer, J. E. Fibronectin matrix as a scaffold for procollagen proteinase binding and collagen processing. *Mol. Biol. Cell* **30,** 2218–2226 (2019).

50. Fogelgren, B. *et al.* Cellular Fibronectin Binds to Lysyl Oxidase with High Affinity and Is Critical for Its Proteolytic Activation. *J. Biol. Chem.* **280,** 24690–24697 (2005).

51. Baneyx, G., Baugh, L. & Vogel, V. Coexisting conformations of fibronectin in cell culture imaged using fluorescence resonance energy transfer. *Proc. Natl. Acad. Sci.* **98,** 14464–14468 (2001).

52. Baugh, L. & Vogel, V. Structural changes of fibronectin adsorbed to model surfaces probed by fluorescence resonance energy transfer. *J. Biomed. Mater. Res.* **69A,** 525–534 (2004).

53. Smith, M. L. *et al.* Force-induced unfolding of fibronectin in the extracellular matrix of living cells. *PLoS Biol.* **5,** e268 (2007).

54. Antia, M., Baneyx, G., Kubow, K. E. & Vogel, V. Fibronectin in aging extracellular matrix fibrils is progressively unfolded by cells and elicits an enhanced rigidity response. *Faraday Discuss.* **139,** 229 (2008).

55. Kubow, K. E. *et al.* Crosslinking of cell-derived 3D scaffolds up-regulates the stretching and unfolding of new extracellular matrix assembled by reseeded cells. *Integr. Biol. (Camb).* **1,**

635–48 (2009).

56. Pankov, R. Fibronectin at a glance. *J. Cell Sci.* **115,** 3861–3863 (2002).

57. Hayman, E. G. & Ruoslahti, E. DISTRIBUTION OF FETAL BOVINE SERUM FIBRONECTIN AND ENDOGENOUS RAT CELL FIBRONECTIN IN EXTRACELLULAR MATRIX.

58. George, E. L., Georges-Labouesse, E. N., Patel-King, R. S., Rayburn, H. & Hynes, R. O. Defects in mesoderm, neural tube and vascular development in mouse embryos lacking fibronectin. *Development* **119,** 1079–91 (1993).

59. Lenselink, E. A. Role of fibronectin in normal wound healing. *Int. Wound J.* **12,** 313–316 (2015).

60. Vogel, V. & Baneyx, G. The tissue engineering puzzle: a molecular perspective. *Annu. Rev. Biomed. Eng.* **5,** 441–63 (2003).

61. Gudzenko, T. & Franz, C. M. Studying early stages of fibronectin fibrillogenesis in living cells by atomic force microscopy. *Mol. Biol. Cell* 1–36 (2015). doi:10.1091/mbc.E14-05-1026

62. McDonald, J. A. Extracellular Matrix Assembly. *Annu. Rev. Cell Biol.* **4,** 183–207 (1988).

63. Little, W. C., Smith, M. L., Ebneter, U. & Vogel, V. Assay to mechanically tune and optically probe fibrillar fibronectin conformations from fully relaxed to breakage. *Matrix Biol.* **27,** 451–61 (2008).

64. Canty, E. G. & Kadler, K. E. Procollagen trafficking, processing and fibrillogenesis. *J. Cell Sci.* **118,** 1341–1353 (2005).

65. Li, S., Van Den Diepstraten, C., D'Souza, S. J., Chan, B. M. C. & Pickering, J. G. Vascular smooth muscle cells orchestrate the assembly of type I collagen via alpha2beta1 integrin, RhoA, and fibronectin polymerization. *Am. J. Pathol.* **163,** 1045–56 (2003).

66. Wenstrup, R. J. *et al.* Type V Collagen Controls the Initiation of Collagen Fibril Assembly. *J. Biol. Chem.* **279,** 53331–53337 (2004).

67. Tsutsumi, K. *et al.* Effects of L-ascorbic acid 2-phosphate magnesium salt on the properties of human gingival fibroblasts. *J. Periodontal Res.* **47,** 263–271 (2012).

68. Velling, T., Risteli, J., Wennerberg, K., Mosher, D. F. & Johansson, S. Polymerization of Type I and III Collagens Is Dependent On Fibronectin and Enhanced By Integrins α 11 β 1 and α 2 β 1. *J. Biol. Chem.* **277,** 37377–37381 (2002).

69. Moriya, K. *et al.* A Fibronectin-Independent Mechanism of Collagen Fibrillogenesis in Adult Liver Remodeling. *Gastroenterology* **140,** 1653–1663 (2011).

70. Kawelke, N. *et al.* Fibronectin Protects from Excessive Liver Fibrosis by Modulating the Availability of and Responsiveness of Stellate Cells to Active TGF-β. *PLoS One* **6,** e28181

(2011).

71. Altrock, E. *et al.* Inhibition of fibronectin deposition improves experimental liver fibrosis. *J. Hepatol.* **62,** 625–633 (2015).

72. Sakai, T. *et al.* Plasma fibronectin supports neuronal survival and reduces brain injury following transient focal cerebral ischemia but is not essential for skin-wound healing and hemostasis. *Nat. Med.* **7,** 324–330 (2001).

73. Ito, Y. & Selenko, P. Cellular structural biology. *Curr. Opin. Struct. Biol.* **20,** 640–8 (2010).

74. Gnutt, D., Gao, M., Brylski, O., Heyden, M. & Ebbinghaus, S. Excluded-Volume Effects in Living Cells. *Angew. Chemie Int. Ed.* **54,** 2548–2551 (2015).

75. Zhou, H.-X., Rivas, G. & Minton, A. P. Macromolecular Crowding and Confinement: Biochemical, Biophysical, and Potential Physiological Consequences. *Annu. Rev. Biophys.* **37,** 375–397 (2008).

76. Banks, A., Qin, S., Weiss, K. L., Stanley, C. B. & Zhou, H.-X. Intrinsically Disordered Protein Exhibits Both Compaction and Expansion under Macromolecular Crowding. *Biophys. J.* **114,** 1067–1079 (2018).

77. Peng, Y. *et al.* Human fibroblast matrices bio-assembled under macromolecular crowding support stable propagation of human embryonic stem cells. *J. Tissue Eng. Regen. Med.* **6,** e74-86 (2012).

78. Chen, B. *et al.* Macromolecular crowding effect on cartilaginous matrix production: a comparison of two-dimensional and three-dimensional models. *Tissue Eng. Part C. Methods* **19,** 586–95 (2013).

79. Kumar, P. *et al.* Macromolecular Crowding: The Next Frontier in Tissue Engineering. *Adv. Sci. Technol.* **96,** 1–8 (2014).

80. Kumar, P. *et al.* Accelerated Development of Supramolecular Corneal Stromal-Like Assemblies from Corneal Fibroblasts in the Presence of Macromolecular Crowders. *Tissue Eng. Part C. Methods* **21,** 660–70 (2015).

81. Lee, M. H. *et al.* ECM microenvironment unlocks brown adipogenic potential of adult human bone marrow-derived MSCs. *Sci. Rep.* **6,** 21173 (2016).

82. Satyam, A., Kumar, P., Cigognini, D., Pandit, A. & Zeugolis, D. I. Low, but not too low, oxygen tension and macromolecular crowding accelerate extracellular matrix deposition in human dermal fibroblast culture. *Acta Biomater.* **44,** 221–231 (2016).

83. Patrikoski, M. *et al.* Effects of Macromolecular Crowding on Human Adipose Stem Cell Culture in Fetal Bovine Serum, Human Serum, and Defined Xeno-Free/Serum-Free Conditions. *Stem Cells Int.* **2017,** 6909163 (2017).

84. Magno, V. *et al.* Macromolecular crowding for tailoring tissue-derived fibrillated matrices. *Acta Biomater.* **55,** 109–119 (2017).

85. Ng, W. L., Goh, M. H., Yeong, W. Y. & Naing, M. W. Applying macromolecular crowding to 3D bioprinting: fabrication of 3D hierarchical porous collagen-based hydrogel constructs. *Biomater. Sci.* **6,** 562–574 (2018).

86. Graceffa, V. & Zeugolis, D. I. Macromolecular crowding as a means to assess the effectiveness of chondrogenic media. *J. Tissue Eng. Regen. Med.* term.2783 (2018). doi:10.1002/term.2783

87. Ranamukhaarachchi, S. K. *et al.* Macromolecular crowding tunes 3D collagen architecture and cell morphogenesis. *Biomater. Sci.* (2019). doi:10.1039/C8BM01188E

88. Bateman, J. F. & Golub, S. B. Assessment of procollagen processing defects by fibroblasts cultured in the presence of dextran sulphate. *Biochem. J.* **267,** 573–577 (1990).

89. Avnur, Z. & Geiger, B. The removal of extracellular fibronectin from areas of cell-substrate contact. *Cell* **25,** 121–132 (1981).

90. Peters, D. M., Portz, L. M., Fullenwider, J. & Mosher, D. F. Co-assembly of plasma and cellular fibronectins into fibrils in human fibroblast cultures. *J. Cell Biol.* **111,** 249–56 (1990).

91. Mitra, S. K., Hanson, D. A. & Schlaepfer, D. D. Focal adhesion kinase: in command and control of cell motility. *Nat. Rev. Mol. Cell Biol.* **6,** 56–68 (2005).

92. Kim, J. S. & Yethiraj, A. Crowding effects on association reactions at membranes. *Biophys. J.* **98,** 951–8 (2010).

93. Chapanian, R. *et al.* Enhancement of biological reactions on cell surfaces via macromolecular crowding. *Nat. Commun.* **5,** 4683 (2014).

94. Chabria, M., Hertig, S., Smith, M. L. & Vogel, V. Stretching fibronectin fibres disrupts binding of bacterial adhesins by physically destroying an epitope. *Nat. Commun.* **1,** 135 (2010).

95. Hertig, S., Chabria, M. & Vogel, V. Engineering Mechanosensitive Multivalent Receptor–Ligand Interactions: Why the Nanolinker Regions of Bacterial Adhesins Matter. *Nano Lett.* **12,** 5162–5168 (2012).

96. Klotzsch, E. *et al.* Fibronectin forms the most extensible biological fibers displaying switchable force-exposed cryptic binding sites. *Proc. Natl. Acad. Sci. U. S. A.* **106,** 18267–72 (2009).

97. Legant, W. R., Chen, C. S. & Vogel, V. Force-induced fibronectin assembly and matrix remodeling in a 3D microtissue model of tissue morphogenesis. *Integr. Biol. (Camb).* **4,** 1164–74 (2012).

98. Li, B., Moshfegh, C., Lin, Z., Albuschies, J. & Vogel, V. Mesenchymal Stem Cells Exploit

Extracellular Matrix as Mechanotransducer. *Sci. Rep.* **3,** 2425 (2013).

99. Li, B., Lin, Z., Mitsi, M., Zhang, Y. & Vogel, V. Heparin-induced conformational changes of fibronectin within the extracellular matrix promote hMSC osteogenic differentiation. *Biomater. Sci.* **3,** 73–84 (2015).

100. Kollmannsberger, P., Bidan, C. M., Dunlop, J. W. C., Fratzl, P. & Vogel, V. Tensile forces drive a reversible fibroblast-to-myofibroblast transition during tissue growth in engineered clefts. *Sci. Adv.* **4,** eaao4881 (2018).

101. Ortiz Franyuti, D., Mitsi, M. & Vogel, V. Mechanical Stretching of Fibronectin Fibers Upregulates Binding of Interleukin-7. *Nano Lett.* **18,** 15–25 (2018).

102. Früh, S. M., Schoen, I., Ries, J. & Vogel, V. Molecular architecture of native fibronectin fibrils. *Nat. Commun.* **6,** 7275 (2015).

103. Hayman, E. G. Distribution of fetal bovine serum fibronectin and endogenous rat cell fibronectin in extracellular matrix. *J. Cell Biol.* **83,** 255–259 (1979).

104. Ugarova, T. P. *et al.* Conformational Transitions in the Cell Binding Domain of Fibronectin. *Biochemistry* **34,** 4457–4466 (1995).

Acknowledgements

I received the support of so many people throughout my PhD journey who helped make this possible and who I would like to recognize here.

I would first like to say a huge thank you to my supervisor Viola Vogel for her guidance and support in completing this work. Thank you for accepting me as an exchange student to your lab, and then giving me the opportunity to stay, thereby enabling me to pursue my professional goals alongside my personal goals. Thank you also for creating such a wonderful lab environment which I have enjoyed working in immensely.

Next, I would also like to say a huge thank you to my former supervisor Denis Wirtz for supporting me when I asked to move to Switzerland during my PhD, even though it eventually meant that I would never move back. I have always really enjoyed your infectious enthusiasm for science and I am very glad that we have been able to stay in touch.

I would also like to thank Michael Raghunath who I serendipitously met after he moved from Singapore to Switzerland at just the right time to become a mentor for me and provide his expertise in crowding. I have really enjoyed our discussions and your guidance and expertise have been very valuable.

The following people also made specific contributions to this work that I would like to recognize:

Jens Möller for many valuable discussions and helpful input, Chantel Spencer-Hänsch for isolating human plasma fibronectin, Sebastian Lickert and Kateryna Selcuk for providing fluorescently-labeled fibronectin, Mario Benn for help with FRET experiments and for providing FRET-labeled fibronectin, Simon Arnoldini for providing Alexa-647 fibronectin and code for FRET analysis, Nikhil Jain for help getting this project started, Justine Kusch and the ScopeM microscopy center at ETH for microscopy support, as well as Malgorzata Kisielow, Anette Schütz, and the Flow Cytometry Core Facility at ETH for flow cytometry support.

I would also like to thank all of the members of the Vogelschar, current and former, who I have had the great pleasure to work with and develop friendships with.

I would like to thank my family in the US for their unwavering support, throughout my entire life, and especially when I moved across the Atlantic. It means everything to have you all with me and on my side wherever I go. Thanks dad for your invaluable guidance, for instilling in me a love of science and engineering, and for telling me to learn coding. Thanks mom for always being my best friend and biggest fan. I would also like to thank my family in Austria for welcoming me so warmly and helping me to create a second home in Europe. Finally, I thank you to my fiancé Lukas Rantner for your invaluable guidance, support, and love, and for creating a great life with me in Switzerland.

Funding sources

This research was supported by ETH Zürich, the National Cancer Institute at the National Institutes of Health (Grant #U54CA210173, Denis Wirtz), and the Institute for International Education (Whitaker International Program Fellowship, Jenna Graham).

Appendix

A. Protocols

A.1. ECM assembly +/- Ficoll (fluorescently labeled fibronectin)

Note: procedure can also be done with fibronectin antibody rather than fluorescently-labeled fibronectin. In this case use 50µg/mL unlabeled fibronectin for the coating and cell culture media and stain for fibronectin at the same time as collagen I with purified mouse anti-fibronectin antibody (BD #610077, 1:200) and donkey anti-mouse-488 (Invitrogen #A-21202, 1:200).

Cells: Normal human dermal fibroblasts (PromoCell, Vitaris AG, Switzerland)

Media: MEM Alpha, (Biowest #L0475), 10% fetal bovine serum (Biowest #S181H), and 1% penicillin-streptomycin (Gibco #15140122)

Crowders:
70kDa Ficoll (GE Healthcare #GE17-0310)
400kDa Ficoll (GE Healthcare #GE17-0300)

Antibodies and dyes:
Abcam anti-collagen I #34710
Invitrogen donkey anti-rabbit-546 (#A10040)
Phalloidin 488 (Invitrogen, #A12379)
Hoechst 33342 (Thermo Scientific #62249)

Other materials:
Human plasma fibronectin (isolated from plasma)
HellmaneX (Hellma #9-307-010-507)
0.25% Trypsin-EDTA (Invitrogen 25200-056)
L-ascorbic acid 2-phosphate (Sigma #A8960)
BSA (AppliChem GmbH #A1391)
Triton X-100 (AppliChem #A4975)
Dako mounting media (Dako #S3023)
Nailpolish

Plate layout: below x3 (one plate each for 16hrs, 24hrs, 6 days)

-Ficoll	+Ficoll		
-Ficoll	+Ficoll		
-Ficoll	+Ficoll		

Procedure:

- Clean coverslips in 2% Hellmane X solution in a sonicator for 30 minutes, and 30 minutes not in sonnicator, wash with DI water and blow dry, store dry (can do ahead)
- Dissolve 37.5mg/mL 70kDa Ficoll and 25mg/mL 400kDa Ficoll in standard media in a water bath, filter through a 0.22um syringe filter. Also filter an appropriate amount of media without Ficoll for control samples.
- Freshly rinse coverslips with DI water, blow dry, place in 12-well culture plate
- Sterilize by UV in the biosafety cabinet for 15min
- Place 100uL drop of fibronectin (45ug/mL unlabeled Fn + 5ug/mL Fn-647 in PBS) on each coverslip. Coat in the biosafety cabinet for 1 hour at room temperature, protected from light.
- Wash x3 with PBS
- Wash cells with PBS, trypsinize (750uL 0.25% trypsin), add 9.5mL media, count, and spin down
- Resuspend cells in standard media to achieve 5,000cells/cm2 in 1mL per well (for 3.6cm2 area of 12 well plate: 18,000 cells/mL), add 1mL cell suspension to each well (careful not to tilt or disturb dish after adding cells. Move carefully to the incubator.
- *Note: swirling or shaking dish side-to-side will result in a high concentration of cells in the center of the well. It is better to mix the cells in the media before and then disturb the dish as little as possible after they are in the well.*
- After 1 hr, change media to +/- Ficoll and the following:
    - L-AA2P (add L-AA2P fresh just after media change, 1:1000 dilution of 100mM stock aliquoted and stored at -20C)
    - 45ug/mL unlabeled FN + 5ug/mL Fn-647
- After 16hrs, fix (wash with PBS, coat with 4% PFA for 20min at room temperature, wash x3 with PBS)
- After 48hrs, fix
- After 3 days, change media on 6 day samples (+/- Ficoll, +Fn, +L-AA2P)
- After 6 days, fix

Staining:

- Block with 5% BSA in PBS for 1hr at room temperature
- Stain with primary antibody in 5% BSA for 1hr at room temperature. Invert each coverslip onto a 100uL drop of antibody solution on parafilm.
    - 1:200 Col1(rb) ab34710, -20Common
- Return coverslips to 12-well plate. Wash x3 with 1% BSA in PBS.
- Stain with primary antibody in 5% BSA for 1hr at room temperature. Invert each coverslip onto a 100uL drop of antibody solution on parafilm.
    - 1:200 donkey-anti rabbit 546
- Return coverslips to 12-well plate. Wash x3 with PBS.
- Permeabilize by covering each coverslip with 0.3% v/v Triton X-100 in PBS for 15min at room temperature
- Wash x3 with PBS.
- Stain actin and nucleus with the following dyes in 5% BSA in PBS for 1 hour at room temperature. Invert each coverslip onto a 100uL drop of antibody solution on parafilm.
    - 1:500 phalloidin 488
    - 1:200 Hoescht
- Return coverslips to 12-well plate. Wash x3 with PBS
- Mount inverted onto glass slides on top of a drop of mounting media
- Let dry overnight, protected from light.
- Seal with nailpolish and image.

A.2. Crosslinked fibronectin coating

Materials:

HellmaneX (Hellma #9-307-010-507)
(3-Aminopropyl)triethoxysilane (APTES) (Sigma-Aldrich #A3648)
Glutaraldehyde (Sigma-Aldrich #G4004)
Human plasma fibronectin (self-isolated)
Plasma cleaner (Harrick Plasma PDC-32G)

Procedure:

- Clean coverslips in 2% Hellmane X in sonicator for 30 minutes, and 30 minutes not in sonicator
- Wash with deionized water and blow dry, store dry or use immediately
- Complete the following steps in a chemical hood:
- Prepare 2% APTES in deionized water
    Note: needs to be made fresh
    Note: purge APTES bottle with inert gas before storing again
- Treat coverslips with air plasma for 30s (approx.. 0.36mbar at 200W) in parafilm coated plastic dish
- Immediately add 200uL 2% APTES, incubate at room temperature for 15 min
- Rinse 3x with deionized water
- Treat with 200uL glutaraldehyde (0.125% in water) for 30 min at room temperature
- Wash x3 with deionized water
- The following 2 steps can be done in open air:
- Coat treated coverslips with plasma fibronectin at 50µg/mL, 100uL per coverslip, 1hr at room temperature
- Wash x3 with PBS
- Sterilize by UV for 15min in biosafety cabinet
- Keep in PBS in sterile conditions until cell seeding

B. MATLAB analysis code

B.1. FRET analysis code

```
%This code completes FRET analysis.  It was written to batch process FRET images stored in nested folders: 'sample name'/Z001/s_001.tif (acceptor) and s_002.tif (donor)
%Code written by Jenna Graham, adapted from Simon Arnoldini
%User should specify the experiment folder containing the images in the file structure stated above as the variable subfolder.
%Variables fiberThresh and labelThresh should be set by the user.  They specify intensity thresholds after dark current subtraction.  Thresholds were typically set to 100.

%Output variables are saved in the inner-most nested folder with the images:
%Output.txt - text file with measured variables (Acceptor Mean, Donor Mean, FRET ratio mean, FRET ratio mode, FRET ratio standard deviations, Number of FRET ratios, 5th percentile, 95th percentile, number of pixels with FRET>1M GdnHCl)
%vector.txt - all FRET ratios saved in a vector (no spatial information saved)
%ir.mat - matrix of all FRET ratios.  Can be used to generate image of FRET ratios (spatial information is maintained)
%FRET.tif - FRET image with FRET histogram below

%Several graphs are shown during analysis and can be suppressed by commenting out the lines starting with figure...
%Analysis waits for user to press any key before continuing to the next z-level or sample.  This can be suppressed by commenting out the pause command

clear all;
clc;

%***User specify this variable***
subfolder = '20180716 Coating analysis';
folders = dir([subfolder '/*']);
a = size(folders);
outputMatrix = [];

%Loop through samples
for i = 1:a(1)
   zs = dir([subfolder '/' folders(i).name '/Z*']);
   b = size(zs);

   %Loop through z-levels (Z001, Z002, Z003, ...)
   for j = 1:b(1)

      %Load images
      path = [subfolder '/' folders(i).name '/Z00' num2str(j) '/']
```

```
files = dir([path 's_C00*.tif']);
donor = imread([path files(2).name]);
acc = imread([path files(1).name]);
filename = 'FRET.tif';

%Dark current from the microscope detector.  Subtracted from both images before analysis.
dc1 = 174 ; dc2 = 174;

%***User specify these thresholds***
fiberThresh = 100;
labelThresh = 100;

%***User can also specify a range for the FRET values.  Default is [0,1].
upLimit = 1; lowLimit = 0; limits = [lowLimit upLimit];
z = 100; binsize = (upLimit-lowLimit)/z;

%Convert to double precision
acc = double(acc); donor = double(donor);

figure(2); imshow(donor, [min(min(donor)) max(max(donor))]);

%Averaging mask
acc = colfilt(acc,[2 2],'sliding', @mean); donor = colfilt(donor,[2 2],'sliding',@mean);

figure(3); imshow(donor, [min(min(donor)) max(max(donor))]);

%Remove dark current offset
acc = acc-dc1; donor = donor-dc2;

%Eliminate pixels below threshold and saturated pixels
threshIndlabel = find(acc <= labelThresh | acc >= 3900); threshIndfiber = find(donor <= fiberThresh | donor >= 3900);
acc(threshIndlabel) = 0; donor(threshIndfiber) = 0;

%FRET correction to account for bleedthrough
acc = acc - 0.2*donor;

%FRET calculation
ir = acc./donor;

%Remove un-realistic ir values and NaNs
realInd = find((isnan(ir) | ir < lowLimit | ir > upLimit));
ir(realInd) = 0;

%Range of possible FRET ratios
fret_range = upLimit-lowLimit;
```

```
%Generate colormap.
%***User can specify the range for the colormap.***
%Default is 0-0.6 because we do not typically see many FRET values above 0.6.
cm = zeros(256,3);
startfret = round((0-lowLimit)/fret_range*256);
endfret = round((0.6-lowLimit)/fret_range*256);
cmjet = jet(256);
cm(startfret+1:endfret,:) = resample(cmjet,endfret-startfret,256);

%Fill rest of colormap
for j=1:startfret+1
   cm(j,:) = cmjet(1,:);
end
for j=endfret+1:256
   cm(j,:) = cmjet(end,:);
end

%Background = black
cm(1,:) = [0,0,0];
cm(cm>1)=1;
cm(cm<0)=0;

%Scale and display image
figure(1);
imagesc(ir,limits); %display image on scaled colormap
axis square;
axis off
colormap(cm);
colorbar('NorthOutside');

%Determine number of ir pixels and ir statistics
 avgirArray=nonzeros(ir);
 avgirsize=size(avgirArray);
 avgirmean=mean(avgirArray);
 avgirstd=std(avgirArray);
per5 = prctile(avgirArray,5); per95 = prctile(avgirArray,95);
avglabelArray=nonzeros(acc); avglabelmean=mean(avglabelArray);
avgfiberArray=nonzeros(donor); avgfibermean=mean(avgfiberArray);

%Generate a histogram for ir mode determination and display
bins = lowLimit:binsize:upLimit;
[histCounts, histX] = hist(avgirArray,bins);
[C,I] = max(histCounts);
modeReal = histX(I);  %Calculate mode from histogram data
histCounts = histCounts/C;  %normalize the image to scale from 0.0-1.0

%Plotting
```

```
    subplot(3,1,[1 2]); imagesc(ir, limits);
    axis off; axis square; colorbar('horiz'); set(gca, 'FontName', 'Times New Roman', 'FontSize', 12);
    subplot(3,1,[3]); bar(histX, histCounts);
    xlabel('intensity ratio (acceptor/donor)', 'FontName', 'Times New Roman', 'FontSize', 12);
    ylabel('events', 'FontName', 'Times New Roman', 'FontSize', 12);
    set(gca, 'FontName', 'Times New Roman', 'FontSize', 12); axis([lowLimit upLimit 0 1]);

    %Save the final data as a .tiff
    saveas(figure(1), [path filename], 'tif');

    %Display FRET image alone
    figure(4);
    imagesc(ir,limits);
    axis square;
    axis off
    colormap(cm);
    colorbar('NorthOutside');

    %Calculate number of pixels above 1M line (representing unstretched fibronectin)
    %***User should specify the FRET ratio in 1M GdnHCl***
    oneMline = 0.337;
    numAboveOneM = sum(avgirArray>oneMline);

    %Output data for further analysis into a text file
    output = [ avglabelmean avgfibermean avgirmean modeReal avgirstd avgirsize(1,1) per5 per95
    numAboveOneM];
    dlmwrite([path 'Output.txt'],output,'delimiter','\t')
    dlmwrite([path 'vector.txt'],avgirArray,'delimiter','\t')
    save([path 'ir.mat'],'ir');

    %Wait for user to press any key before continuing to the next sample or z-level.  Comment out
    to suppress.
    pause;
  end
end
```

B.2. Code to generate FRET histograms of -Ficoll and +Ficoll conditions overlayed (2-day matrices)

```
%This code makes a combined histogram of two different conditions, with all FRET ratios from each individual image combined into one histogram for each condition
%It should be run from within the experiment folder, where there are folders for each ROI named +Ficoll... and -Ficoll...
%It considers only the first z-slice (Z001).
%The 1M and 4M GdnHCl lines are included in the graphs.  User should change the values according to the calibration of their FRET-Fn batch.

clear all;
clc;

%Initialize vectors
all_vector_no_ficoll = double.empty;
all_vector_ficoll = double.empty;

%Collect all FRET ratios for each condition into vectors
files_no_ficoll = dir('-*');
files_ficoll = dir('+*');
a = size(files_no_ficoll);
b = size(files_ficoll);
for i = 1:a(1)
   vec = dlmread([files_no_ficoll(i).name '/Z001/vector.txt']);
   all_vector_no_ficoll = cat(1, all_vector_no_ficoll,vec);
end
for j = 1:b(1)
   vec = dlmread([files_ficoll(j).name '/Z001/vector.txt']);
   all_vector_ficoll = cat(1, all_vector_ficoll,vec);
end

%Generate the histograms
upLimit = 1; lowLimit = 0;
z = 100; binsize = (upLimit-lowLimit)/z;
bins = lowLimit:binsize:upLimit;

[histCounts, histX] = hist(all_vector_no_ficoll,bins);
[C,I] = max(histCounts);
histCountsNorm = histCounts/C;

[histCounts2, histX2] = hist(all_vector_ficoll,bins);
[C2,I2] = max(histCounts2);
histCounts2Norm = histCounts2/C2;
```

```
%***User should change the values for the GdnHCl lines here***
oneMLine = 0.34;
fourMLine = 0.23;

%Plot the non-normalized histograms
figure(1);
plot(histX,histCounts,'b',histX2,histCounts2,'r');
hold on;
line([oneMLine oneMLine],get(gca,'YLim'),'Color',[0 0 0],'LineStyle','--');
line([fourMLine fourMLine],get(gca,'YLim'),'Color',[0 0 0],'LineStyle','--');
hold off;

%Plot the normalized histograms
figure(2);
plot(histX,histCountsNorm,'b',histX2,histCounts2Norm,'r');
hold on;
line([oneMLine oneMLine],get(gca,'YLim'),'Color',[0 0 0],'LineStyle','--');
line([fourMLine fourMLine],get(gca,'YLim'),'Color',[0 0 0],'LineStyle','--');
hold off;
```

B.3. Code to generate FRET histograms of -Ficoll and +Ficoll conditions overlayed (6 day-matrices)

```
%This code is used to generate combined histograms from 6 day old matricies.  The z-level with the highest number of FRET ratios is added to the combined vector.  This is meant to select the depth with the most in-focus fibronectin.

clear all;
clc;

all_vector_no_ficoll = double.empty;
all_vector_ficoll = double.empty;

folders = dir('-Ficoll*');
a = size(folders);
outputMatrix = [];
for i = 1:a(1)
   zs = dir([folders(i).name '/Z*']);
   b = size(zs);
   outputmatrixTemp = [];
   for j = 1:b(1)
      outputmatrixTemp(j,:) = dlmread([folders(i).name '/Z00' num2str(j) '/Output.txt']);
   end
   [M,I] = max(outputmatrixTemp(:,6));
   outputMatrix(i,:) =
   [str2num(folders(i).name(10)),str2num(folders(i).name(13)),I,outputmatrixTemp(I,:)];
   vec = dlmread([folders(i).name '/Z00' num2str(I) '/vector.txt']);
   all_vector_no_ficoll = cat(1, all_vector_no_ficoll,vec);
end

folders2 = dir('+Ficoll*');
a2 = size(folders2);
outputMatrix2 = [];
for i = 1:a2(1)
   zs2 = dir([folders2(i).name '/Z*']);
   b2 = size(zs2);
   outputmatrixTemp2 = [];
   for j = 1:b2(1)
      outputmatrixTemp2(j,:) = dlmread([folders2(i).name '/Z00' num2str(j) '/Output.txt']);
   end
   [M2,I2] = max(outputmatrixTemp2(:,6));
   outputMatrix2(i,:) =
   [str2num(folders2(i).name(10)),str2num(folders2(i).name(13)),I2,outputmatrixTemp2(I2,:)];
   vec2 = dlmread([folders2(i).name '/Z00' num2str(I2) '/vector.txt']);
   all_vector_ficoll = cat(1, all_vector_ficoll,vec2);
```

```
end

upLimit = 1; lowLimit = 0;
z = 100; binsize = (upLimit-lowLimit)/z;
bins = lowLimit:binsize:upLimit;

[histCounts, histX] = hist(all_vector_no_ficoll,bins);
[C,J] = max(histCounts);
histCountsNorm = histCounts/C;

[histCounts2, histX2] = hist(all_vector_ficoll,bins);
[C2,J2] = max(histCounts2);
histCounts2Norm = histCounts2/C2;

%***User should change the values for the GdnHCl lines here***
oneMLine = 0.34;
fourMLine = 0.23;

figure(1);
plot(histX,histCounts,'b',histX2,histCounts2,'r');
hold on;
line([0.34 0.34],get(gca,'YLim'),'Color',[0 0 0],'LineStyle','--');
line([0.23 0.23],get(gca,'YLim'),'Color',[0 0 0],'LineStyle','--');
hold off;

figure(2);
plot(histX,histCountsNorm,'b',histX2,histCounts2Norm,'r');
hold on;
line([0.34 0.34],get(gca,'YLim'),'Color',[0 0 0],'LineStyle','--');
line([0.23 0.23],get(gca,'YLim'),'Color',[0 0 0],'LineStyle','--');
hold off;
```

B.4. Code to display image of FRET ratios

```
%This code is an excerpt from the FRET analysis code that displays the FRET image from the ir variable
%User should load ir.mat into the workspace if it is not already there

upLimit = 1; lowLimit = 0; limits = [lowLimit upLimit];
fret_range = upLimit-lowLimit;
cm = zeros(256,3);
startfret = round((0-lowLimit)/fret_range*256);
endfret = round((0.6-lowLimit)/fret_range*256);
cmjet = jet(256);
cm(startfret+1:endfret,:) = resample(cmjet,endfret-startfret,256);
for j=1:startfret+1
   cm(j,:) = cmjet(1,:);
end;
for j=endfret+1:256
   cm(j,:) = cmjet(end,:);
end;
cm(1,:) = [0,0,0];
cm(cm>1)=1;
cm(cm<0)=0;
figure(1);
imagesc(ir,limits);
axis square;
axis off
colormap(cm);
c = colorbar('EastOutside');
set(c,'FontName','Arial','FontSize',14,'FontWeight','bold');
```

B.5. Code to analyze cell density and matrix assembly

```
%This code analyzes the cell density, summed fibronectin and collagen I, and area covered by
fironectin
%It expects a folder with many tiff images (like from an exported tilescan)
%ch00 = Hoescht
%ch01 = Fibronectin
%ch02 = Collagen I
%(These channel assignments can be changed below)
%User will be prompted to select the folder to be analyzed.  There should be no folders inside the
folder selected, only the images that should be analyzed.
%Each image will go through nuclear segmentation and then be displayed and the user must decide
for each if it is to be analyzed.  This way images with poor segmentation or debris can be excluded.
%User should define the background for fibronectin and collagen, and the threshold for fibronectin
area determination
%Output matrix data is generated with calculated values for each image.  This output file is only
saved in the MATLAB workspace.  It should be copied or saved elsewhere to keep data.

clc;
clear all;

%Select folder
folder =  uigetdir()
files = dir(fullfile(folder, '*ch00.tif'));
[numFiles,~] = size(files);

%Initialize variables
numNuclei = [];
cellDensity = [];
fnSum = [];
colSum = [];
area_fn = [];
index = 0;

%Increment through images
for h = 1:numFiles

   %Import images
   %***User can change channel assignments
   Idna = imread([folder '\' files(h,1).name]); %Hoechst
   Ifn = imread([folder '\' files(h,1).name(1:end-5) '2.tif']);
   Icol = imread([folder '\' files(h,1).name(1:end-5) '1.tif']);

   %Segment nuclei
```

```
%***User can adjust this parameter to tune the nuclear segmentation.  If nuclei are excluded, the fudge factor should be lowered.  If tracing is larger than the nucleus, the fudge factor should be lowered.  Usually a value between 0.6 and 1.5 works well.
fudgefactor = 1;  %Change to adjust tracing

%Detect edges
[a threshold] = edge(Idna, 'sobel');
threshold = threshold * fudgefactor;
edges = edge(Idna,'sobel', threshold);

%Dilate edges
disk = strel('disk',1);
dilated = imdilate(edges, disk);

%Fill holes
filled = imfill(dilated, 'holes');

%Erode edges
eroded = imerode(filled,disk);

%Remove small objects
cleaned = bwareaopen(eroded,150);

%Display tracing overlayed on original nuclei image
outline = bwperim(cleaned);
traced = Idna;
[r,c] = size(Idna);
for i = 1:r
   for j = 1:c
      if outline(i,j) == 1
         traced(i,j) = max(max(Idna));
      end
   end
end

%Threshold Fn image to exclude background and coating
%***User should define this threshold to include fibronectin fibers but not coating.  Threshold is 0-1, so intensity should be divided by the maximum possible intensity.***
fnbinary = im2bw(Ifn,500/65535);
fnbinary = imcomplement(fnbinary);

%Display segmented nuclei, Fn image, binary Fn image
figure(1), imshow(traced, [min(min(Idna)) max(max(Idna))]), title('Traced nuclei');
figure(2), imshow(Ifn, [0 8000]), title('Fibronectin');
figure(3), imshow(fnbinary), title('Thresholded Fn');

%Ask if image should be analyzed.
```

```
  %***User should type 0+Enter (no) if nuclei segmentation not good, coating not good, or
 threshold not good, otherwise they should type 1+Ener (yes).
  analyze = input('Analyze this image? (0/1)');
  if analyze
     index = index+1;

     %Calculate #cells, cell density
     [~, numNuclei(index)] = bwlabel(cleaned);
     %***User should adjust the line below based on the size of the image***
     cellDensity(index) = numNuclei(index)/(749.82*749.82*(10^-4)*(10^-4));  %Cells/cm2

     %Calculate summed intensity of Fn and Col
     totalArea = 1616*1616;
     %***User should set Fn background here***
     Ifn = Ifn-305;
     fnSum(index) = sum(sum(Ifn));
     %***User should set Col background here***
     Icol = Icol-204;
     colSum(index) = sum(sum(Icol));

     %Calculate area coverage of fibronectin in microns^2
     %***User should adjust the line below based on the size of the image***
     area_fn(index) = sum(sum(fnbinary))*(749.82*749.82)/totalArea;
  end
end

%Save data
for i = 1:index
  data(i,:) = [numNuclei(i) cellDensity(i) fnSum(i) colSum(i) fn_cell(i) col_cell(i) area_fn(i)];
end
```

B.6. Code to sum the intensity of a marker in the nucleus

```
%This code segments nuclei and sums the intensity of the label in Channel 1
%An additional segment of code if included to exclude nuclei with circularity <0.65.  This helps to exclude debris and nuclei that are segmented together.
%Code loops through several images in one folder
%Output data for all nuclei analyzed is in the vector sumChannel1 in the workspace.  This data needs to be copied or saved elsewhere.
%Nuclei that are cut off at the edges of the image are not included in the analysis.

clc;
clear all;

%Load files
folder =  uigetdir();
files = dir(fullfile(folder, '*ch00.tif'));
[numFiles,~] = size(files);

numObjects = zeros(numFiles, 1);
sumChannel1 = [];

for h = 1:numFiles
   I0 = double(imread([folder '\' files(h,1).name])); %Hoechst
   I1 = double(imread([folder '\' files(h,1).name(1:end-5) '1.tif']));

   fudgefactor = 1;

   %Detect edges
   [a threshold] = edge(I0, 'sobel');
   threshold = threshold * fudgefactor;
   edges = edge(I0,'sobel', threshold);

   %Dilate edges
   disk = strel('disk',1);
   dilated = imdilate(edges, disk);

   %Fill holes
   filled = imfill(dilated, 'holes');

   %Erode
   eroded = imerode(filled,disk);

   %Remove small objects
   cleaned = bwareaopen(eroded,200);
```

```
%Exclude objects cut off at border
excluded = imclearborder(cleaned);

%Display tracing overlayed on original image
outline = bwperim(excluded);
traced = I0;
[r,c] = size(I0);
for i = 1:r
   for j = 1:c
      if outline(i,j) == 1
         traced(i,j) = max(max(I0));
      end
   end
end
figure(10), imshow(traced, [min(min(I0)) max(max(I0))]), title('Traced nuclei');

%Exclude non-circular nuclei
[labeledn, numObjectsn(h)] = bwlabel(excluded);
perimeters = regionprops(labeledn,'Perimeter');
areas = regionprops(labeledn,'Area');
pixels = regionprops(labeledn,'PixelList');
for i = 1:numObjectsn(h)
   circularity = ((4*pi).*areas(i,1).Area)./(perimeters(i,1).Perimeter.^2);
   %If circularity is low, remove object from binary image
   if circularity < 0.65
      pix = pixels(i,1).PixelList;
      [j1,~] = size(pix);
      for j = 1:j1
         excluded(pix(j,2),pix(j,1)) = 0;
      end
   end
end

%Display tracing overlayed on original image
outline = bwperim(excluded);
traced = I0;
[r,c] = size(I0);
for i = 1:r
   for j = 1:c
      if outline(i,j) == 1
         traced(i,j) = max(max(I0));
      end
   end
end
figure(11), imshow(traced, [min(min(I0)) max(max(I0))]), title('Traced nuclei');

%Exclude images with poor segmentation
```

```
  analyze = input('Analyze this image? (0/1)');
  if analyze
    %Count and label objects
    [labeledn, numObjectsn(h)] = bwlabel(excluded);

    %Get pixel values for each nucleus
    Channel1int = regionprops(labeledn,I1,'PixelValues');

    %Calculate sum Channel1 for each cell and add to array
    for i = 1:numObjectsn(h)
      sumCh1temp = sum(Channel1int(i,1).PixelValues);
      sumChannel1 = cat(1,sumChannel1,sumCh1temp);
    end
  end
end
```

C. Notes about ECM visualization

C.1. Collagen visualization without permeabilization

Collagen was visualized by antibody staining without permeabilization throughout this work. The reason is that there is a lot of intracellular collagen that gets stained if cells are permeabilized before, and this intracellular collagen is much brighter than the extracellular fibers that we want to visualize. Figure C.1 shows an example of two different samples from the same experiment, where one was stained for collagen before permeabilization and the other was stained after permeabilization. Both were stained with Abcam primary antibody #34710 (1:200) and donkey anti-rabbit-546 secondary antibody (Invitrogen #A10040, 1:200). Permeabilization was performed with 0.3% Triton X-100 (AppliChem #A4975) for 15 minutes. It is clear that collagen fibers can only be visualized if they are stained before cell permeabiliztion. The second row of images shows the corresponding Alexa 647-fibronectin. The colocalization of collagen and fibronectin can only be seen when collagen is stained before permeabilization. See section 10.5 for the protocol for collagen staining that was used consistently throughout this work.

When fibronectin was visualized by antibody staining, it was also stained before permeabilization.

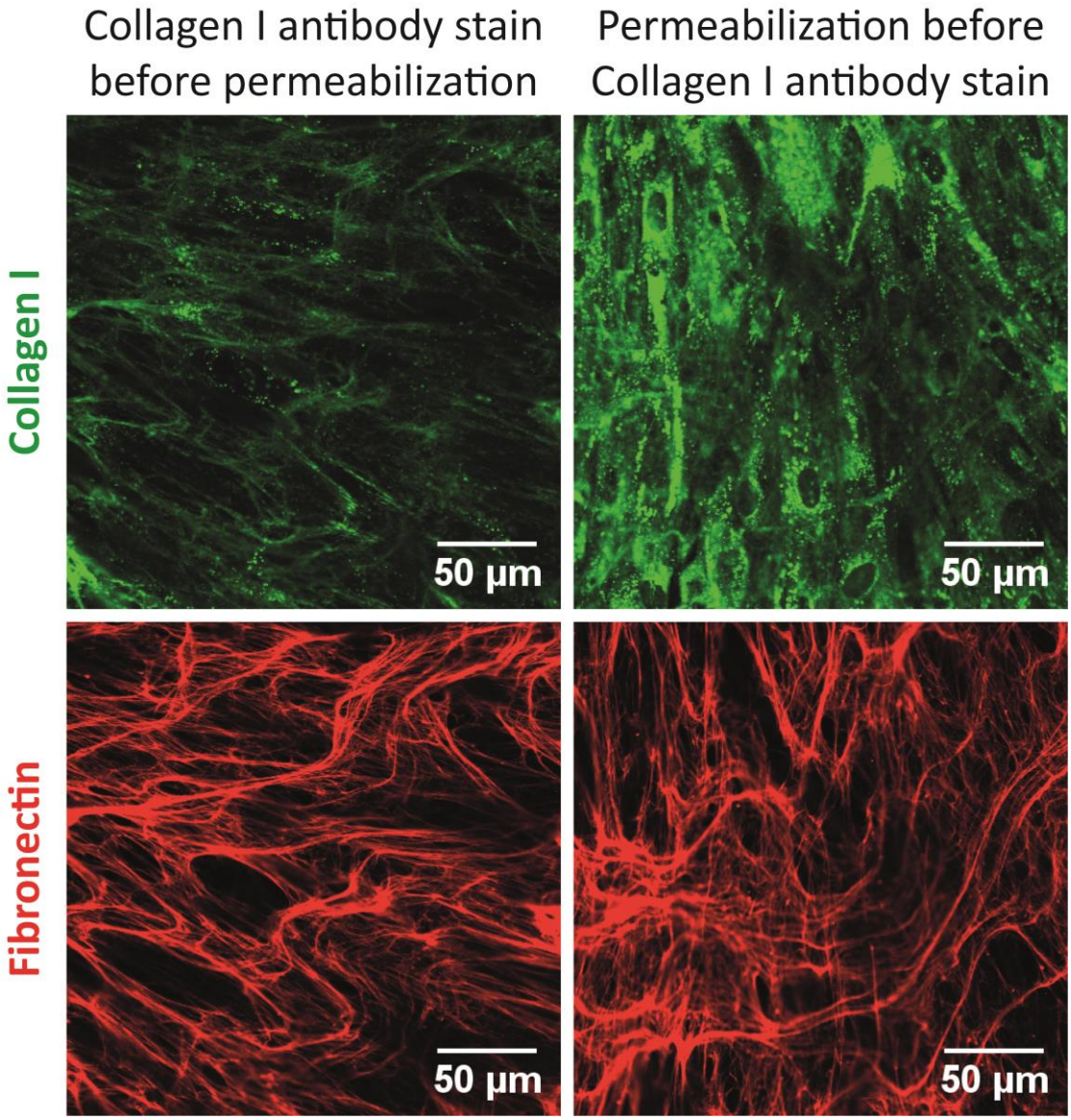

Figure C.1 Representative 6-day matricies from the same experiment that were stained differently for collagen (green). The left image shows the signal when collagen is stained before cell permeabilization. The right image shows the signal when collagen is stained after cell permeabilization. The second row shows corresponding Alexa-647-labeled fibronectin (red). Abcam antibody #34710 was used to visualize collagen (see materials and methods for procedure).

C.2. Comparison of fibronectin visualization with antibody staining and fluorescent labeling

As mentioned previously, we labeled fibronectin both with antibody staining and fluorescent labeling in the course of this work. Figure C.2 shows representative images of 6-day fibronectin matrix visualized with these two different methods. Note that these are from independent experiments with the same culture conditions. We never visualized with both techniques in the same sample. There are some differences in the appearance of the matrix based on the method used. Most notably, the fluorescently labeled fibronectin tends to show a larger variation in fluorescent intensity of fibers, whereas the antibody labeling tends to show a more uniform intensity. One possible reason for the difference in appearance of the matrix is that the labeled fibronectin only visualizes plasma fibronectin (since we only label the plasma fibronectin that we supplement) whereas the antibody visualizes both cellular and plasma fibronectin. Another difference is that the Alexa-647 fibronectin preferentially labels matrix assembled on the days that it is added (day 1 and day 3 upon media change). This is because the Alexa-647 fibronectin is progressively depleted from the media as it is incorporated into fibers. The antibody stain, on the other hand, labeled all matrix equally. However, the antibody staining was done before permeabilization to avoid intracellular stain, and this means that the high density of the cell layer could limit the accessibility of the antibody to the matrix fibers. Fluorescently labeled fibronectin does not have this problem. However, quantification of fibronectin matrix as several timepoints with these two techniques gave similar results (see Figures 3.2, 3.4, 3.6, and 3.9). Therefore, we conclude that both are valid methods to visualize and quantify fibronectin matrix.

See sections 10.5 and 10.6 for the methods for each visualization technique.

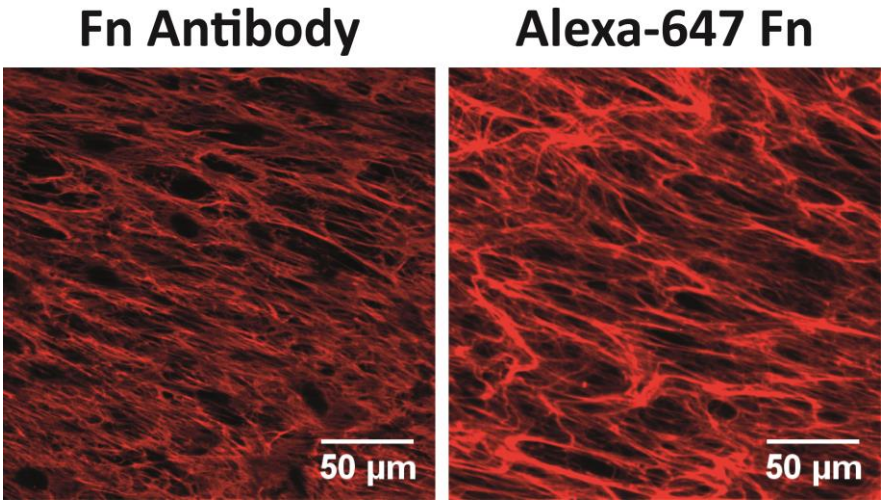

Figure C.2 Comparison of fibronectin visualization in 6-day matricies with antibody vs fluorescently labeled fibronectin. BD antibody #610077 was used (see materials and methods for full procedure).

D. Optimization of threshold for FRET analysis

Analysis of FRET required setting a threshold to exclude low intensity pixels from the background and FRET-Fn adsorbed to the glass. The threshold was varied and the optimal level was chosen to avoid including coating pixels but include as many small fibers as possible. Figure D.1 shows example FRET analyses of the same ROI (shown in the first row) with various threshold levels (50, 90, and 130). When the threshold was set to 50, a lot of fibronectin adsorbed to the glass was included. Increasing the threshold to 90 excluded this adsorbed fibronectin but still included many small fibers. Increasing the threshold further to 130 excluded many small fibers as well. A threshold of 90 was chosen to be optimal.

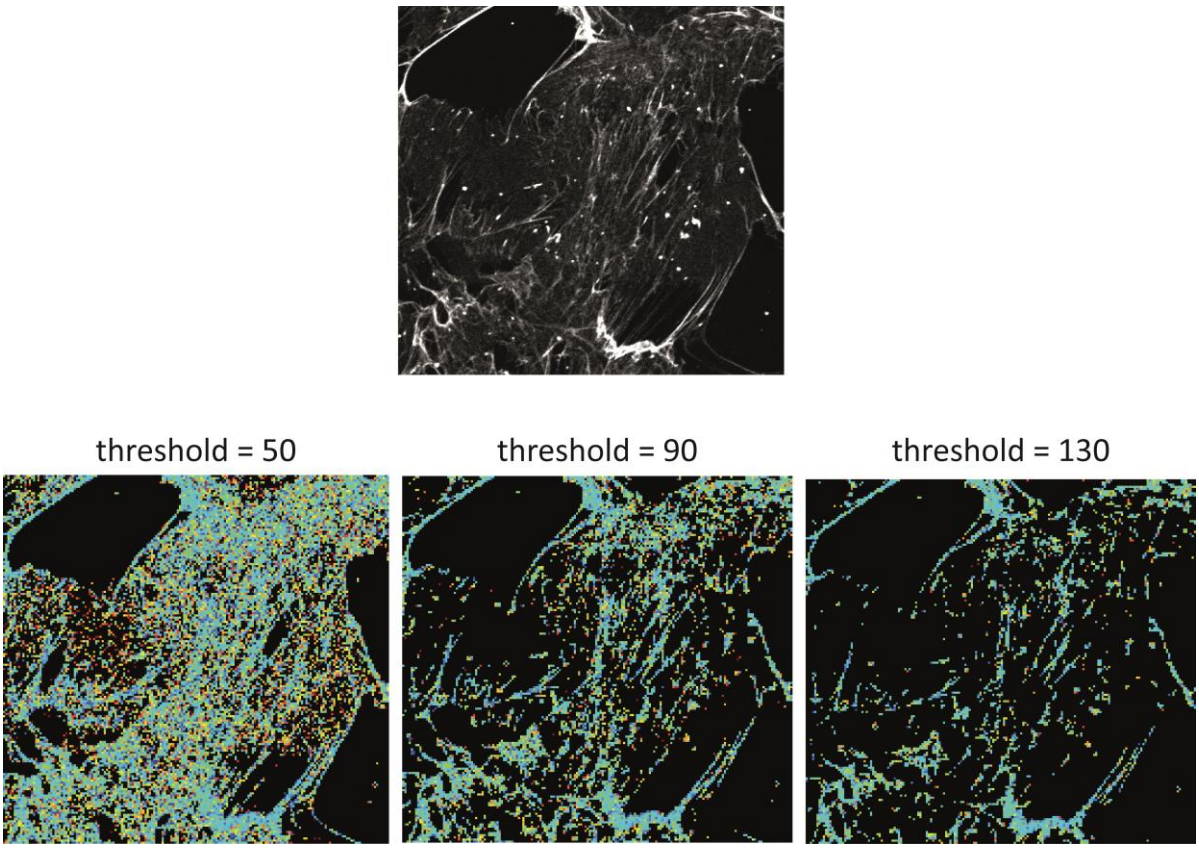

Figure D.1 Impact of threshold on FRET analysis. The top image is the donor channel and the three below show FRET analysis of this area with different thresholds. A threshold of 90 was chosen as optimal to exclude fibronectin adsorbed to the glass but include as many small fibers as possible.

E. Unknown Toxicity effect of Ficoll from Sigma Aldrich

At the start of this work we used Ficoll from two different companies: Sigma Aldrich (#F2878 and #F2637) and GE Healthcare (#GE17-0310 and #GE17-0300). All previous work using Ficoll to enhance matrix assembly has been done with Ficoll from GE Healthcare, except for one study that found Ficoll from Sigma-Aldrich to be quite unsuccessful for producing 3D cartilage tissue (Chen *et al. Tissue Eng. Part C. Methods* (2013), ref 73 in main text)[78]. According to the companies, these 2 products are the same. In fact, we contacted Sigma-Aldrich and they said that their Ficoll is produced by GE Healthcare, even though it is packaged differently, so there should be no difference. However, we found that the two have very different impacts on cell proliferation. We consistently found that Ficoll from Sigma-Aldrich significantly reduced cell density relative to control, whereas Ficoll from GE Healthcare had little effect on cell density (Figure E.1).

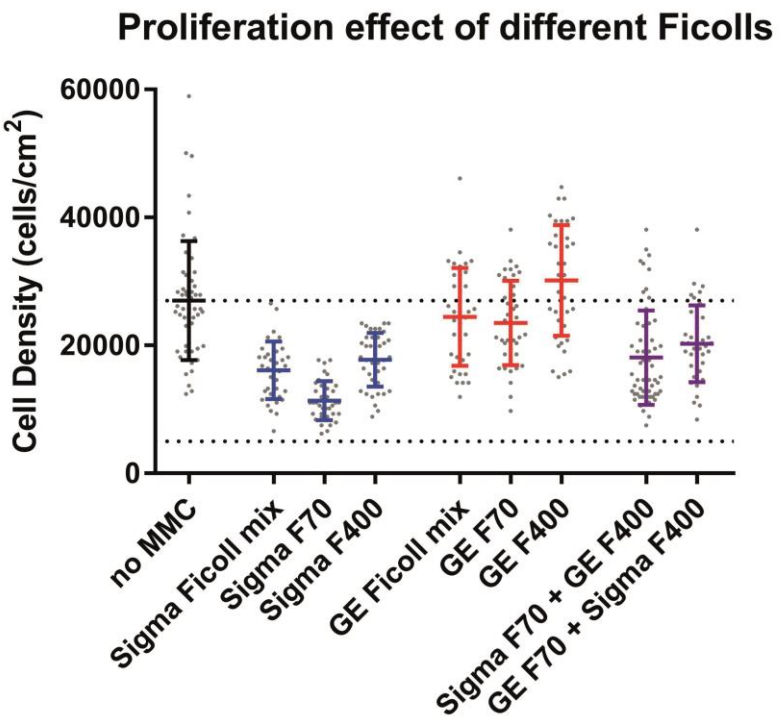

Figure E.1 Cell density is significantly reduced by Sigma Ficoll, not by GE Ficoll. Fibroblasts were cultured on fibronectin coated glass (adsorbed) for 48 hours in media supplemented with different types of Ficoll, after a 24 hour adhesion period. Media contained 100uM L-ascorbic acid 2 phosphate, but no supplemental fibronectin. Cells were plated at 5,000 cells/cm^2, which is indicated with the lower of the two dotted lines. The upper dotted line represents the density of cells in control media (without crowders) after 24 hours adhesion time and 48 hours culture time. Several different mixtures of Ficoll from the two different companies (Sigma-Aldrich and GE Healthcare) were tested. All mixtures have the same level of crowding: 18% FVO. Sigma Ficoll mix refers to 37.5mg/mL 70kDa Ficoll and 25mg/mL 400kDa Ficoll, both from Sigma-Aldrich. Sigma F70 refers to 75mg/mL of 70kDa Ficoll from Sigma-Aldrich. Sigma F400 refers to 50mg/mL 400kDa Ficoll from Sigma-Aldrich. The same mixtures were tested for Ficoll from GE Healthcare. The last two conditions (purple) represent mixtures of one component from each company, as indicated. In both of these, the 70kDa component was at 37.5mg/mL and the 400kDa component was at 25mg/mL. Results show that Ficoll from Sigma-Aldrich resulted in a reduced cell density compared to control, whereas Ficoll from GE Healthcare had little effect on cell density. Even mixtures with only one component from Sigma-Aldrich reduced cell density. Note: Ficoll from Sigma Aldrich with the unknown toxicity effect was only used in experiments presented in Appendix E. All other experiments were conducted with Ficoll from GE Healthcare.

We did not explore this result deeply, but we did collect some data regarding this unknown effect of Ficoll from Sigma-Aldrich, which we present here.

In order to determine if the reduced cell density was due to cell death or reduced proliferation, we first used trypan blue to quantify the ratio of dead to live cells after 24 hour incubation with Sigma

Ficoll. The media was collected as well to make sure that both adherent and non-adherent cells were analyzed. We found that there was no increase in cell death with Ficoll treatment in 24 hours (Figure E.2).

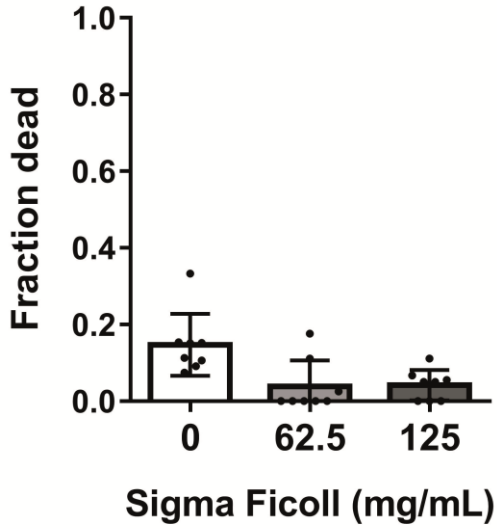

Figure E.2 Ficoll from Sigma-Aldrich does not cause an increase in cell death. Fibroblasts were plated at 4,000 cells/cm2 onto glass coated with adsorbed fibronectin. Cells were plated already in media containing Ficoll from Sigma-Aldrich (or none for control sample), meaning there was no adhesion time before media was changed to media containing Ficoll. 62.5mg/mL Ficoll was the standard mixture of 37.5mg/mL 70kDa Ficoll and 25mg/mL 400kDa Ficoll. 125mg/mL was 2x this. After 24 hours, trypan blue was added 1:25 into the media and incubated for 5 minutes at 37°C. The media was collected and saved. Adherent cells were washed with PBS, which was added to the saved media. Cells were then trypsinized and added to the saved media and PBS. The whole volume was spun at 1100rpm for 3 minutes, supernatant was remove, cells were washed with PBS, and spun again. Supernatant was again removed and cells were resuspended in 20µL of PBS. A hemocytometer was then used to count the fraction of cells that were live and dead (only dead cells were stained with trypan blue). Eight different areas were measured for each condition. Note: Ficoll from Sigma Aldrich with the unknown toxicity effect was only used in experiments presented in Appendix E. All other experiments were conducted with Ficoll from GE Healthcare.

Since cells are not dying, the large decrease in cell density compared to control suggests that proliferation is slowing down in response to Ficoll from Sigma-Aldrich. To confirm this we measured proliferation markers EdU and ki67. EdU binds to DNA while it is being replicated, so it can be used to tag all cells that divide during the time window of incubation. Ki67 is a protein that is expressed in all active phases of the cell cycle, but not in the quiescent phase (G_0). Both markers give a measure of the cells that are actively proliferating. We found both markers to show a significant decrease in proliferation in response to Ficoll from Sigma-Aldrich (Figures E.3 and E.4).

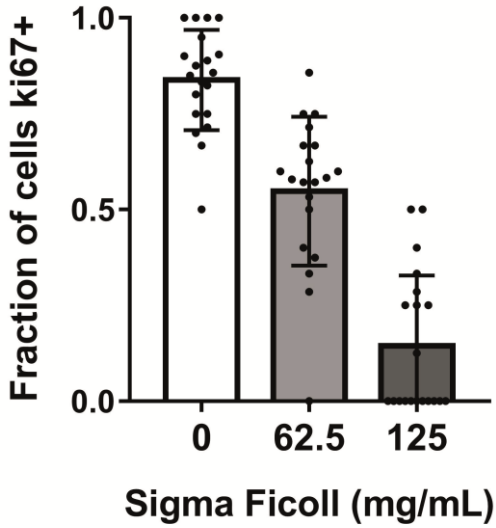

Figure E.3 Fraction of cells actively proliferating goes down in response to Ficoll from Sigma-Aldrich. Fibroblasts were plated on glass preadsorbed with fibronectin at 4,000 cells/cm2, directly into Ficoll containing media and cultured for 48 hours. The media did not contain ascorbic acid or supplemental fibronectin. After culture time the cells were fixed, permeabilized, and stained with anti-Ki67 antibody ab15580 (abcam, 1:1000) and goat anti-rabbit 555 secondary antibody (Invitrogen, #A21429, 1:200). Staining procedure proceeded as described in the main text materials and methods (Section 10.5). Cells were imaged and an intensity threshold was set to determine which cells were expressing ki67. The fraction of cells expressing Ki67 went down with Sigma Ficoll treatment, in a dose dependent manner. Note: Ficoll from Sigma Aldrich with the unknown toxicity effect was only used in experiments presented in Appendix E. All other experiments were conducted with Ficoll from GE Healthcare.

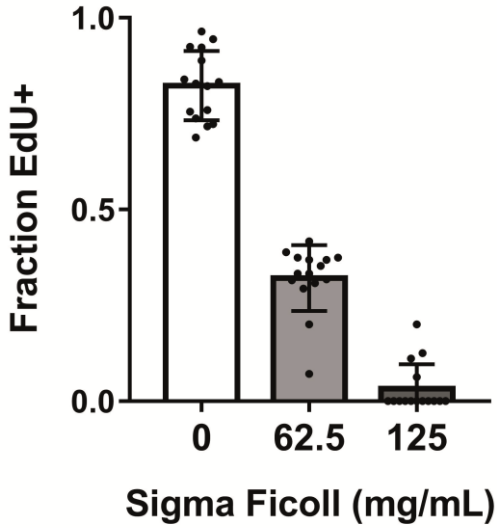

Figure E.4 Fraction of cells proliferating in 24 hours goes down in response to Ficoll from Sigma-Aldrich. Fibroblasts were cultured as described in Figure E.3. After the first 24 hours, half of the media was replaced with EdU containing media to reach a final concentration of 20nM. The cells were cultured for an additional 24 hours, fixed, permeabilized, and stained following the protocol of the Click-iT EdU Alexa Fluor 647 Imaging Kit (Invitrogen, #C10340). Note: Ficoll from Sigma Aldrich with the unknown toxicity effect was only used in experiments presented in Appendix E. All other experiments were conducted with Ficoll from GE Healthcare.

We further explored the time dependency of the decrease in proliferation in response to Sigma Ficoll. The found that proliferation decreased in the first 48 hours. After 48 hours the proliferation (as measured by fraction of cells EdU positive) stayed steady and perhaps slightly increased (Figure E.5).

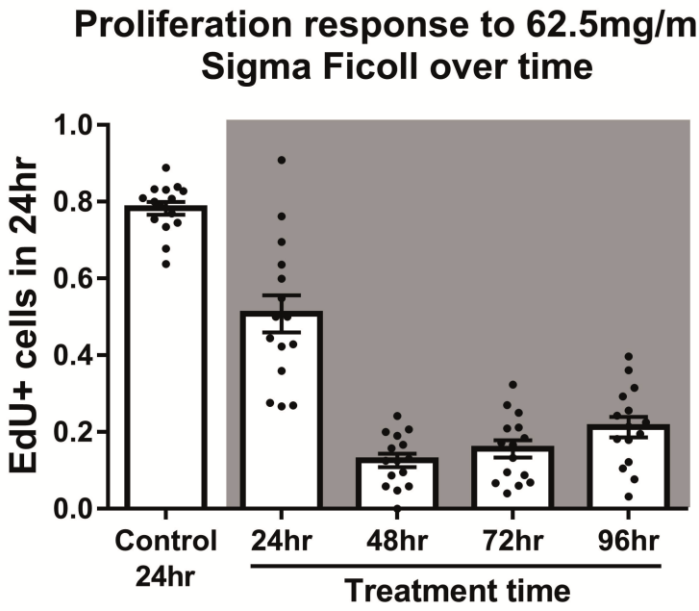

Figure E.5 Proliferation decreases sharply in the first 48 hours of treatment with 62.5mg/mL Sigma Ficoll. Fibroblasts were cultured for increasing length of time before incubation with EdU. The treatment time indicated on the x-axis refers to the time before EdU was added. Cells were then incubated with EdU for 24 hours. Proliferation seemed to recover slightly after 48 hours, but very slowly. Note: Ficoll from Sigma Aldrich with the unknown toxicity effect was only used in experiments presented in Appendix E. All other experiments were conducted with Ficoll from GE Healthcare.

We also explored the dose dependency of the reduced proliferation in response to Sigma Ficoll. We found that the fraction of cells proliferating after 48 hours treatment was linearly dependent on the concentration of Sigma Ficoll (Figure E.6).

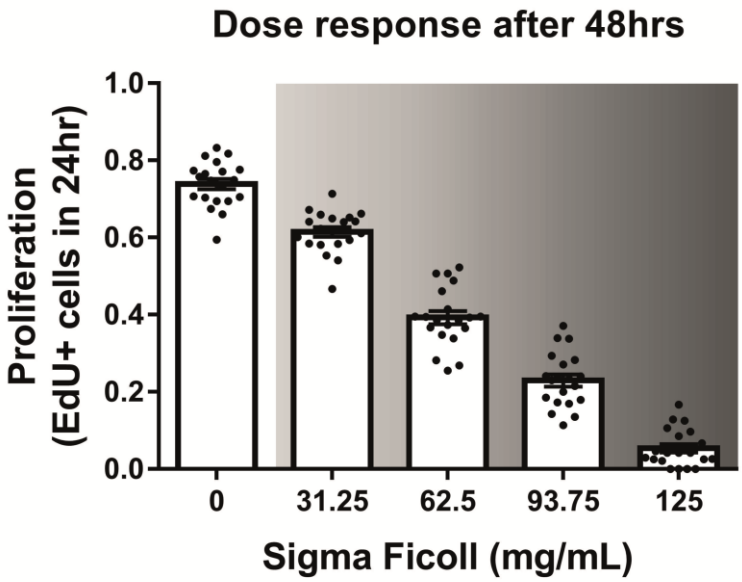

Figure E.6 Proliferation is linearly dependent on Sigma Ficoll concentration. Fibroblasts were exposed to several different concentrations of Sigma Ficoll for 48 hours, and then treated with EdU for an additional 24 hours to assess proliferation. All formulations of Ficoll have the same ratio of 70kDa and 400kDa Ficoll. 31.25mg/mL is a 1:2 dilution of the standard Ficoll mixture (62.5mg/mL). 93.75mg/mL is a 1.5x and 125mg/mL is a 2x version of the standard mixture. Note: Ficoll from Sigma Aldrich with the unknown toxicity effect was only used in experiments presented in Appendix E. All other experiments were conducted with Ficoll from GE Healthcare.

In order to understand better why the fibroblasts slowed proliferation in response to Sigma Ficoll, we analyzed the cell cycle distribution at different timepoints with and without Ficoll treatment. The first row of Figure E.7 shows what happened in control media over time as the cells proliferated and reached confluence. The proportion of cells in the G_2 and S phases progressively decreased while the proportion in G_0/G_1 phase increased. This technique is based on DNA quantification, so it cannot distinguish between the G_0 and G_1 phases, in which cells have the same amount of DNA (1n). The second row shows that there is not much change in cell cycle distribution with Ficoll after 6 hours. However, after 1 day there is a very large difference. The portion of cells in the S and G_2 phases is much larger in the Ficoll treated sample. This suggests that cells are not becoming quiescent in Ficoll media (which would show up as an increase in G_0 phase) but rather they are getting stuck in or slowing down progression through the S and G_2 phases. After 2 days there are still more cells in each of the S and G_2 phases with Ficoll, but much less than after 1 day, suggesting that the cells are not permanently frozen in these phases and do eventually complete the cell cycle. After 6 days, cells in both conditions are confluent and show a cell cycle distribution consistent with quiescence. Interestingly, even though proliferation is slowed with Ficoll, after 6 days fibroblasts have also reached confluence when exposed to Sigma Ficoll. This further supports the idea that progression through the cell cycle is slowed but not arrested.

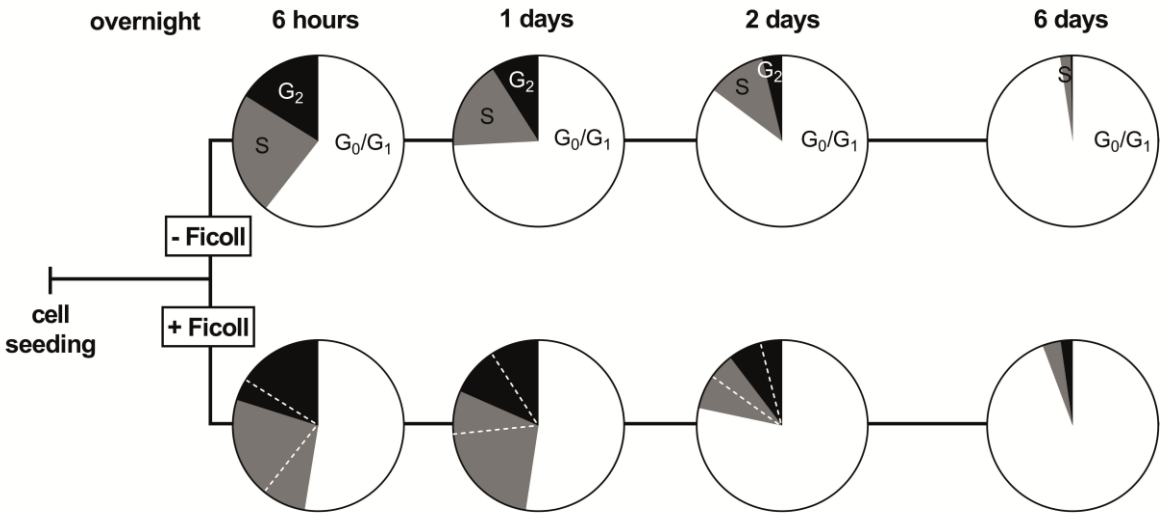

Figure E.7 Cell cycle distribution is altered by exposure to Sigma Ficoll. Fibroblasts were cultured in polystyrene tissue culture flasks (75cm^2 area) with a starting cell density of 4,000 cells/cm2. Polystyrene was used because a large quantity of cells was needed for FACS analysis and we needed to keep the starting cell density low. The surface area requires for cell culture was not practical to achieve with glass and fibronectin coating. Cells were allowed to adhere overnight before media change to include Sigma Ficoll (62.5mg/mL mixture). 6 day samples received one media change at 3 days. After the specified culture time, cells were trypsinized, fixed with ethanol, and stained with propidium iodide. Cells were analyzed with a BC LSRFortessa flow cytometer immediately after staining. Histograms of the DNA signal were fit with ModFit LT 3.3 software in order to get the fraction of cells in each phase. Note: Ficoll from Sigma Aldrich with the unknown toxicity effect was only used in experiments presented in Appendix E. All other experiments were conducted with Ficoll from GE Healthcare.

We next explored how the matrix environment affects the proliferation response to Sigma Ficoll. We compared cell density after 48 hours on adsorbed fibronectin coating, crosslinked fibronectin coating, a fibronectin-rich decellularized matrix, and a collagen- and fibronectin-rich decellularized matrix. Interestingly, we found that the response was very different (Figure E.8). There was no big difference in cell density on the crosslinked coating or either matrix. This suggests that signals from the matrix can override whatever anti-proliferation signal is coming from the Sigma Ficoll.

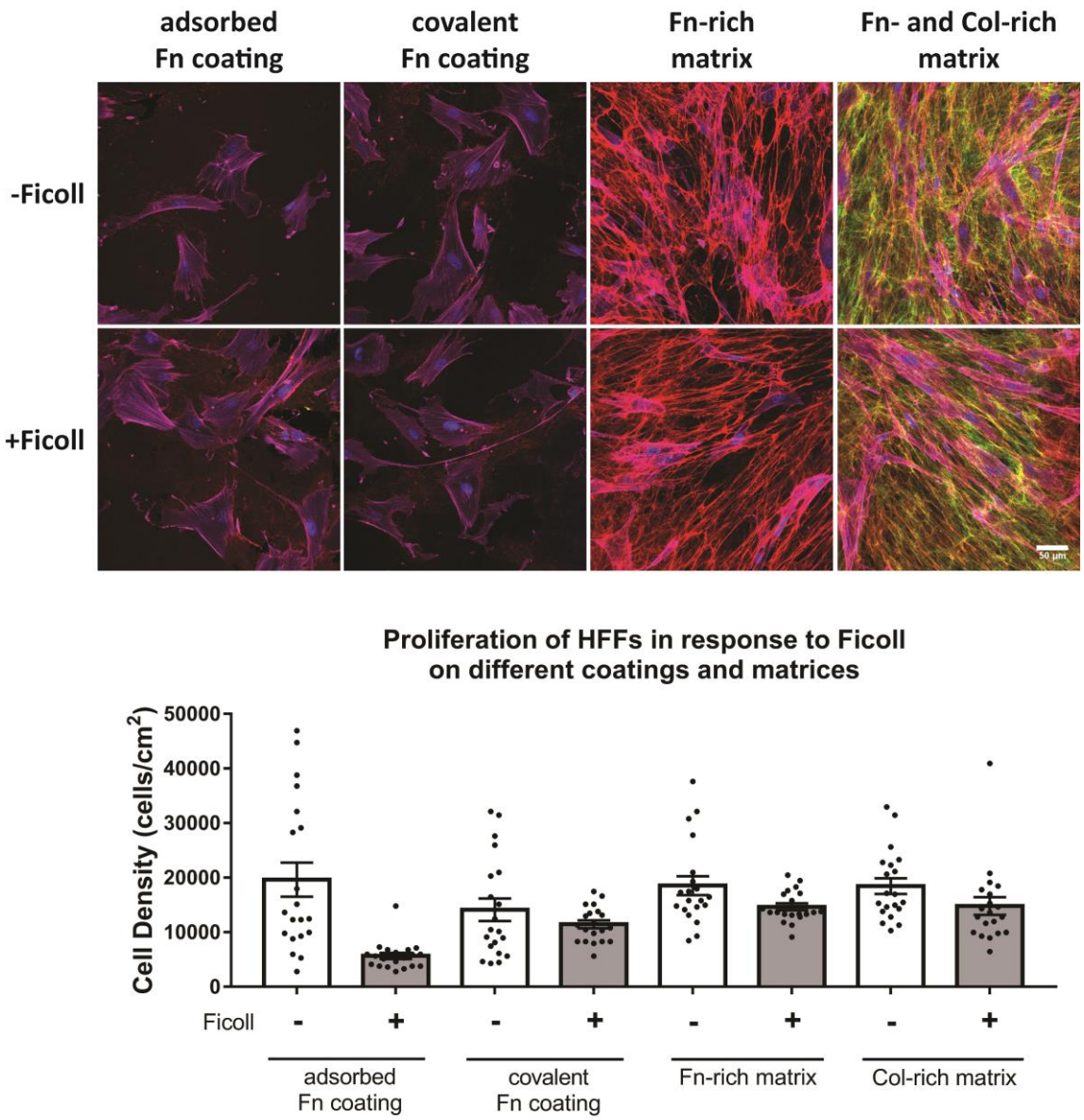

Figure E.8 Proliferation response of fibroblasts to Sigma Ficoll depends on the matrix environment. Fibroblasts were cultured on several different substrates for 48 hours, after an overnight adhesion period, and the cell density was compared with and without Sigma Ficoll. The different substrates were adsorbed fibronectin, covalently cross-linked fibronectin, fibronectin-rich decellularized matrix, and fibronectin- and collagen rich-decellularized matrix. Fibroblasts were plated at 45,000 cells/cm2 onto crosslinked fibronectin coating and cultured for 4 days in standard media with 50µg/mL supplemental fibronectin to produce the matricies. To produce matricies rich in both fibronectin and collagen 100µM sodium ascorbate was added. Media was changed once after 2 days. Cells were removed by vigorous washing with 0.5% sodium deoxycholate. Images show actin (magenta), DNA (blue), fibronectin (red), and collagen (green). Note: Ficoll from Sigma Aldrich with the unknown toxicity effect was only used in experiments presented in Appendix E. All other experiments were conducted with Ficoll from GE Healthcare.

Key takeaways from this investigation of Ficoll from Sigma Aldrich are the following:

- Ficoll from Sigma Aldrich has an unknown toxicity effect that reduces proliferation but does not cause cell death
- The cells do not become quiescent, but rather slow down progression through the cell cycle
- Signals from the ECM can override the signals from the Sigma Ficoll

Given the lack of clarity about what exactly this toxic effect is and what other effects it might have, and also given the fact that information from the company provides no reason to think cells should behave differently to Sigma vs GE Ficoll, we strongly recommend only using Ficoll from GE Healthcare for supplementation into cell culture media.